Dissertation

Synthesis and Characterization of Pd-supported Fluoro-dodecavanadates

Graduate School of
Natural Science and Technology
Kanazawa University

Division of Material Chemistry

Student ID No. : 1424022006
Name : Miftahul Khair
Chief advisor : Prof. Yoshihito Hayashi
Date of Submission : June 30, 2017

TABLE OF CONTENTS

ABBREVIATION

POM(s)	Polyoxometalate(s)
POV(s)	Polyoxovanadate(s)
DMSO	Dimethyl sulfoxide
DMF	Dimethylformamide
FT-IR	Fourier Transform Infrared Spectroscopy
TGA	Thermogravimetric analysis
NMR	Nuclear magnetic resonance
UV-VIS	Ultraviolet-visible
XRD	X-ray diffractometry
SXRD	Single Crystal X-ray diffractometry
PPhh4	Tetraphenylphosphonium
TEA	Tetraethylammonium
n-Bu_4N / TBA	Tetra-*n*-butylammonium

PUBLICATION

The following article were published as a result of work undertaken over the course of this PhD programme :

Khair, Miftahul, Yuji Kikukawa, and Yoshihito Hayashi. "Synthesis and Characterization of a Palladium-Supported Fluoride-Incorporated Dodecavanadate." Chemistry Letters 46 (2017).

ABSTRACT

In Metal Organic Framework (MOF) chemistry, bidentate ligands are key factor to construct highly porous materials. To get best properties of MOF, we develop inorganic linker building unit for to substitute the organic ligand linker unit. The need of the new inorganic linker units is solved by making use of polyoxometalate functionalized with a metal.

To overcome the weak coordination ability of POM, halide anion is incorporated on a spherical polyoxovanadate (POV) because halide incorporation can reduce the surface charge and increases electronegativity. This in turn increases the coordination capability of POV.

In order to develop the intended inorganic linker, Pd is attached to the Fluoride incorporated dodecavanadate. The linker would not only be beneficial for framework (POMOF) material construction unit, but also would be beneficial for the purpose of oxidation catalysis.

Complex **1**

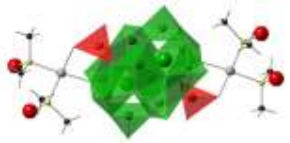

Complex **2**

Complex **3**

Herein we report the synthesis of these types of POVs: [*n*-$Bu_4N]_4[V_{12}O_{30}F_2].CH_3CN$ **(1)**, $[VO(DMSO)_5]_2[\{Pd(DMSO)_2\}_2V_{12}O_{32}(F)_2].2CH_3CN$ **(2)**, and $\{n\text{-}Bu_4N\}_4[\{Pd(NO_3)(DMSO)\}_2V_{12}O_{32}(F)_2]\cdot 2DMSO$ (3). Complex [1] is prepared by reduction with hydrazine of $(n\text{-}Bu_4N)_4[HV_{11}O_{29}F_2]$. Addition of Pd^{2+} to DMSO solution of [1] gave complex [2]. Addition of nitrate salt of Pd^{2+} to DMSO solution of $[V_{10}O_{26}]^{4-}$ and F^- ion gave complex **(3).**

The successfully synthesized three complexes have spherical shapes anions containing two anions F^-. Anion **(1)** is mixed valence $[V^{V}_{10}V^{IV}_{2}O_{30}F_2]^{4-}$ which shows electrochemical behavior potential for electron sponge application. The reaction of precursor complex **(1)** with Pd^{2+} and DMSO afforded complex **(2)** which is a first mixed valence Pd supported fluorododecavanadate linker. Spherical compound **(2)** anion consists of ten VO_5 units and two VO_4 units. Two palladiums with two DMSO ligands at both sides attached on the main cage. Cation $[VO(DMSO)_5]^+$ comes from the partial decomposition of complex **(1)** during the reaction. By the oxidation of decavanadate $\{n\text{-}Bu_4N\}_4[V_{10}O_{26}]$ in the presence of F^- and $Pd(NO_3)_2$ in DMSO, a palladium-supported fluoride-incorporated dodecavanadate **(3)** was synthesized. Even if sharing similar main cage shapes with **(2)**, complex **(3)** is a fully oxidized form with nitrate and DMSO ligands attached to Pd.

These complexes have potential linker capabilities that can bind the connection of building units to cultivate new field of molecular inorganic frameworks.

ACKNOWLEDGEMENT

First of all, I would like to express my deep appreciation to Professor Yoshihito Hayashi, Dr. Yuji Kikukawa, and Dr. Keisuke Kawamoto for their supervision, patience and support. It was a pleasure and an honor to join the group and to have an opportunity to deal with great people and interesting research themes over the past three years.

I would like to express my appreciation to many people at the Inorganic Chemistry Laboratory Kanazawa University. I am very grateful to Mr. Saito Masahiro for preliminary work on underlying the synthesis procedures of some complexes I explored during his master Thesis 2004. Special thanks Mr. Sho Kuwajima and Mr. Sugiarto for their kind help and for technical cooperation in particular. I would like to thank Prof Shigehisa Akine, Prof Hideki Furutachi, Prof. Tomonori Ida, and Prof Masahiro Mizuno as the examiners of this dissertation.

I am also very grateful to State University Padang, Indonesia for the opportunity to continue this wonderful research, and the Directorate General of Higher Education (DIKTI) Indonesia – Kanazawa University for the financial support through a joint scholarship program.

I must also admit my friends and family, especially. My parents, Chairul Amri and Asnawiyar, my wife Hafni Ziad, my kids Thariq, Syamil, Faishal, and Salman, who smile and cry that makes my world more beautiful.

CHAPTER 1 INTRODUCTION

1.1 Polyoxometalates

Polyoxometalate (POM) is an outstanding class of oxo-cluster materials. The first report of POM dates back to Berzelius (1826) when he noticed a yellow solid from a reaction between molybdate and phosphoric acid. The formed solid was $(NH_4)_3(PMo_{12}O_{40})$ compound. After that, POM had been a large and quickly growing class of compound. Researchers from synthetic/structural chemistry, physics, biology and theoretical chemistry from all over the world have been devoting themselves on the study of POM.

With the availability of new analytical methods, most POM molecular science (chemistry, biology, physics, and materials science) has been developed recently. Single Crystal X-ray Diffraction and Mass Spectroscopy are examples of methods not available before that allow the POM study to be easier nowadays.

The interdisciplinary research of synthetic/structural chemistry, theoretical chemistry, physic, and biology focuses on study of the manifold structures and properties of POMs. The outstanding compositional and structural diversity of POMs enables fine-tuning of their electronic properties, redox properties, and chemical stability together with robustness in the objective of designing future applied devices[1]. Today, POM chemistry is still an important emerging area where over 500 papers (not including patents) were published each year and this number is rapidly increasing[2]. POM is currently very attractive even in the most challenging leading research areas, e.g., water splitting, magnetism, catalysis, electronic materials and bio-medical applications.

1.1.1 Structure

Polyoxometalates (POM) are inorganic metal oxide anions containing individual $\{MO_x\}_n$ where M is limited to groups of 5 and 6 metals (M = vanadium, niobium, tantalum, molybdenum and tungsten, x = 4-7) (figure 1) in their highest oxidation state. The units can be combined to form a series of groups from low to high nuclearity, ranging from 2 to 368 (for example $H_xMo_{368}O_{1032}(H_2O)_{240}(SO_4)_{48}^{48-}$ anion) metal atoms in a single molecule[3]. The versatile nature of polyoxometalate derives from their ability to polymerize these MO_x units to form highly symmetric groups. POM clusters are generally anionic and hardly coordinate with additional cations as linkers. Removal of some of the cage atoms to form vacancies that can be filled results in lacunary structure of POM .

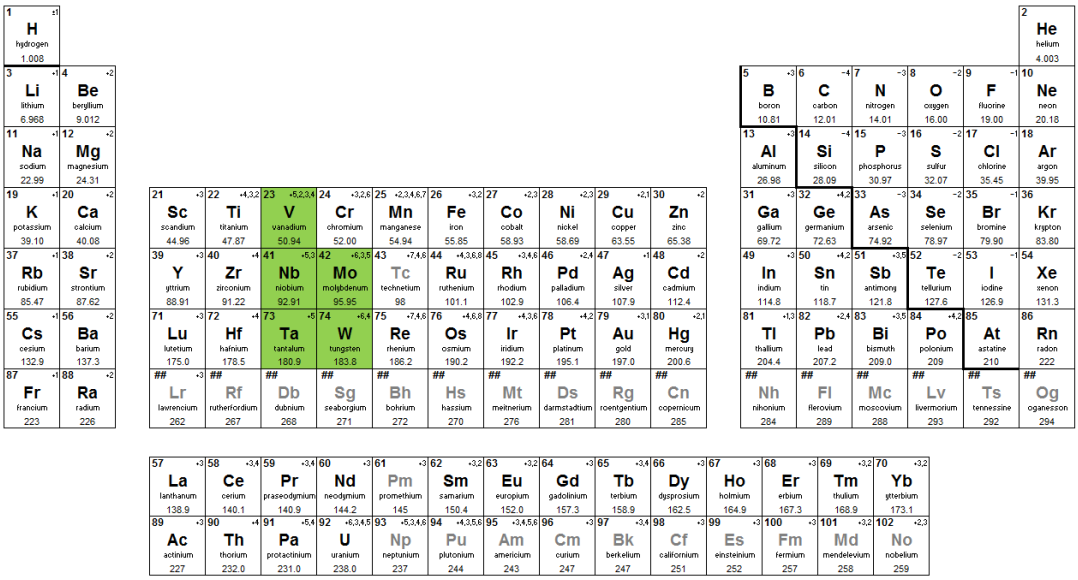

Figure 1 Periodic Table of the Element. The elements that form p1olyoxometalates are in green.

POMs embrace certain structural motifs. The POM family is divided into *iso*-polyoxometalates (isopolyanion) and *hetero*-polyoxometalate (heteropolyanion) based on the types of transition metal atoms involved in their composition.

Isopolyanions only involve one type of transition metal atoms in their metal oxide framework. They have interesting properties, e.g. high charges and strongly basic oxygen surfaces, which is a good unit as a building block[4]. The example is illustrated by dodecavanadate $[V_{10}O_{28}H_3]^{3-}$ (figure 2).

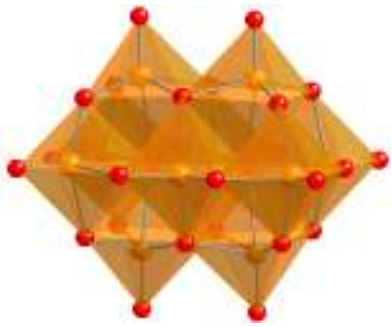

Figure 2 Decavanadate $[V_{10}O_{28}H_3]^{3-}$

The *hetero*-polyoxometalate type (heteropolyanions) involve more than one type of metal atoms. In the other word, heteropolyanions are metal oxide clusters that contain heteroanions. Heteropolyanions are the most studied POMs especially for catalysis, with much focus on the well-known Keggin $[XM_{12}O_{40}]^{n-}$ anions and Wells–Dawson $[X_2M_{18}O_{62}]_n$ anions (where M= Mo or W, X is the heteroatom usually P^{5+}, Si^{4+}, or B^{3+}).

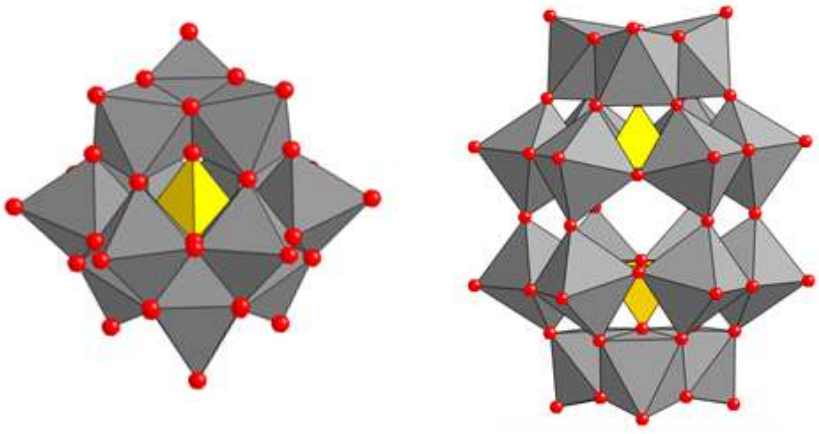

Figure 3 Polyhedral Representation of Keggin Structure (*LHS*) and Dawson Structure (*RHS*)

The most stable POMs Keggin structure general formula is $[XM_{12}O_{40}]^{n-}$ (where X = heteroatom, most common are P^{5+}, Si^{4+}, or B^{3+}), M is the addenda atom (generally Mo and W), and O represents oxygen. The structure shows self-assembly in acidic aqueous solution. Since their properties are finely tunable by controlling the constituent elements, structures, and counter cations, POMs can be used as the unique functionalized materials, such as optical materials, single molecule magnets, electronic interfaces, adsorbents, medicine, and catalysts.

Tungsten and molybdenum dominate many polyoxometalate chemistry primarily because of its stability and rich redox chemistry. These properties enable them to be part of a class of inorganic compounds that exhibit semi-conduction, magnetic, thermal and photochemical properties. Vanadium is also interesting because it forms various structures and with various structural units and oxidation states.

1.1.2 Representation

Like most of inorganic compounds, POMs' building blocks tend to be formed from groups of atoms. The structure of POMs seems to be governed by the principle of electrostatic and radius ratios observed for extended ionic lattices. Therefore, it is easier to describe the structure and bonding of POMs by replacing this metal-oxide building block with a polyhedron where the metal ion resides at the center with oxygen ligands at the vertices (figure 4).

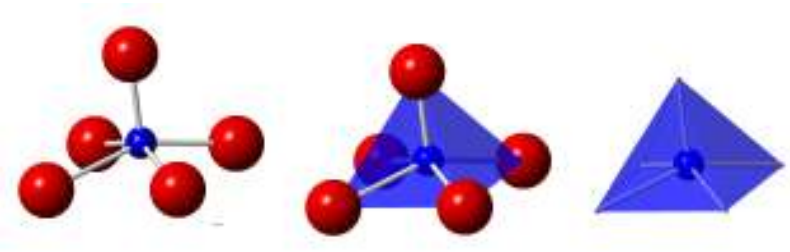

Figure 4 Ball stick (*left*) and polyhedral representation (*middle* and *right*) of MO_5 square pyramid unit where M = V, Mo or W. M: blue, O: red.

At each case, the metal ion does not lie in the center of the polyhedra of oxide, instead it is strongly displaced outward of the POM structure, i.e. toward the vertex of the polyhedron (figure 5).

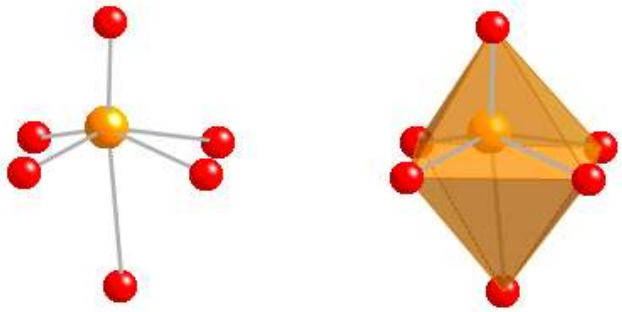

Figure 5 Ball stick and polyhedral representation of the VO_6 octahedron, where V: orange, O: red. V atom is no longer sit in the center of the polyhedron.

These polyhedra are connected together through the edge sharing, corner sharing, and (rarely) faces sharing or a combination of them to build up the structure[5] (figure 6).

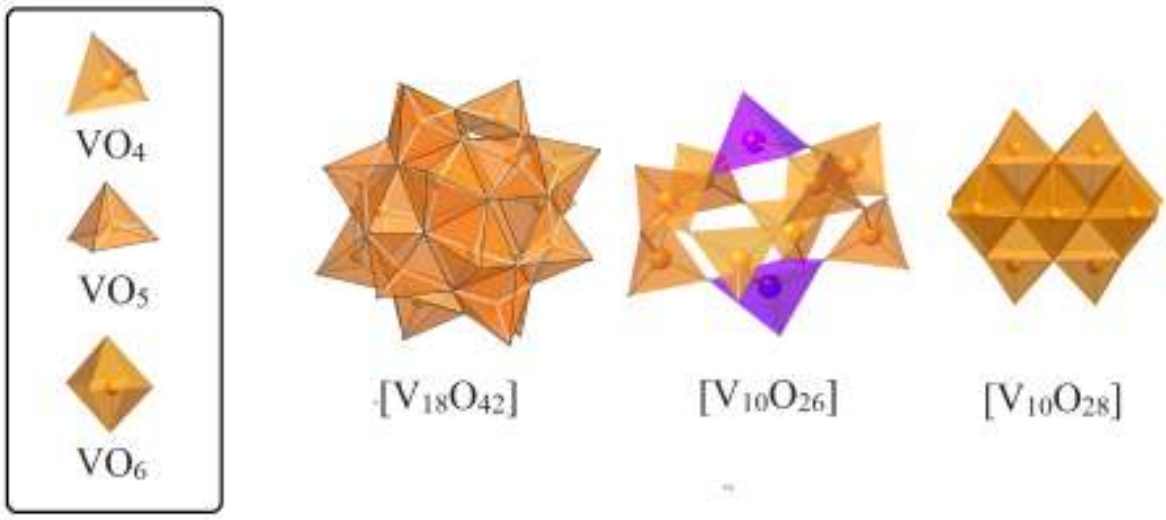

Figure 6 Units for construction of POVs *(LHS* box), edge sharing and corner sharing types of assembled POVs from the units (*RHS*).

If molybdenum and tungsten with d^0 anionic clusters use octahedral shaped building blocks in their construction, then vanadium in the other hand can use tetrahedral $\{VO_4\}$, square-pyramidal $\{VO_5\}$, and octahedral $\{VO_6\}$ building units. The availability of these various building units (coordination environment) make polyoxovanadates have a unique structural chemistry[6] (figure 6).

1.1.3 Properties

POMs molecule in term of charge can be regarded as a conjugating system. It is because for most POMs the charge is always uniform across molecules and all units. So which atom holding up electrons cannot be indicated. POM have moieties for receiving electrons in the charge transfer system which is good for energy storage application. The donor/acceptor interactions in such charge-transfer materials are controlled by the shape and size the POMs as well as by their redox potentials, which are readily tuned by changing the metal centers and with smart synthetic methods. Cations accompanying POMs for charge balancing consideration, make salt which can be both water soluble and organic soluble, allowing POMs applications in both media.

POMs are robust and have large number of metallic centers, so that POMs can undergo reversible and multi- electron photoredox processes and keeping their structure intact. These properties make POMs as electron mediators in solar cell and photocatalytic process. The reversible multielectron-transfer reactions of POMs are the basis for catalytic application of POMs. Polyoxometalate-based catalysts are interesting because their acidic and redox properties can be controlled at molecular levels. In addition, POM has unique electrochemical, magnetic, photonic and chemical reactivity. While the catalysis and materials science are two main fields of applications of POMs, their biochemical and biological properties are the subject of increasing interest.[7,8]

1.1.4 Characterization of Polyoxometalates

There are various methods for characterization of POM both in solid state and in solution. Spectroscopy is the most common and easy to use technique. To identify the M-O bond presence one can use vibration spectroscopy. FTIR spectroscopy is a powerful and fast method to characterize POM products from established syntheses.

The characteristic absorption of infrared spectra of POM are in the region of 1100-400 cm^{-1} associated with oxygen-stretching vibrational frequency. There are distinct areas where the oxygen terminal and oxygen bridging peaks can be found in that region. The infrared spectrum also gives information about the symmetry of polyoxoanion. It can be used to distinguish POMs and provide information on structures. Infrared and ultraviolet-visible spectroscopy, and also thermogravimetric and differential thermal analyses has been used for POM characterization methods since 1960s [9,10,11].

To determine the environment of specific atom in POM, one can use Nuclear Magnetic Resonance (NMR) spectroscopy. ^{31}P NMR is used to identify POMs such as phosphotungstates and phosphomolybdates. ^{29}Si NMR is to identify the POM structure

that includes non Si as P heteroatoms. Polyoxovanadate and polyoxotungstate can be characterized by ^{51}V NMR and ^{183}W NMR respectively.

Associated with NMR is electron paramagnetic resonance spectroscopy (EPR). EPR can detect and identify free radical, paramagnetic centers, and geometry of atomic coordination.[12] The energy dispersive x-ray spectroscopy (EDS) paired with a microscope can help to determine element composition. Transmission electron microscope (TEM) can be used to observe individual polyoxometalate clusters. Scanning Electrons Microscopy (SEM) can be used to observe crystals or bulk powder.

Mass spectrometry is a useful technique for identifying species present in solution by separating them based on mass to charge ratio. The relative percentage of each species can also be determined. Mass spectrometry can be augmented by various techniques such as chromatography, thermogravimetric analysis, ionization electrospray, etc.

The method of Electrospray Ionization Mass Spectrometry (ESI-MS) is suitable for the analysis of ionic species in aqueous and polar solvent, and as such complements the other methods for the characterization of POMs structurally and chemically[13]. ESI-MS has enabled the real time monitoring of the formation of a complex of organic–inorganic POM hybrid system[14]. X-ray photoelectron spectroscopy (XPS) can be used to identify substitution of elements into clusters and also study the surface of films stored from POMs.

Beside some of the traditional tools, non-traditional analytical tools are also used currently to characterize the aqueous inorganic clusters and POMs ions. Some examples of the techniques are nuclear magnetic resonance spectroscopy (NMR), Raman spectroscopy, dynamic and phase analysis light scattering (DLS and PALS), small angle

X-ray scattering (SAXS), and quantum mechanical computations (QMC). The cluster species in the solid state or in the solution can be determined with this techniques.[12]

Computational chemistry provides valuable information to complement characterization of polyoxometalate. Simulation data can be produced for some data different methods such as vibration spectroscopy, NMR, scattering data, etc. Computation can also determine the energetics of the group under various conditions, and can helps us to understand the speciation and formation of this attractive metal oxide cluster.

1.1.5 Application of Polyoxometalates

By extensive structural range of POMs, attractive POM applications continue to grow. The extensive application of POMs are due to (i) the ability of POM to act as a conjugated electron sponge and (ii) great variability of its molecular properties, including size, shape, redox potential, charge density, solubility, acidity, etc. Some noted area of POMs application are on the catalysis, medicine, bioanalysis and materials science[15].

The group VI and vanadium POMs possess extensive redox properties relevant to catalysis and electron transfer processes. Therefore, the silico- and phospho- tungstates and molybdates are the most referenced examples for applications.

Inorganic-organic hybrid POMs can be used to synthesize new multi-functional POM materials. Hybrid POMs can be applied in enantioselective catalysis and separation by incorporating chiral organic molecules into the structure. Photo induced electron transfer in POM-porphyrin hybrids provides photosensitive systems for catalysis, photovoltaics, and for environmental applications such as depollution and recovery of valuable or toxic metals.

1.1.6 Synthesis

Most POM synthesis depends on the use of a conventional solution-based synthetic method such as solvent evaporation, precipitation method and crystallization technique where ambient pressure and temperature conditions have been used. The solution-based approach so far has resulted in the synthesis of a large number of POM compounds. There are also some precaution regarding the use of this method. One must take care of the low solubility of metal oxide starting materials, inclusion and co-crystallization water and solvent molecules, poor controllability of reaction parameters etc.

The experimental variables which should be controlled in the synthesis of a POM are: (1) pH, (2) type and concentration metal oxide anion, (3) ionic strength, (4) type of heteroatom and its concentration, (5) additional ligands presence, (6) temperature and pressure (7) reducing environment, (8) counter-ion and metal-ion effect and (9) processing methodology (one-pot, continuous flow conditions.[16] Some of these problems are seen for obtaining high yield synthesis. Changes of acid type, solvent (aqueous or non-aqueous systems), use of a ligand, heteroatom or reducing agent, all play a role in the assembly of new clusters of POMs.[5]

POMs have been synthesized and isolated from both aqueous and non-aqueous solutions. In aqueous solution, the common method involves the acidification of aqueous solutions of simple oxoanions and the necessary heteroatoms as follows,

$$12\ WO_4^{2-} + HPO_4^{2-} + 23\ H^+ \rightarrow [PW_{12}O_{40}]^{3-} + 12\ H_2O$$

$$4\ VO_4^{3-} + 8\ H^+ \rightarrow V_4O_{12}^{4-} + 4\ H_2O$$

$$7\ MoO_2^{4-} + 8\ H^+ \rightarrow [Mo_7O_{24}]^{6-} + 4\ H_2O$$

In some cases, the product is crystallized at room temperature since the equilibrium constants and the rate of formation are large. Furthermore, careful temperature and pH control is required for the desired reaction to occur.

1.2 Polyoxovanadate

1.2.1 Introduction

Vanadium is group 5 transition metal which is known for production of alloys. Vanadium also has function in biological system and plays role in bioinorganic chemistry.[17] Vanadium has many oxidation states with the common oxidation state between +2 and +5 associated with certain characteristic colors. Vanadium exhibits various coordination geometries that provide more structural flexibility and have general tendency to form cluster with shell and cages like topologies. Specific reaction parameters such as temperature, pressure, reaction time, stoichiometry, solvent, concentration, and pH determine the oxovanadium ions' nuclearity, structural motifs and net charge.

Vanadium oxide compounds have application in the field of catalysis, biochemistry, sensor, geochemistry, sorption and intercalated layered material surface and nanoscience and perform their role in smart material for energy[18]. A compound containing an oxoanion of vanadium is known as a vanadate, generally with the highest +5 oxidation state of Vanadium. The simplest vanadate ion is the tetrahedral, orthovanadate, VO_4^{3-} anion, and in solutions of V_2O_5 in strong base (pH > 13). Conventionally this ion is represented with a single double bond, however this is a resonance form as the ion is a regular tetrahedron with four equivalent oxygen atoms.

Polyoxovanadate (POV) represents an important subclass of POMs. POV's fast growing research are motivated by the their versatile redox properties and prospective in various branch of chemical, physical and biological sciences.[18]

POVs show structural versatility due to the variety of the coordination number of vanadium. POVs have different basic types of polyhedra, ({VO_4}, {VO_5}, and {VO_6}) building blocks (units), to form cluster shells or cages. Further, they can be divided into four families: "highly-reduced" (V^{III}), "fully-reduced" (V^{IV}), mixed-valent (V^{V}/V^{IV} or V^{IV}/V^{III}), and fully-oxidised (V^{V}), species (figure 7).[18] The cage-, basket-, and sphere-like shape of POVs enables them to entrap small guest molecules in their central cavities, to behave like a "molecular container" like *e.g.* fullerenes.

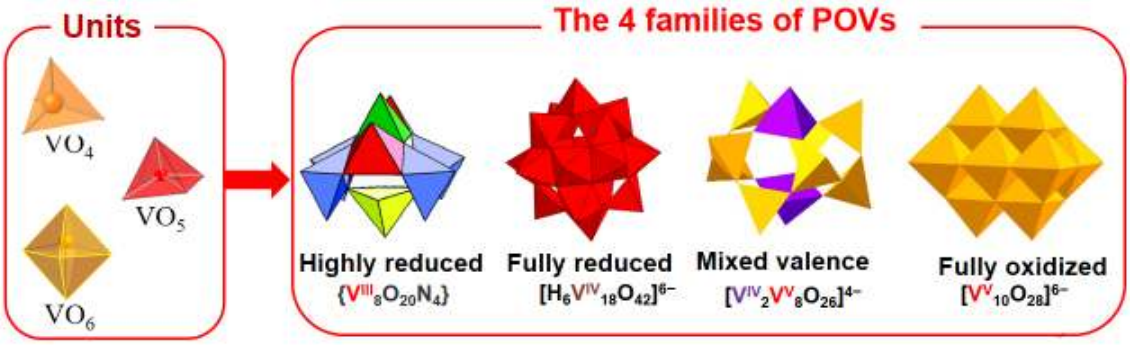

Figure 7 The four families of POVs (*RHS)* constituted by different building units (*LHS*)

POV clusters that contain mixed valence species ($V^{IV/V}$) arise from the full or partial delocalization of the single 3d electrons of the vanadium ions over either valence types or the complete localization over the paramagnetic ions. [19,20] This type of POV are highly attractive for magnetic studies.

1.2.2 Synthetic procedure

Polyoxovanadates are almost always synthesized under aqueous or hydrothermal conditions which may limit the isolation of different cluster types. A variety of POV synthetic methods have been used to construct complex molecules by considering synthetic parameters (concentration, pH, molar ratio, temperature, solvent choice and counter cation). Exploration of new synthetic routes may need long time and patience. POV Materials doesn't include those which do not form crystals with distinct chemical

compositions and the atoms must be organized in an orderly array of repeating units. The choice of counter cation and condensation method is very important for the synthesis of POVs. [21]

Adjusting the pH to a specific level can give rise to POMs with different nuclearities. For example, in the synthesis of POVs in very alkaline conditions, the formation of polyoxo species is not easy, because only orthovanadate $[VO_4]^{3-}$ is formed. On the acidification of solution, the protonation reaction begin against the oxido group with the formation of the intermediate $[HVO_4]^{2-}$, $[H_2VO_4]^-$, and H_3VO_4. As the solution becomes more acidic, condensation reactions of orthovanadates occurs to form of various POVs species.[21]

At pH 8 to 13, monovanadates $[HVO_4]^{2-}$, divanadates $[V_2O_7]^{4-}$, and metavanadates, $[VO_3]_n^{n-}$ (n = 3 or 4) are stable.[21] Simple illustration of the effect of pH on the transformation of POVs can be seen in figure 8.

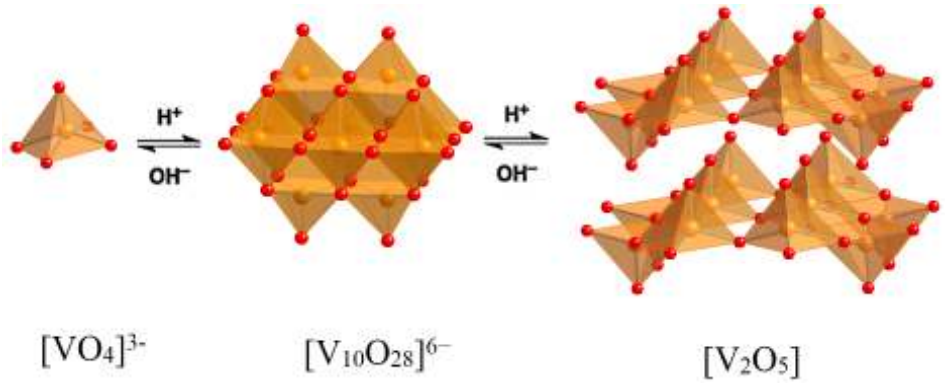

Figure 8 The effect of pH on the anions and oxides in vanadium (V) chemistry

1.3 Mixed valence POMs

The names ‘mixed valency’ or ‘intermediate valence’ or ‘mixed oxidation state’ or ‘non-integral oxidation state’ are used to describe inorganic or metal-organic compounds in which an element is present in more than one oxidation state. The transfer of an electron from one metal ion to another cause the colouration. The distribution of oxidation states

within the molecule can exchange under the influence of light resulting in the light absorption and hence the colour. This happens very frequently in inorganic chemistry when the same element is present in different valence states in the same molecule. [22]

There is a type of reduced POM, the so-called heteropoly blue, which are is stable in alkaline solutions. They are able to receive or release electrons without any change or decomposition of their structures. Moreover, since redox systems based on POMs are electrochemically fast; thus the reduced POMs can participate in numerous electrocatalytic cycles. Based on the above considerations, it is possible to use reduced POMs as a catalyst or an assistant catalyst substrate in oxidation–reduction reactions. [23]

Reduced polyoxovanadates is a relatively recent development in polyoxometalates chemistry. While readily available V^V isopolyvanadates are mainly limited to have decavanadate structures, mixed valent species exhibit unique structures, such as cage-like spherical clusters. The spherical vanadate clusters have been observed with encapsulating negatively charged ions.[24]

1.4 Noble Metals in Polyoxometalates

Noble metals are interesting to discuss in POM field especially for the catalysis purpose. The noble metals related are ruthenium, rhodium, palladium, silver, osmium, iridium, platinum and gold. The combination of noble metal with POMs can be in the form of introduction a noble metal atom in a POM structure or the complete formation of different structures.

Polyoxoanions substituted by noble metal cations are interesting due to the rich and extensive multi-electron redox chemistry displayed by noble metal elements.[25] In the field of catalysis, noble-metal-substituted polyoxometalate catalysts showed high activity and selectivity in alkane and alkene epoxidations.[26]

1.5 Palladium POM complexes

Palladium is a noble metal that is difficult to oxidize because of a combination of high sublimation energy and high ionization potential. The coordination chemistry of palladium is mostly related with their oxidation states. The most common oxidation state of Pd is 0 and +2. Oxidation states of +1 and +4 are also found and the rarest one is +3. The Pd(0) complexes cover compounds with many possible ligands (L) e.g. in [PdL_2], [PdL_3], and [PdL_4] stoichiometries. All Pd(I) compounds have feature Pd-Pd or Pd-M bonds. Some tridentate macrocyclic ligands containing S and N as donors can stabilize mononuclear complexes of Pd(III). Pd(IV) is common oxidation state. Complexes with many different ligands, which have octahedral coordination are also identified.[27]

Pd(II) compounds are frequently four-coordinated square planar. Square-planar Pd(II) fragments are building blocks in the construction of extended structures. There is no report of three-coordinated Pd(II) compounds. Coordination to *cis*-PdL_2 fragments can be used to express corners, while *trans*-PdL_2 moieties can help build linear edges[27]. Some interesting features of palladium (II) chemistry are (1) formation of square-planar complexes and (2) bonding properties intermediate between the first transition series and the heavy metals[28].

Palladium (II) is a class b or a soft metallic center. Therefore, it forms various stable complexes with soft ligands. A vast palladium (II) coordination chemistry is found for S-, N-, P-, and As-donor ligands. Complexes containing O–donor ligands are less abundant and monodentate ligands of this type readily undergo substitution reactions by other ligands[29].

The strong motivation on research on Palladium-POM is because Pd has attractive catalytic properties beside its relatively high abundance in the Earth's crust. Some

palladium- substituted polyoxometalates have been synthesized. Most palladium (II) ions in these structures are generally coordinated in a square planar geometry to oxygen atoms of lacunary Keggin, or Dawson POMs. Among few examples are reports on sandwich-type polyoxotungstates substituted by Pd.

1.6 POMOFs

Metal organic frameworks (MOFs) are complexes containing of metal ions or clusters coordinating to organic ligands (linker) to form framework structures (figure 9). MOFs are a subclass of coordination polymers that is particularly porous. However, the organic linkers can decompose by oxidation or high temperature. Obtaining inorganic linker can overcome the problem, and POMs is potential linker for MOF chemistry.

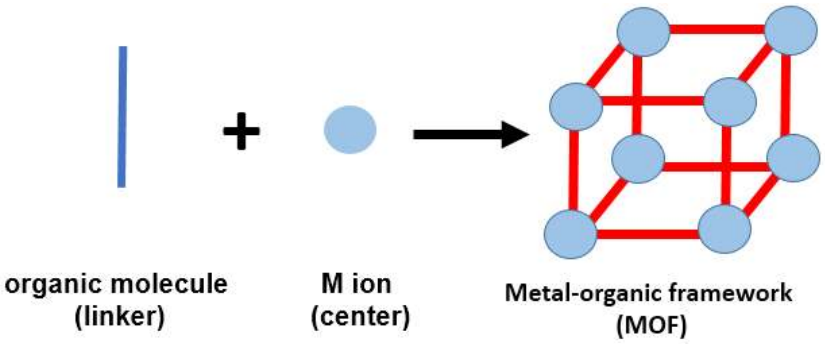

Figure 9 Schematic view of MOF formation

Recently, new class of POM-based Metal Organic Frameworks, so-called POMOFs has developed. The schematic connection among metal ion, ligand and POMs in POMOF is presented in figure 10. [30]

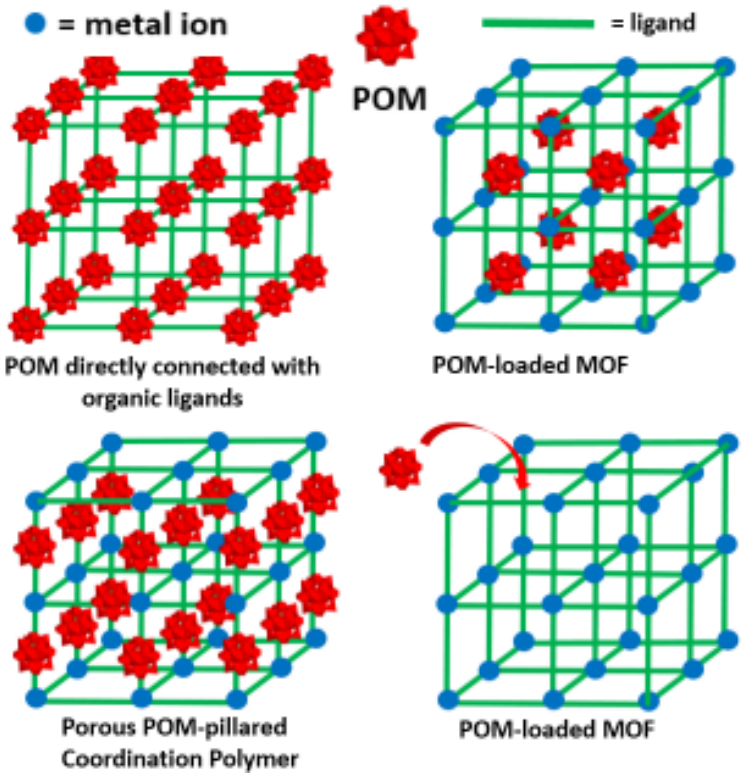

Figure 10 Schematic POM based MOF materials [30]

The POM clusters can be bridged into chain and networks by inclusion of secondary transition metals, rare-earth metals, and main group metals[31] [32]. POMs can be regarded as inorganic multi-dentate ligands that can bind to secondary transition metals. Small metal-oxide clusters have well-defined binding sites, known oxidation states and definite solubility preferences. So in POMOF chemistry, the way one can assemble the connection of POMs to one another are by using bridging organic linkers [33] or by ligand-supported transition-metal bridges.[34]

The design of coordination polymers based on polyoxometalates (POMOFs), how to introduce a linker unit on the polyoxometalate frameworks, is essential. Even if the coordination ability of polyoxometalates are commonly small due to the relatively small surface electron density, the introduction of the metal binding sites with available coordination sites are suitable for inorganic functional nanoscale structures.[35]

1.7 Aims and Overview of the Research

Most of POMs materials are molecular under standard conditions of pressure and temperature. There are only a few examples of 1-D POMs reported at standard condition. The problem of the formation of POM based frameworks structure is related with the POMs' weak ligand properties that have weak coordination ability of the POMs. Even if POMs have high negative charges, they actually have only weak coordination ability. This problem is due to the delocalization of surface charge along the POMs clusters.

This means that the construction of POMOFs basically is not easy. This can be seen from very few publications reported for this topics. For example, SciFinder produced by Chemical Abstracts Service (CAS) that has the most comprehensive database for the chemical literature, journal articles and patent records, chemical substances and reactions only listed 38 references containing "POMOF" entry or 36 references containing "POM and MOF" entry until the writing of this thesis.

So, the aim of this project is to overcome the weak ligand POMs in the objective of constructing POM based frameworks (POMOFs) materials. This aim is approached by functionalization of POMs with introduction of transition metal on the surface of POMs. The transition metals should be a well-known linker metal in MOF chemistry and should have definite coordination geometry. Pd^{2+} fulfill this criterion as it is the known superior linker metal in MOF chemistry and supramolecular chemistry. The synthesized materials would be the first Pd-POM linker which can become a building block of POM based MOFs materials via coordinative-Pd bridge.

Overview of the research

For the ease of discussion of this dissertation, we describe the overview of the synthetic scheme of this research with the three important complexes synthesized (figure

11). In the next chapters 3, 4 and 5, we will discuss the three complexes, compound **(1),** compound **(2),** and compound **(3)** subsequently in detail.

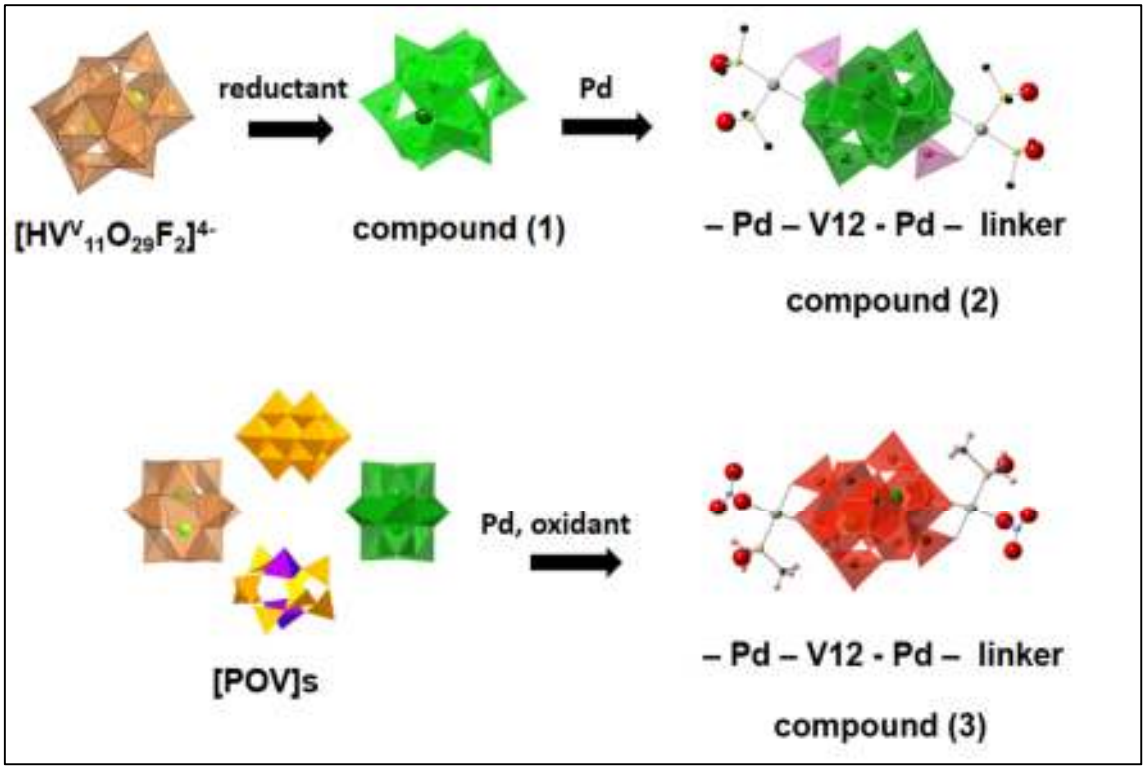

Figure 11 Research overview where a reduced inorganic linker (comp 2) is synthesised from the precursor (comp 1) and fully oxidized inorganic linker (comp 3) is prepared with addition of oxidant

The synthesis of the three complexes is to create new inorganic ligands for supramolecular or Metal Organic Frameworks. Since POM itself is generally weak coordinator, we started from special kind of POV where Fluoride is incorporated at the center of the POV so that it can enhance the coordination ability of POV (compound **1**).

Then Pd is put at both end of compound **(1)** to provide actual linker site (compound **2)**. Compound **(2)** is still in reduced state so that it is air sensitive against oxidation. Therefore, we need a really stable complex which is the oxidized one. This the final product is air stable with two linkers (compound **3**).

CHAPTER 2 EXPERIMENTAL METHOD

2.1 Synthetic Procedure

The synthesis of inorganic solids can be performed by a variety of methods. Some noted methods are the ceramic method, combustion method, precursor method, topochemical routes, intercalation compounds, ion-exchange method, sol-gel process, alkali-flux method, electrochemical methods, high pressure methods, etc.[36] Chemical methods of material synthesis play an important role in designing new materials and in providing better practical methods for preparing the already known materials.

The synthesis is expected to give solids products. When the solids are formed, the next step is the characterization of the material to determine the structure, and to reveal the chemical and physical properties of these materials. For this purpose, the solid should be single crystalline form. Special attention must be taken to make sure the formation of single crystal growth which is vital for structural characterization. The most widely used characterization method of structures for crystalline solids is Single Crystal X-ray Diffraction (SXRD). After revealing the arrangement of atoms and overall structure of the solids, predictions about the characterization of potential properties can be made based on structural analysis.

2.2 Characterization techniques

The need for the synthesis of new materials is driven mainly by the potential properties that can be exploited. Knowing the arrangement atoms and or molecules in three-dimensional space (3D) is one of the most important steps in allowing ones to understand the chemical principles and processes responsible for material properties (e.g. conductivity, energy storage, etc.). Understanding of material structures in terms of bonding and oxidation states, for example, allows researchers to discover material properties.

In this dissertation, we routinely focus on the characterization of newly discovered crystalline solid using Single Crystal XRD. In addition to the structural characterization, the compounds are also characterized by other appropriate characterization techniques. These characterization methods include UV-vis spectroscopy, IR spectroscopy, CHN, S and F elemental analysis, and thermal analysis (TGA).

2.3.1 Single Crystal X-ray Diffraction (SXRD)

The atoms and molecules can be arranged in a non-periodic array to form amorphous or periodic array to form crystalline materials. Crystalline solids are most generally characterized using both single crystal and powder X-ray diffraction techniques. SXRD method can determine the atomic positions, crystal structures, and the overall composition of a crystalline solid. Since the atomic arrangement determines the material properties, it is essential to know the structure before further doing the property characterization.

Before performing SXRD measurement, one must have a bit large (0.1 - 0.3 mm in each dimension) single crystal (not only the crystalline) material in question. The crystal lattice in a single crystal is continuous and unbroken to the edges of the crystal without any grain boundaries. It is different from polycrystalline (crystallite) that has random orientation or an amorphous structure that has atomic positions limited to short range order only. The crystal should also not be twinning which can be problematic in X-ray crystallography, because a twinned crystal produce complicated a simple diffraction pattern. The twinning itself is caused by the symmetrical intergrowths of crystals.

Once the single crystals were obtained from reaction solution, the crystals were quickly placed in mineral oil. This is to prevent the decomposition in air if the crystal is

moisture sensitive. The glue also functions as a protective film to prevent the possibility of single crystal decomposition in air. The crystal was then mounted on diffractometer.

X-ray crystallographic analysis measurement.

Single crystal structure analysis was performed at 90 K by using a Bruker D8 VENTURE diffractometer with graphite monochromated Cu Kα radiation (λ = 1.54178 Å). The data reduction and absorption correction were done using *APEX3* program.[37] The structural analyses were performed using *APEX3*, and *WinGX*[38] for Windows software. The structures were solved by SHELXS-2014[39] (direct methods) and refined by SHELXL-2014.[39] Non-hydrogen atoms were refined anisotropically. Hydrogen atoms are positioned geometrically and refined using a riding model.

2.3.2 IR Spectroscopy

Spectroscopy is a very important tools used to investigate the structure of materials through the interaction of electromagnetic radiation with matter. Infrared spectroscopy (IR) was used for the study the vibration between atoms when infrared radiation is absorbed. By measuring the vibrational characteristics occurring in the material, information about the composition of the materials can be obtained. The infrared region of the electromagnetic spectrum is found from 400 cm^{-1} to 4000 cm^{-1}.

From the study of the vibration frequencies of some synthesized POMs for years, it was found that the IR spectra of POMs result from stretching vibration frequency of the metal-oxygen. The characteristic absorption peak is 1100-400 cm^{-1}. The infrared spectrum also has information about the symmetry of polyoxoanion. The infrared spectrum, as an analytical means, can be used to differentiate heteropolyanion. In addition, different functional groups in POMs also absorb characteristic frequencies of IR radiation.

IR spectrum can be obtained from samples in the forms of liquid, solid, and gas. Pellets are used for the solid samples. The solid sample (0.5 to 1.0 mg) is finely ground and intimately mixed with approximately 100 mg of dry potassium bromide (KBr). The mixture is then pressed to be transparent disk at sufficiently high pressure. The introduction of the KBr pellet method has made possible the determination of infrared spectra of most insoluble materials.

IR spectra measurement:

FTIR were measured on Jasco FT/IR-4100 using KBr disks. The sample was mixed in with dry KBr salt. KBr was kept in a desiccator. The crystals along with KBr were ground in a mortar until the mixture is homogenous. Then, the ground mixtures were pressed into disk-like pellets using pellet press. The transparent pellets were attached to the sample holder for performing measurements. The samples, including the KBr blank, were measured in the wavenumber of 400 cm^{-1} to 4000 cm^{-1}.

2.3.3 Nuclear magnetic resonance (NMR) spectroscopy

NMR spectroscopy is used to determine the environments of specific atoms in a POMs either in solution or solid state. For identifying POMs such as the phosphotungstates and phosphomolybdates, ^{31}P NMR is utilized. ^{29}Si NMR is also used to study POMs that contain Si heteroatom. Polyoxovanadates and Polyoxotungstates can be characterized with the corresponding nuclei ^{51}V NMR and ^{183}W NMR respectively. Unluckily, there are some nuclei with quadrupole moments that cause line broadening and therefore makes characterization extremely difficult (tantalum and molybdenum for example).

Vanadium complexes of V^{V} (d^0), low-spin V^{III} (d^2), low spin V^{I} (d^4), low spin V^{-I} (d^6) and V^{-III} (d^8) are diamagnetic and vanadium NMR come to be observable. Among the transition metal nuclei, ^{51}V NMR have a relatively higher sensitivity because of its excellent NMR properties. Its receptivity is close to that of the proton, a consequence of the high natural abundance and the favorable magnetogyric ratio, the latter also accounting for its accessibility at a frequency close to that used for the detection of ^{13}C. The nuclear spin of the ^{51}V nucleus is $^{7}/_{2}$. Distinctive ^{51}V NMR signals can often be detected down to micromolar concentrations. Even minor variations in the electronic status at the vanadium nucleus are thus detectable through variations of the chemical shift.[17]

Nuclear magnetic resonance (NMR) spectroscopy measurement:

NMR spectra were performed with JEOL JNM-LA400. ^{1}H, ^{51}V and ^{19}F NMR spectra were measured at 399.78, 105.15, and 376.17 MHz, respectively. All spectra were obtained in the solvent indicated, at 25ºC unless otherwise noted. ^{19}F NMR spectra were referenced to neat CF_3COOH (δ = 0.00). ^{51}V NMR spectra were referenced using a sample of 10 mM $NaVO_3$ in 2.0 M NaOH (−541.2 ppm).

2.3.4 UV-Vis Spectroscopy

UV-Vis spectroscopy can be used to study the electronic changes in solids or liquid samples occurring upon the absorption of UV-Vis radiation. In transition metal compounds, electronic transitions occur upon the absorption of UV-Vis radiation. For example, ligand to metal charge transfer (LMCT) and *d-d* transitions occur in the UV-Vis region.

For vanadium complexes, electronic absorption spectra from the near-infrared (NIR) to the visible (Vis) and ultraviolet (UV) region may be caused by intra-metal d–d transitions (parity forbidden), metal-to-ligand charge transfer (MLCT), ligand-to-metal charge transfer (LMCT), intra ligand transitions and, in complexes containing more than one vanadium center with the vanadium centers in different oxidation states, inter-valence charge transfer (IVCT).[17]

The more intriguing information on the electronic situation of the metal comes from the *d–d* transitions. Extinction coefficients ε for the 'allowed' MLCT, LMCT and IVCT transitions generally are several thousand $lmol^{-1}cm^{-1}$, whereas the 'forbidden' d–d transitions are between 20–200 $lmol^{-1}cm^{-1}$.[17]

Vanadium(V) which does not contain d electrons, obviously is restricted to intra-ligand LMCT absorptions. Simple V^V compounds such as vanadate are colorless, because LMCT bands lie in the UV region. Decavanadate $[V^V_{10}O_{28}]$ are yellow, because the LMCT tails from the UV region into the violet range.

More complex vanadium(V) complexes can be very colorful when the LMCT shifts into the visible region. Examples are hydroxamate complexes, which can be used to for the colorimetric quantitative determination of vanadium(V), and other complexes with noninnocent ligands, such as catecholato–vanadium complexes with low-energy ligand-to-metal transitions.[17]

UV-Vis Absorption Spectra Measurement:

UV/Vis spectra were recorded using a JASCO V-570 spectrophotometer. The data of solid samples was collected in the absorbance mode between 300 nm and 800 nm or 1600 nm.

2.3.5 Thermal Analysis TG:

Thermal analysis of is used to study the new discovered compounds' thermal stability. When the compound is heated some temperature-dependent changes can occur. For instance, the decomposition of the compound to a more stable one is reached after certain temperature. Usually, the decomposition of the compound results in the loss of a gas species or solvent of crystallization.

In addition, we can study the phase changes and transformation by calculating the amount of heat absorbed or the heat released by the sample. For example, crystallization of solids results in the release of energy while melting requires energy input.

Thermogravimetric analysis is an essential laboratory tool used for material characterization. In thermogravimetric analysis the mass of a sample is monitored continuously as a function of temperature or time when the sample specimen is exposed to a controlled temperature in a controlled atmosphere.

TGA is used to determine the loss in mass at particular temperatures, so the information provided is quantitative. It is limited to decomposition and oxidation reactions and to such physical processes as vaporization, sublimation, and desorption. A sample purge gas controls the sample environment by flowing over the sample and exits through an exhaust. Nitrogen or argon is usually used to prevent oxidation of the sample.

TGA measurements

TGA measurements were done on ground powders (~10 mg). The heating profile for the measurement included a heating rate of 10 °C/min starting from room temperature to 300 °C, followed by a return cooling rate of 10 °C/min in the presence of nitrogen gas flow.

2.3.6 Cyclic voltammetry

Applications of cyclic voltammetry have been extended to almost every aspect of chemistry, including the examination of the ligand effect on the metal complex. Cyclic voltammetry is a method in which information about the analyte is obtained from measurement of the Faradaic current as a function of the applied potential.

Cyclic voltammetry is a very useful electrochemical technique in modern analytical chemistry for the characterization of the electroactive species. This method provides valuable information regarding the stability of the oxidation states and the electron transfer rate between the analyte and the electrode.

The current response over a range of potentials is measured. The measurement starts from an initial value, varies of the potential in a linear way until a limiting value, and to reverse the direction of the potential scan at this limiting potential, and finally the same potential range is scanned in the opposite direction. Consequently, the species formed by oxidation on the forward scan can be reduced on the reverse scan. This technique is accomplished with a three-electrode arrangement: the potential is applied to the working electrode with respect to a reference electrode while an auxiliary (or counter) electrode is used to complete the electrical circuit.

Reduction-oxidation (electronic) properties of POMs can be tested in solution by cyclic voltammetry. The cyclic voltammograms contain reversible or reversible waves that correspond to the oxidation and reduction of POM anions. So it is necessary to have POMs soluble in specific solvent of choice for cyclic voltammetry measurement.

Ferrocene/ bis-cyclopentadienyl iron(II) $Fe(C_5H_5)_2$ as standard

The ferrocene $Fe(C_5H_5)_2$ oxidation to the ferrocenium cation $Fe(C_2H_5)_2^+$ is a standard one-electron transfer reversible process for CV measurement because the rate of

electron transfer is incredibly fast.[40] The redox system $Fe(C_2H_5)_2^+/Fe(C_5H_5)_2$ has received considerable attention in electrochemistry because it can be used for instrumental and reference potential calibrations in organic media [4142]

Cyclic Voltammetry (CV) Measurement

An ALS/CH Instruments electrochemical analyzer (Model 600A) was used for voltammetric experiments. The working electrode was glassy carbon, the counter electrode was Pt wire, and the reference electrode was Ag/Ag^+. The voltage scan rate was set at 100 mV s^{-1}. The potentials in all voltammetric experiments were converted using data derived from the oxidation of Fc (Fc/Fc^+ Fc = ferrocene) as an external reference.

2.3.7 Elemental analyses

Elemental analyses of C, H, and N were done by the Research Institute for Instrumental Analysis, Kanazawa University. Elemental analysis of F was conducted at the Center for Organic Elemental Microanalysis Laboratory in Kyoto University.

2.4 Materials

The starting materials used in the synthesis of our new polyoxometalate in this dissertation are not sensitive to air and/or oxygen. For this reason, there is no need to use of a nitrogen-purged drybox (solvent-free glovebox). The reactants were weighed on an analytical microbalance with a precision of 0.1 mg. The chemicals and reagents were purchased from various commercial sources and were used without further purification unless otherwise stated. Table 1 reports all of the chemicals used in synthesis of compounds presented in this dissertation.

Table 1 Materials used

Compounds	Chemical Formula	Source
Hydrazine, Monohydrate	$NH_2NH_2.H_2O$	NACALAI
Hydrogen peroxide	H_2O_2	WAKO
Silver Nitrate	$AgNO_3$	WAKO
Tetrabutylammonium nitrate	$(CH_3CH_2CH_2CH_2)_4N(NO_3)$	WAKO
Tetrabutylammonium fluoride trihydrate	$(C_4H_9)_4NF(H_2O)_3$	Sigma Aldrich
Vanadium(V) Oxide	V_2O_5	NACALAI
Triethylamine	$C_6H_{15}N$	WAKO
Tetrabutylammonium Bromide	$C_{16}H_{36}BrN$	TCI
Palladium chloride	PdC_{l2}	HPC
1,5-Cyclooctadiene	C_8H_{12}	KCC
Silver tetrafluoroborate	$AgBF_4$	TCI
Et-OH	C_2H_5OH	WAKO
diethyl ether	$(C_2H_5)_2O$	WAKO
Nitromethane	CH_3NO_2	TCI
Acetone	$(CH_3)_2CO$	WAKO
Acetonitrile	CH_3CN	WAKO
Hydrochloric acid	HCl	WAKO

Some precursors were prepared according the literature procedures, $(n\text{-}Bu_4N)_4[HV_{11}O_{29}F_2]$, $\{n\text{-}Bu_4N\}_4[V_{10}O_{26}]$, $VOSO_4.3H_2O$, and $Pd(cod)Cl_2$.

2.4.2 Synthesis of starting materials

$\{n\text{-}Bu_4N\}_4[HV_{11}O_{29}F_2]$ from reported procedure.[43]

To a solution of 1 (379 mg, 0.20 mmol) and tetra-*n*-butylammonium fluoride (315 mg, 1.0 mmol) in dichloromethane (20 mL) was added *tert*-butyl hydroperoxide (60 mg, 0.5 mmol); the purple solution gradually turned intense red. The solution was dried with anhydrous magnesium sulfate and then concentrated to 10 mL by heating; chloroform (20 mL) was then added. Red crystals were obtained after 2 d. Yield: 200 mg (54% based on V).

$Pd(cod)Cl_2$ from reported procedure. [44]

First 200 mg (1.13 mmol) of palladium (II) chloride was dissolved in 0.50 mL conc. HCl by warming the mixture. The solution was cooled to ambient temperature, diluted with 17 mL ethanol, and then filtered. Under stirring, 0.30 mL (2.244 mmol) of 1,5 cyclooctadiene was added to the filtrate. The yellow product precipitated immediately. After 10 min storage, the precipitate was separated and washed three times with 3 mL of diethyl ether to yield 308 mg (1.08 mmol, 96%) of yellow solid;

{*n*-Bu_4N}$_4$[$V_{10}O_{26}$] from reported procedure[45].

Firstly, V_2O_5 (3.62 g, 20 mmol) was suspended in water 20 mL and this solution was heated at 60 °C. Triethylamine 4.04 g, 5.56 mL (40 mmol) was added dropwise into the solution. This solution was stirred for 20 min at 60 °C, then the suspended solution turned yellow clear solution. Acetone 100 mL was added to the solution, then the milky-white suspended solution was obtained. $VOSO_4$-xH_2O (2.17 g, 10 mmol) was dissolved in water 5 mL (solution B). After dissolution, the solution A was filtered out, solution B was added slowly to the filtrate, the yellow solution turned dark purple, and the dark purple was formed immediately. The solution was to be kept stirred for 10 min at room temperature. The dark purple solid was filtered, washed with H_2O, ethanol, and diethyl ether, and dried under vacuum and in a desiccator. Yield 7.77 g (82% based on V)

CHAPTER 3 SYNTHESIS OF FLUORIDE INCORPORATED DODECAVANADATE

{*n*-Bu_4N}$_4$[$V_{12}O_{30}(F)_2$]·CH_3CN

Abstract

In the objective of synthesizing metal inorganic polyoxovanadate (POV) linkers, a core structure for the linker is firstly synthesized. Because POM itself is generally weak coordinator, we started from special kind of POV where Fluoride is incorporated at the center of the POV cluster so that it can enhance the coordination ability of POV. It is a fluoride-incorporated polyoxovanadates {*n*-Bu_4N}$_4$[$V_{12}O_{30}(F)_2$]·CH_3CN **(1)** that play important role as core structure for the linker target.

Anion of **(1)** $[V_{12}O_{30}(F)_2]^{4-}$ a structural modification of its precursor $[HV_{11}O_{29}F_2]^{4-}$. $[V_{12}O_{30}(F)_2]^{4-}$ is a mixed valence V^{IV}/V^{V} state polyoxovanadate which has square pyramidal vanadium units. Crystallographic study of this complex shows that the polyoxoanion has two fluoride anions incorporated and four $\{n\text{-}Bu_4N\}^+$ counter cations. No hydrogen bond interactions were observed.

Graphical abstract

The environmental condition may vary that effect the fate of POMs. The acidic, basic, oxidizing, reducing, etc. environments are pertinent at which POMs may exist and may transform themselves to other products.

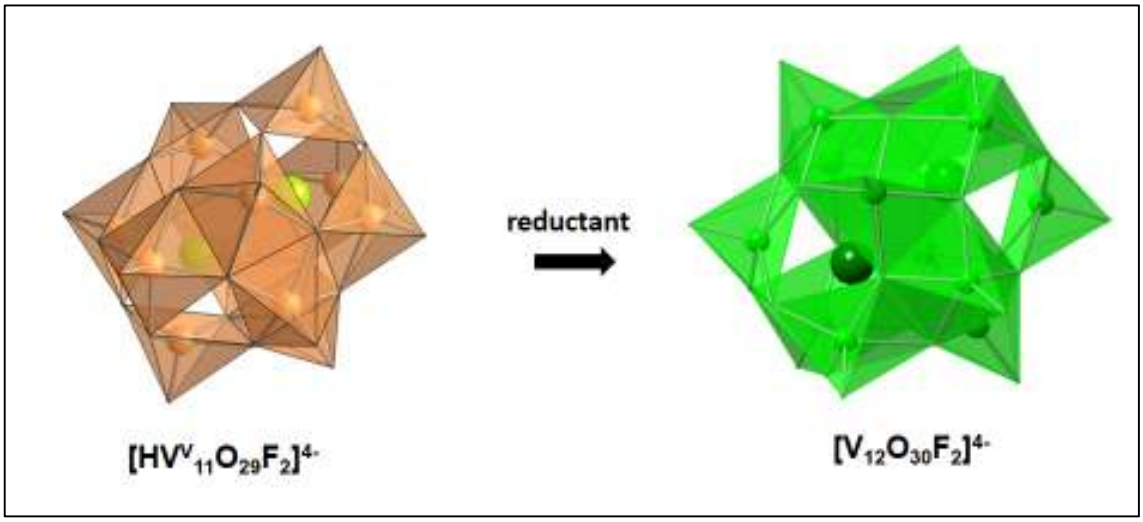

Figure 12 Synthetic scheme to product $\mathbf{[V_{12}O_{30}F_2]^{4-}}$

Reduction of $[HV^{V}_{11}O_{29}F_2]^{4-}$ has significant effect which not only reduces the vanadium atoms, but also modifies the structure giving rise to $[V^{IV}_2V^{V}_{10}O_{30}(F)_2]^{4-}$.

3.1 Introduction

Host–guest chemistry is common in supramolecular chemistry. It is about complexes composed of two or more molecules or ions held together by forces other than full covalent bonds. Polyoxovanadates are potential to be an inorganic host molecule which can exhibit potential application for molecular recognition, ion separation, or molecular switching.[46] POV anions which have shell-like clusters are molecular containers in which the guest molecule or ion is situated inside as the entrapped guest. Some cluster anions of dodecavanadates are of this types and reveal the host –guest systems against halides incorporated.

Relatively recent development in polyoxometalates chemistry is the synthesis of reduced POVs. If the V^V POVs are mainly limited to have decavanadate structures, then the mixed valent species have unique structures, such as cage-like spherical clusters. The spherical vanadate clusters have been observed with encapsulating negative charged ions[24].

3.1.1 Fluoride incorporated POV

Generally, coordination ability of polyoxovanadate is weak. So supporting transition elements to POV is difficult that the examples are very small. However, by changing electrostatic valence by putting two fluorides inside the cluster, then Fluoride incorporated POV would be able to coordinate with transition elements.

Halide incorporated POVs can be prepared by halide anions reaction with polyoxovanadates, for example the formation of $[HV_{11}O_{29}F_2]^{4-}$ and $[HV_{12}O_{32}(Cl)]^{4-}$. The advantage of incorporation of F^- into POMs are to decrease the surface charge, to make them small and in purpose of obtaining high electronegativity POMs[47,48]. These aspects in turn have promising properties. This advantages ignites the synthesis of fluoride

complexes of vanadium numerously, e.g. $[VOF_4]^-$, $[VOF_5]^{2-}$, $[VO_2F_2]^-$, $[VO_2F_3]^{2-}$, $[V_2O_4F_5]^{3-}$, $[V_2O_6F_2]^{4-}$, $[V_2O_2F_8(H_2O)]^{2-}$, $[V_3O_3F_{12}]^{3-}$ and etc.[48] Furthermore, the mixed valence fluorinated isopolyvanadates are still rare, where $[H_6V^V_2V^{IV}_{10}O_{30}F_2]^{6-}$ and $[V^{IV}_2V^V_{12}O_{36}F_4]8^-$ are among the few examples.

3.1.2 Related fluoro dodecavanadate compounds

Compound $Na_6(H_6V_{12}O_{30}F_2]\cdot 22H_2O$

Fluoro incorporated dodecavanadate was first synthesized by Müller et al [49] for the first time in 1993 and then the magnetic properties of the complex $Na_6(H_6V_{12}O_{30}F_2]\cdot 22H_2O$ was studied later.[50] $Na_6(H_6V_{12}O_{30}F_2]\cdot 22H_2O$ consists of two groups of three octahedra sharing edges as in a Keggin ion but with μ3-F centers, linked through six square pyramids. The repulsion or direct contact of the F^- ions in the center (F···F = 311 pm) apparently controls the structure. Complex $Na_6(H_6V_{12}O_{30}F_2]\cdot 22H_2O$ have six octahedral units and six square pyramids units, with mixed valent V^{IV}/V^V centers of cluster anions. The $Na_6[H_6V^{IV}_{10}V^V_2O_{30}F_2].22H_2O$ compounds was prepared from aqueous vanadate solutions in the presence of pentaerythritol[49].

Compound $Na_6[V^{IV}_{10}V^V_2O_{30}F_2\{(CH_2)_3CCH_2OH\}_2].22H_2O$

At the year 1998 he also claimed the synthesis of $Na_6[V^{IV}_{10}V^V_2O_{30}F_2\{(CH_2)_3CCH_2OH\}_2].22H_2O$, but a single-crystal X-ray structure analysis could not be executed at that time because of the inadequate quality of the crystals. However, from the comparison of the spectroscopic, analytical, and magnetochemical data, this complex is structurally closely related to compound $Na_6[H_6V^{IV}_{10}V^V_2O_{30}F_2].22H_2O$ previously prepared.

Compound $(NMe_4)_4[V_{12}O_{30}F_4(H_2O)_2]\cdot 9H_2O$

Lukáš Krivosudský on 2014 prepared $(NMe_4)_4[V_{12}O_{30}F_4(H_2O)_2]\cdot 9H_2O$. The anion $[V_{12}O_{30}F_4(H_2O)_2]^{4-}$ comprises two groups of three VO_5F units capped by one $VO_4F(H_2O)$ unit at the outer layers and four VO_5 units in the central layer. Strong O–H···F hydrogen bonds running in the *a* axis direction of the anion.

Our lab also has successfully synthesized $[HV^{V}_{11}O_{29}F_2]^{4-}$ prepared from $[V_{10}O_{26}]^{4-}$. The structure of $[HV^{V}_{11}O_{29}F_2]^{4-}$ that contains of five VO_5 and six VO_5F units with two μ3-F bridges.[51] The molecular structure of $[HV^{V}11O_{29}F_2]^{4-}$ consists of five VO_5 and six VO_5F units with two μ3-F bridges and can be derived from $[H_6V^{V}_2V^{IV}_{10}O_{30}F_2]^{6-}$ by removal of one VO unit.[48]

In this chapter we will discuss the modification of the precursor $[HV_{11}O_{29}F_2]^{4-}$ for the synthesis of other F incorporated POVs. In this study also, we investigated reduction of $[HV_{11}O_{29}F_2]^{4-}$ in nitromethane solvent which leads to a discovery of simple syntheses of $[V_{12}O_{30}(F)_2]^{4-}$. The successful isolation of the product allows the full characterization by X-ray crystallography, IR, UV/visible (UV/Vis), and cyclic voltammetry.

3.2 Experimental

In fact, many mixed valent and reduced vanadium-oxygen compounds were synthesized by reduction of vanadate(V) or oxidation of vanadate(IV)/vanadate(V).[49] The use of a conventional solution-based synthetic method accompanied by standing for crystallization at ambient pressure and temperature conditions have been used for the synthesis of compound **(1)**. The solution-based approach so far has resulted in the synthesis of a large number of POM compounds.

Synthesis of {n-Bu_4N}$_4$[$V_{12}O_{30}(F)_2$]·CH_3CN ***(1)***

(n-Bu_4N)$_4$[$HV_{11}O_{29}F_2$] (500 mg, 0.25 mmol) was dissolved in 5 cm^3 of nitromethane, and the addition of hydrazine-monohydrate (7.5 mg, 0.15 mmol) gave deep green solution after stirring for 1 h. The resulting mixture was precipitated by adding enough amount of ether and washed with acetone then diethyl ether. The deep green powder was dried under reduced pressure. Yield 400 mg. It was recrystallized in acetonitrile through ether diffusion method. Yield 68 % based on V. IR (KBr) 985, 877, 781, 734, 669, 624 cm^{-1}. Elemental Analysis calcd for C64H144F2N4O30V12 : C 36.62%, H 6.91%, N 2.67%, found : C 36.5%, H 6.83%, N 2.88%.

3.3 Characterization

3.3.1 Materials and Measurements.

The precursor for the synthesis of complex **(1)** is {n-Bu_4N}$_4$[$HV_{11}O_{29}F_2$] prepared according literature method.[43] Hydrazine-monohydrate and solvents were purchased from commercial sources and used as received unless otherwise is stated.

3.3.2 X-ray crystallographic analysis.

The crystallographic data can be seen in Table 1. The atomic coordinates, anisotropic thermal parameters, bond distances and angles and bond valence sums calculations can be seen in Tables the following tables.

Table 2 Crystallographic data for (1)

Crystal System	orthorhombic
Lattice Type	Primitive
Lattice Parameters	a = 22.2064(7) Å
	b = 23.6891(7) Å
	c = 17.3462(5) Å
	V = 9125.0(5) $Å^3$
Space Group	Pccn (#56)

Z value	4
D_{calc}	1.553 g/cm^3
No. Observations (All reflections)	8582
Residuals: R (I>2.00σ(I))	0.0431
Residuals: R (All reflections)	0.0000
Residuals: wR (All reflections)	0.1132
Goodness of Fit Indicator	1.024

Table 3 Atomic coordinates and Biso/Beq of (1)

atom	x	y	z	Beq
V1	0.43783(3)	0.56635(2)	0.38478(3)	1.199(10)
C3	0.0665(2)	0.5105(3)	0.6327(3)	4.74(13)
C5	0.0323(6)	0.5037(7)	0.5679(8)	4.3(4)
C4	0.0433(3)	0.4566(3)	0.6230(3)	2.24(13)
V2	0.45971(3)	0.54186(2)	0.66801(3)	1.258(10)
V3	0.46129(3)	0.62846(2)	0.53639(3)	1.209(10)
C1	0.1871(8)	0.6868(8)	0.9237(10)	8.8(4)
C2	0.2086(9)	0.7136(9)	0.8694(11)	9.0(4)
N3	0.25	0.75000	0.82930	9.027
V4	0.37054(3)	0.50724(2)	0.50345(3)	1.186(10)
V5	0.56731(3)	0.57483(2)	0.39930(3)	1.185(10)
V6	0.58057(2)	0.58403(2)	0.60345(3)	1.154(10)
F7	0.49996(8)	0.54346(7)	0.55226(10)	1.09(3)
O8	0.39643(10)	0.50093(9)	0.60553(12)	1.29(4)
O9	0.39985(10)	0.57983(9)	0.48461(13)	1.32(4)
O0A	0.50669(10)	0.53549(9)	0.33877(12)	1.27(4)
O0B	0.63945(11)	0.61214(9)	0.64073(13)	1.63(4)
O0C	0.53620(10)	0.64467(9)	0.57445(12)	1.25(4)
O0D	0.60743(10)	0.57168(9)	0.49577(12)	1.30(4)
O0E	0.39551(10)	0.49784(9)	0.39731(13)	1.29(4)
O0F	0.40294(11)	0.60251(9)	0.32109(13)	1.67(4)
O0G	0.49818(10)	0.61404(9)	0.43299(13)	1.28(4)
O0H	0.29894(11)	0.51106(10)	0.50410(13)	1.61(4)
O0I	0.43126(10)	0.60897(9)	0.62965(13)	1.37(4)
O0J	0.53412(10)	0.56965(9)	0.68864(12)	1.33(4)
O0K	0.43359(11)	0.69002(9)	0.52189(13)	1.60(4)
O0L	0.60439(10)	0.61596(10)	0.34380(13)	1.59(4)
O0M	0.42878(11)	0.53952(10)	0.75125(13)	1.74(4)

N0N	0.49306(15)	0.77757(12)	0.31079(17)	2.04(6)
N0O	0.22837(13)	0.48786(12)	0.71260(16)	1.65(5)
C0P	0.24730(16)	0.44042(14)	0.65864(19)	1.63(6)
C0Q	0.26152(16)	0.54026(14)	0.6856(2)	1.84(6)
C0R	0.45264(19)	0.73270(15)	0.2754(2)	2.26(6)
C0S	0.57624(18)	0.76818(15)	0.5080(2)	2.13(6)
C0T	0.51638(19)	0.75456(15)	0.3870(2)	2.01(6)
C0U	0.54597(19)	0.79120(15)	0.2576(2)	2.38(7)
C0V	0.16043(16)	0.49642(17)	0.7109(2)	2.32(7)
C0W	0.23778(18)	0.35132(16)	0.5340(2)	2.23(6)
C0X	0.58174(19)	0.73972(16)	0.2306(2)	2.51(7)
C0Y	0.21627(17)	0.38370(15)	0.6709(2)	2.01(6)
C0Z	0.31148(18)	0.46653(18)	0.8099(2)	2.53(7)
C10	0.24985(19)	0.59350(16)	0.7320(2)	2.41(6)
C11	0.24461(18)	0.33891(15)	0.6197(2)	2.01(6)
C12	0.4582(2)	0.83202(15)	0.3231(2)	2.53(7)
C13	0.24490(18)	0.47344(17)	0.7954(2)	2.18(6)
C14	0.5497(2)	0.79710(15)	0.4372(2)	2.33(7)
C15	0.62874(19)	0.72920(16)	0.4902(2)	2.52(7)
C16	0.3953(2)	0.6999(2)	0.1585(3)	3.32(9)
C17	0.4043(2)	0.82726(18)	0.3771(2)	3.03(8)
C19	0.6809(2)	0.70186(19)	0.1862(3)	3.48(9)
C1A	0.4236(2)	0.75019(19)	0.1996(3)	3.43(9)
C1B	0.1352(2)	0.5130(3)	0.6321(3)	3.96(10)
C1C	0.6467(2)	0.75239(19)	0.2159(3)	3.61(9)
C1D	0.2915(2)	0.64031(18)	0.7047(3)	3.55(9)
C1E	0.3822(3)	0.8851(2)	0.4016(3)	4.33(11)
C1G	0.3895(3)	0.4329(2)	0.9036(4)	5.76(16)
C18	0.3232(2)	0.44337(19)	0.8904(2)	3.45(9)
C1H	0.2848(2)	0.6570(2)	0.6221(3)	4.00(9)
C1I	0.4401(3)	0.6633(2)	0.1214(3)	5.13(13)
C1K	0.3248(3)	0.8830(3)	0.4489(3)	4.91(12)

Table 4 Anisotropic displacement parameters

atom	U_{11}	U_{22}	U_{33}	U_{12}	U_{13}	U_{23}
V2	0.0177(4)	0.0151(5)	0.0230(5)	0.0004(3)	0.0000(3)	-0.0018(3)
V3	0.0157(4)	0.0161(4)	0.0194(4)	-0.0005(3)	0.0000(3)	0.0027(3)
V4	0.0179(4)	0.0163(5)	0.0194(4)	-0.0008(3)	-0.0012(3)	0.0036(3)
V5	0.0171(4)	0.0162(4)	0.0191(5)	-0.0014(3)	-0.0009(3)	0.0004(3)
V6	0.0166(4)	0.0170(5)	0.0213(5)	0.0007(3)	0.0008(3)	0.0015(3)
V7	0.0198(5)	0.0193(5)	0.0194(5)	-0.0007(3)	0.0010(3)	-0.0021(4)

Table 5 Bond lengths (Å)

atom	**atom**	**distance**		**atom**	**atom**	**distance**

V1	V3	3.0582(7)		V1	V4	2.9036(8)
V1	V5	2.8933(9)		V1	O9	1.952(2)
V1	O0A	1.873(2)		V1	O0E	1.888(2)
V1	O0F	1.598(2)		V1	O0G	1.942(2)
C3	C5	1.366(15)		C3	C4	1.387(10)
C3	C1B	1.527(6)		C5	C4	1.489(17)
V2	V3	3.0696(7)		V2	V5[1]	3.0601(7)
V2	V6	3.0749(8)		V2	F7	2.1981(18)
V2	O8	2.022(2)		V2	O0A[1]	1.982(2)
V2	O0I	1.836(2)		V2	O0J	1.814(2)
V2	O0M	1.600(2)		V3	V6	3.0785(8)
V3	F7	2.2063(18)		V3	O9	1.999(2)
V3	O0C	1.830(2)		V3	O0G	2.001(2)
V3	O0I	1.810(2)		V3	O0K	1.603(2)
C1	C2	1.23(3)		C2	N3	1.44(2)
V4	V5[1]	2.9207(8)		V4	V6[1]	3.0483(7)
V4	O8	1.868(2)		V4	O9	1.867(2)
V4	O0D[1]	1.933(2)		V4	O0E	1.936(2)
V4	O0H	1.593(3)		V5	O8[1]	1.969(2)
V5	O0A	1.945(2)		V5	O0D	1.897(2)
V5	O0G	1.887(2)		V5	O0L	1.598(2)
V6	F7	2.2173(18)		V6	O0B	1.603(2)
V6	O0C	1.813(2)		V6	O0D	1.982(2)
V6	O0E[1]	2.011(2)		V6	O0J	1.834(2)
N0N	C0R	1.521(5)		N0N	C0T	1.521(5)
N0N	C0U	1.528(5)		N0N	C12	1.519(5)
N0O	C0P	1.522(4)		N0O	C0Q	1.517(4)
N0O	C0V	1.523(5)		N0O	C13	1.521(4)
C0P	C0Y	1.525(5)		C0Q	C10	1.518(5)
C0R	C1A	1.522(6)		C0S	C14	1.525(5)
C0S	C15	1.519(6)		C0T	C14	1.524(5)
C0U	C0X	1.529(5)		C0V	C1B	1.529(6)
C0W	C11	1.523(5)		C0X	C1C	1.495(6)
C0Y	C11	1.520(5)		C0Z	C13	1.509(6)
C0Z	C18	1.523(5)		C10	C1D	1.520(6)
C12	C17	1.524(6)		C16	C1A	1.524(7)
C16	C1I	1.468(7)		C17	C1E	1.516(7)
C19	C1C	1.508(6)		C1D	C1H	1.494(7)
C1E	C1K	1.517(9)		C1G	C18	1.510(8)

3.4 Result and Discussion

Compound **(1)** was synthesized using simple solution method. The use of the cluster compound $\{n\text{-}Bu_4N\}_4[HV_{11}O_{29}F_2]$ as starting material for modification to give compound **(1)** is straightforward.

3.4.1 Hydrazine monohydrate as reducing agent

Preparation of compound **(1)** made use of hydrazine as the reducing agent. Reaction of hydrazine with KVO_3 or V_2O_5 was already known to prepare most halide-encapsulating polyoxovanadates, e.g., $[V_{15}O_{36}X]^{6-}$ (X = Cl, Br), and $[H_XV_{18}O_{42}(X)]^{(13-x)-}$ (X =Cl, Br, and I) by thermal reactions in aqueous solutions[52].

Hydrazine compounds are also known to reduce fully oxidized POV, e.g. $[V_6O_{13}(tris)_2]^{2-}$ can be reduced with organohydrazines to give the reduced protonated derivatives $[V^{IV}_3V^{V}_3O_{10}(OH)^{3-}\ (tris)_2]^{2-}$, $[V^{IV}_4V^{V}_2O_9(OH)_4(tris)_2]^{2-}$ and $[V^{IV}_6O_7(OH)_6\text{-}(tris)_2]^{2-}$ [5352]. So, complex **(1)** was the other type of the use of hydrazine to prepare the F encapsulated POV reducing fully oxidized POV. The crystallization of compound **(1)** was succesfully done with good crystal quality (68% yield based on V).

3.4.2 Single Crystal X–ray Diffraction (SXRD) Analysis

Addition of hydrazine into the nitromethane solution of $\{n\text{-}Bu_4N\}_4[HV_{11}O_{29}F_2]$ gave complex $\{n\text{-}Bu_4N\}_4[V_{12}O_{30}(F)_2]\cdot CH_3CN$ crystallized in by acetonitrile-ether. The molecular structure was determined by X-ray crystallographic analysis (figure 11).

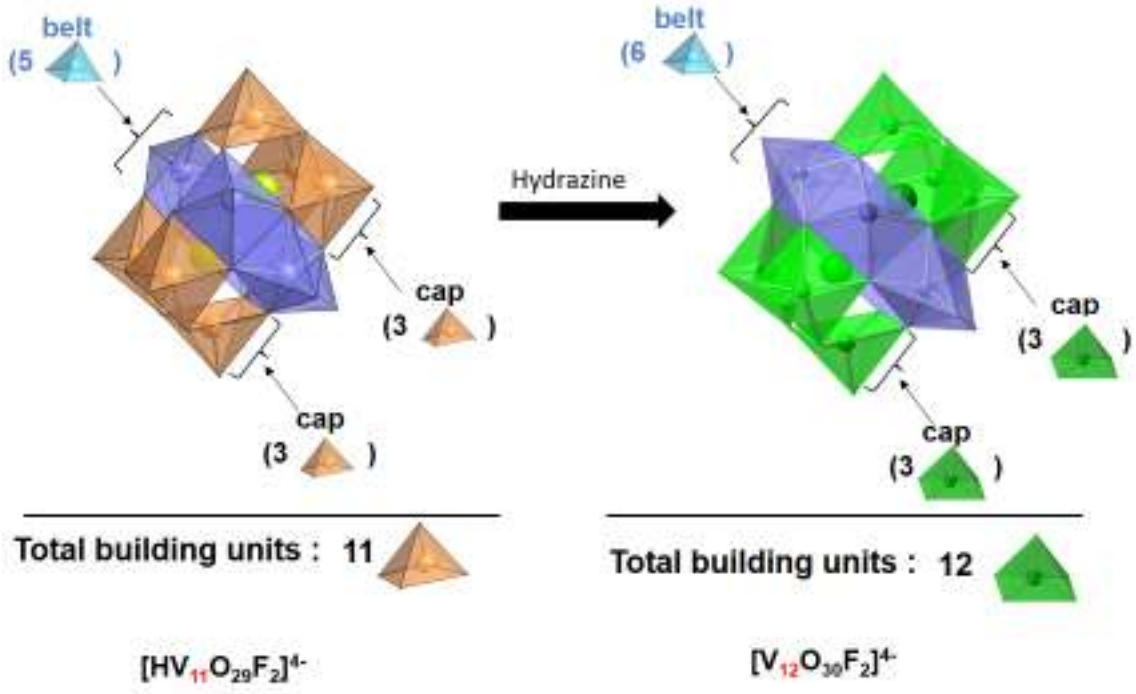

Figure 13 Structural comparison between precursor $[HV_{11}O_{29}F_2]^{4-}$ and product $[V_{12}O_{30}(F)_2]^{4-}$. The anion $[V_{12}O_{30}(F)_2]^{4-}$ is constructed of six belt VO_5 square pyramids (blue) and six capping VO_5 square pyramids (green). Four counter cations $\{n\text{-}Bu_4N\}^+$ and the solvated CH_3CN molecule are omitted for clarity.

The anionic $[V_{12}O_{30}(F)_2]^{4-}$ cluster anion consists of twelve VO_5 square pyramids with V−O bond lengths range from 1.8010(2) - 2.022(2), while the V-F range from 1.593(3) - 2.217(2). The V–O bond lengths decrease with the decreasing coordination number of the oxygen atom, with values for coordination: μ1-O = 1.593(3) - 1.603(2), μ2-O = 1.810(2) - 1.836(2) and μ3-O = 1. 867 – 2.011. The crystallographic data were summarized previously in table 2-5. The comparison of compound **(1)** anion with related POVs $[HV^{V}_{11}O_{29}F_2]^{4-}$ [54] and $[H_6V^{V}_2V^{IV}_{10}O_{30}F_2]^{6-}$ and is summarized in table 6.

Table 6 Selected average bond lengths (Å) for $[HV^{V}_{11}O_{29}F_2]^{4-}$ [54], $[H_6V_{12}O_{30}(F)_2]^{4-}$ [49] and anionic (1)

	$[HV_{11}O_{29}F_2]^{4-}$	$[H_6V_{12}O_{30}(F)_2]^{4-}$	$[V_{12}O_{30}(F)_2]^{4-}$
V=O	1.60	1.62	1.60
V_{bottom} –μ-O(-V_{bottom})	1.83		1.83
V_{bottom}-μ-O(-V_{middle})	1.99		2.00
V_{middle}-μ-O(-V_{bottom})	1.83		1.92
V···F	2.21	2.18	2.22
F···F	2.75	3.11	2.74

The μ3-F bridge is an interesting feature of all of these anions. Bond distance of V-F 2.18 Å can be said that F in the sphere just sit and floating in the sphere by having ionic interaction with spherical POV in the surrounding. As can be seen from the table 6, even if F^- ion is too small to be a guest in the cavity without covalent interaction with V, but it creates a strong V-F interaction. The V- μ3-F distances in $[V_{12}O_{30}F_4(H_2O)_2]^{4-}$ are V1–F1 2.20 Å similar also with that of compound **(1)** anion.[48]

In many cases, electronic influences can also play a role, for instance the occurrence VO_4 tetrahedra only in the case of V^V compounds [49], so this happen to anionic $[V_{12}O_{30}F_2]^{4-}$ which is a mixed valence V^{IV}/V^V then it is all VO_5 square pyramid. The existence of mixed valence will be described BVS calculation and proven by CV analysis later.

There are no "classical hydrogen bonds" between the $\{n\text{-}Bu_4N\}^+$ cations and the $[V_{12}O_{30}(F)_2]^{4-}$ anion in **(1),** however there are several CH···O short contacts in the range 2.591–2.714 Å between these units. These interactions involve both terminal and bridged oxo groups of $[V_{12}O_{30}(F)_2]^{4-}$ anions.

3.4.3 Bond Valence Sum (BVS) Calculation

The oxidation states of the Vanadium atoms in complex **(1)** are established by a combination of charge balance considerations, check of bond lengths, and bond valence sum (BVS)calculations.[55] BVS values for V atom in complex **(1)** are between 4.400 and 5.058, indicating that the respective valences are +4 and +5, respectively. The unclear /slight difference of whether which V atoms holding +4 suggest that there is delocalization of charge due to the spherical shape of anionic **(1)**.

Table 7 BVS calculation of compound (1)

V^{IV}	V^{V}		V1	V2	V3	V4	V5	V6
0	12	V^{IV}	4.479	4.807	4.818	4.606	4.4	4.8
		V^{V}	4.715	5.047	5.058	4.849	4.632	5.04

The mixed valence of V^{IV} / V^{V} is supported by CV analysis. From BVS calculation, complex **(1)** is mixed valence $[V^{V}_{10}V^{IV}_{2}O_{30}F_{2}]^{4-}$ where delocalization of charge happens due to spherical shape.

3.4.4 Cyclic Voltammetry (CV) analysis

The reversible reductive peaks in CV (figure 11) coupled with oxidative peaks appeared in the range. There are four reductive peaks at 0.39, 0.08, -0.67, and -1.27 V, and four oxidative peaks at -1.00, -0.50, 0.12, 0.53 V. The reductive peaks (V^{V} - V^{IV}) and oxidative peaks (V^{IV} - V^{V}) are redox pairs and reversible. The voltage at 0.08 V is the initial state of $V^{V}_{10}V^{IV}_{2}O_{30}F_{2}]^{4-}$

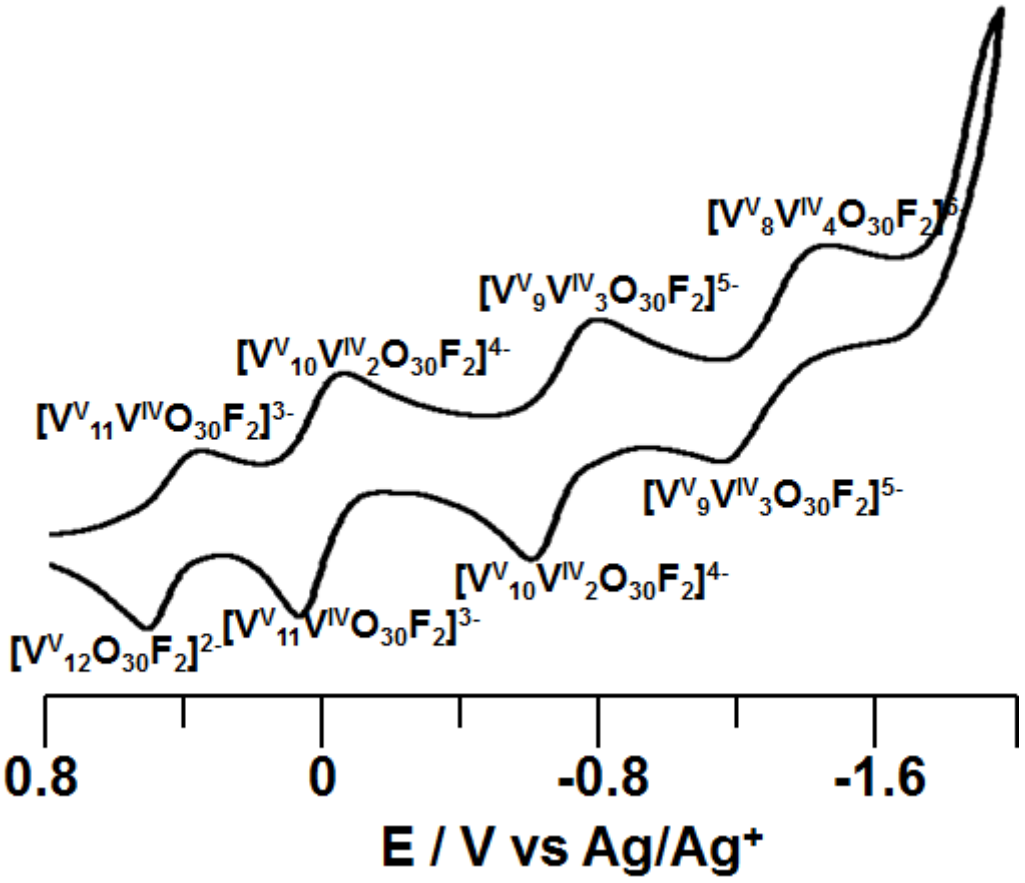

Figure 14 Cyclic voltammograms of (a) (n-$Bu_4N)_4[V_{12}O_{30}F_2]$ in acetonitrile solvent. (Scan rate was 0.05 V/s, the supporting electrolyte used was {n-Bu_4N}PF_6, solvent was acetonitrile, scan rate was 0.05 V/s, working electrodes was glassy carbon, and counter electrode was Pt)

Electrochemical behavior of **(1)** show that complex **(1)** can accept reversibly up to four electrons (Figure 14). The reduction process is reversible (reaction **1**) and the structure of the anion is basically unchanged .

$$[V^{V}{}_{12}O_{30}(F)_2]^{2-} + 4\ e^- \rightleftharpoons [V^{IV}{}_4V^{V}{}_8O_{30}(F)_2]^{6-} \qquad \textbf{(1)}$$

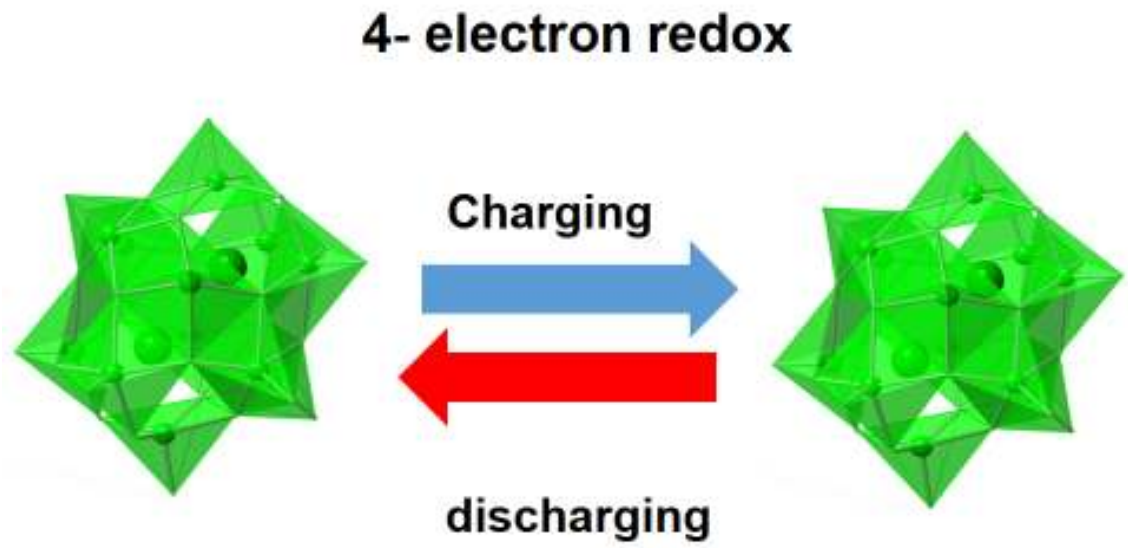

Figure 15 Four electron redox electron sponge system of anion (1)

This is a promising material for electron sponge for energy storage application, compared with single reversible electron transfer in currently used Li ion battery. This behavior of the ability in accepting and releasing specific number of electrons without any change or decomposition of the structures of compound **(1)** is attributed to reduced POMs, for the so-called heteropoly blue.[23]

3.4.5 UV-Vis Absorption Spectra

Figure 14 shows the UV-vis absorption spectra on solid samples of compound **(1)**. The UV−vis spectrum of the compound 1 showed absorption bands above 600 nm, suggesting that the vanadium species are mixed valence of reduced V^{IV} and the oxidized to V^{V}.

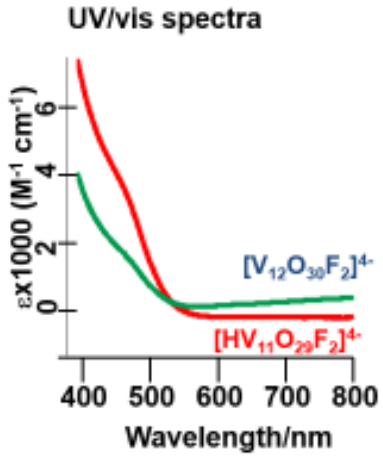

Figure 16 UV Vis spectra of complex (1) (blue) compared with precursor {n-Bu_4N}$_4$[$HV_{11}O_{29}F_2$] (red)

The intervalence charge-transfer (IVCT) bands is corresponding to electronic transfer between d^1 and d^0 Vanadium moieties. The overall charge of the cluster is -4, indicating that it is a mixed-valence system consisting of two V^{IV} and ten V^{V} centers.

3.4.6 The IR spectrum

The complex **(1)** exhibits characteristic absorption peaks of POV located in the range of 400 – 1000 cm^{-1}.

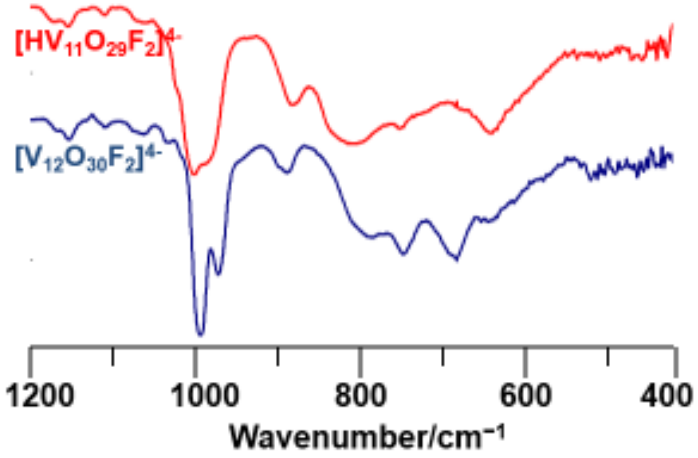

Figure 17 FTIR spectra of {*n*-Bu_4N}$_4$[$V_{12}O_{30}(F)_2$]·CH_3CN

The IR spectrum of **(1)** shows strong bands around 989 cm^{-1}, which correspond to the $\nu(V{=}O_{terminal})$ stretching frequencies (Figure 5). Stretching of the $V–O_{bridge}$ bond appears in the range 500–900 cm^{-1}. Complex **(1)** also has μ_2-O bridges and exhibits distinct peaks in the 750–900 cm–1 region. The relatively weak spectrum in the range of 750 – 900 cm^{-1} is due to the lack of μ_2-O bridges (5 bridges) compared with μ_3-O bridges (13 units) [51].

3.4.7 Thermogravimetric (TG) Analysis

The thermal stability of compounds **1** were investigated on powder samples in an air atmosphere in the temperature range 30-300 ºC.

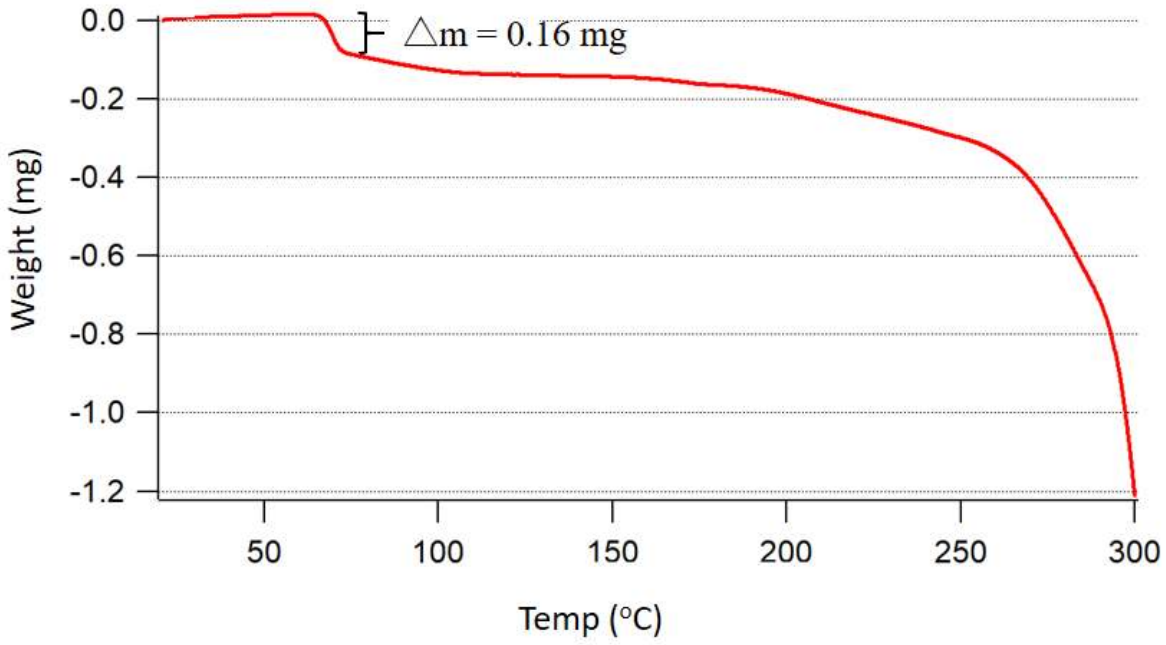

Figure 18 TG of crystalline complex [1]

The TGA data shows that the title compound is thermally stable up to about 65 °C and has weight loss 0.16 mg corresponding to about 1.6% weight loss attributed to evaporation and loss of solvent of crystallization acetonitrile. The weight loss of temperature range 250 - 300°C corresponds to the decomposition of the POV.

TG analysis coupled with elemental analysis suggest the acetonitrile was part of the solvated solvent in the structure of compound **(1)**. So, the formula is best written as $(n\text{-}Bu_4N)_4[V_{12}O_{30}F_2].(CH_3CN)$

3.5 Conclusions

As fluorine incorporation in POV is very important to enhance POV coordination ability with transition metal, we achieved a new fluorine incorporated dodecavanadate. This complex can later be used coordinate with Pd ion to form the actual linker. Here, F^- inclusion dodecavanadate clusters is presented and characterized.

Reduction of $[HV_{11}O_{29}F_2]^{4-}$ to give $[V_{12}O_{30}(F)_2]^{4-}$ means that addition of electron that change the electrostatic balance makes structural change of the dodecavanadate. Beside the use of precursor for polyoxometalates framework which will be described in chapter 4, compound **(1)** is good catalyst and potential energy storage material with high capacity.

CHAPTER 4 SYNTHESIS OF A REDUCED PALLADIUM SUPPORTED FLUORIDE INCORPORATED DODECAVANADATE $[VO(DMSO)_5]_2[\{Pd(DMSO)_2\}_2V_{12}O_{32}(F)_2].2CH_3CN$

Abstract

This chapter describe the construction for the first time of a new POM based inorganic linker unit. The linker is in a reduced form synthesized from the reduced POV precursor (compound **1**). To provide a bidentate coordination site of the linker unit, Pd^{2+} was chosen to react with anion **1** while the remaining two coordination sites of Palladium ion are occupied by leaving group ligands. The synthesized complex is $[VO(DMSO)_5]_2[\{Pd(DMSO)_2\}_2V_{12}O_{32}(F)_2].2CH_3CN$ (compound **2**).

The synthesis by using reaction of Pd^{2+} ion wit precursor synthesized before $\{n\text{-}Bu_4N\}_4[V_{12}O_{30}(F)_2]\cdot CH_3CN$ was performed by solution-based synthetic method and crystallization process was in ambient pressure and temperature. The POM starting materials are dissolved in the DMSO solvent by which the reaction with Pd^{2+} solution results in the reformation of metal oxide fragments to form a discrete mixed valence Pd-V_{12} anionic clusters.

This chapter will discuss the synthesis and characterization of the two electron reduced Pd- supported dodecavanadate compound featuring spherical Fluoride incorporated cluster isolated for the first time. The dodecavanadate component consisted of ten VO_5 units and two VO_4 units in the framework with two fluorides inside and each VO_4 unit was coordinated to Pd^{2+}.

This chapter will also describe some synthetic parameters by which the title compound can be obtained. Furthermore, discussion of structure will also be presented. Lastly, potential application will be discussed based on the structure.

Graphical Abstract

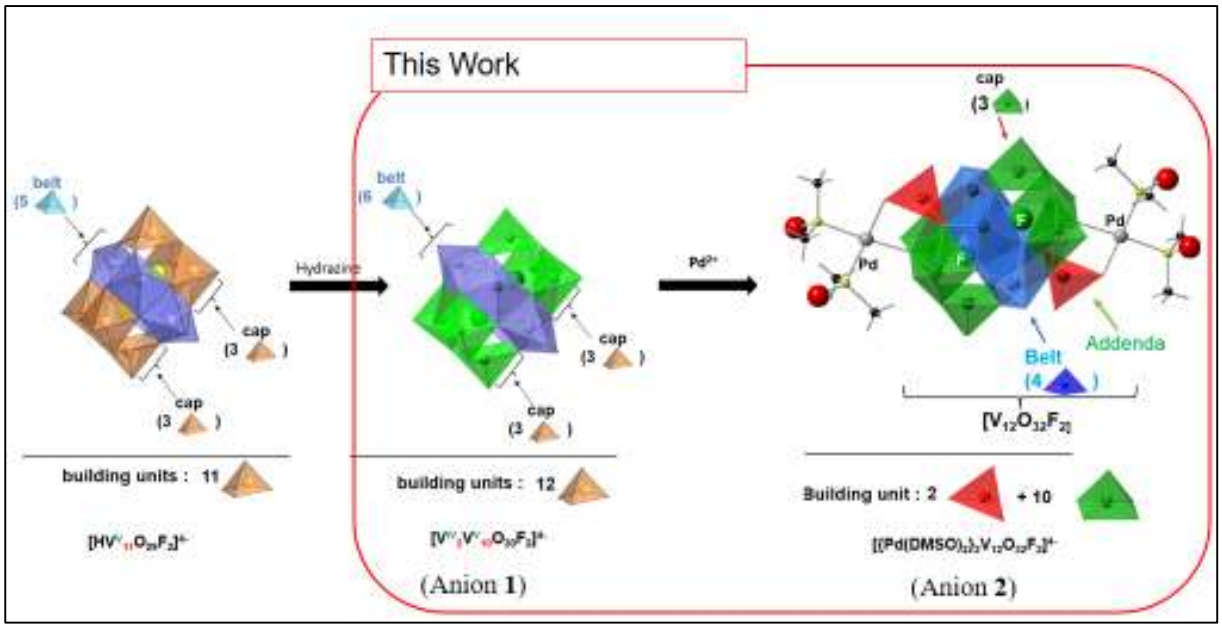

Figure 19 Synthetic Scheme to product $[\{Pd(DMSO)_2\}_2V_{12}O_{32}(F)_2]^{4-}$

4.1 Introduction

The negatively charged polyoxometalate can serve as an inorganic ligand that is able to form a metal complex through the coordination of the oxido groups. However, the coordination ability is very weak that only few examples of metal coordinated POV found so far. Successful incorporation of two fluorides anion inside the dodecavanadate cluster (compound **1)** before would overcome this problem. This would open up the possibility for its coordination with transition metal, especially specified transition metal with definite coordination mode for making a inorganic linker for framework structure.

Among the few examples, our lab has studied the coordination chemistry of polyoxometavanadate species against Cu^{2+}, Ni^{2+}, and Pd^{2+} cations. In Cu^{2+} and Pd^{2+} complexes, the heteropolyoxovanadate complexes incorporated the metal cations without the coordination of hydroxide or water ligands.[56]

Furthermore, our group has succeeded in the synthesis of tetravanadate-supported organopalladium complex $[\{(\eta^3\text{-}C_4H_7)Pd\}_2V_4O_{12}]^{2-}$ which was obtained by reaction of $[Pd(\eta^3\text{-}C_4H_7)Cl]_2$ with $(n\text{-}Bu_4N)VO_3$ in acetonitrile. The two (η3-C4H7)Pd groups on both side of the tetra- vanadate ring supported the cyclic tetravanadate structure with an inversion center on the center of the molecule[57].

However, the Pd supported POV complex above is limited only on a blocked Pd coordination sites complex, so that there is no possible free site of Pd which is available to coordinate with others. All the coordination sites of Pd are occupied, so that it is not available for supramolecular or other complexes formation.

Our research now has unique in creating Pd supported POV that is able to provide two free sites of Pd for coordination. It is a good point of the complex **2** and complex **3** we synthesize, because the ligand DMSO or Nitrate is easy to remove from Pd resulting in a free coordination site of Pd to coordinate with others.

DMSO has sulfur center which is nucleophilic toward soft electrophiles and the oxygen that is nucleophilic toward hard electrophiles. The coordination sites of DMSO can be O or S atom or both, for example in the complex $(RuCl_2(DMSO)_4)$, three DMSO ligands are bonded to ruthenium through sulfur, while the fourth DMSO is bonded through oxygen.[58]

Diao et.al has studied DMSO coordination to Palladium(II) in solution and solid state on complex Pd-(DMSO)2(TFA)2 (TFA = trifluoroacetate). He found that coordination of DMSO to palladium(II) in both the solid state and in solution. has one O-bound and one S-bound DMSO ligand (figure 19)[59].

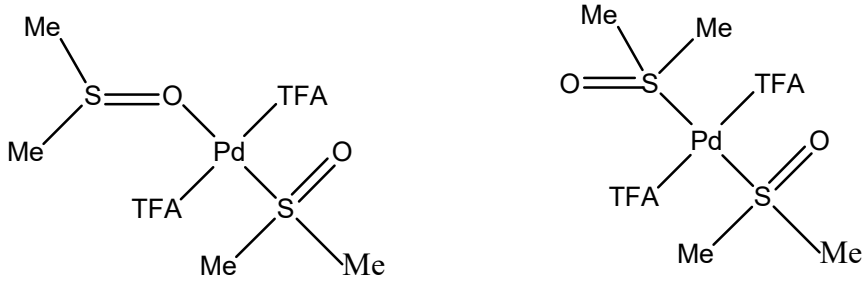

Figure 20 DMSO coordination to Pd(TFA)2 with O or S coordination of the DMSO are possible.

In general, the anion of POVs sits in the sphere, for example NO_3^- and Br^-. This is not the case for F^- where two anion F- sit inside the sphere to stabilize the structure of the sphere. Polyoxovanadates with both VO_5 and VO_4 units have the potential to stabilize both anions and metal cations. The Pd^{2+} units are exploited without conventional organic ligands to provide a linker site in POMOF chemistry and also this material is potential in the field of catalysis.

4.2 Experimental

4.2.1 Hypothetic polymeric structure of $\{n\text{-}Bu_4N\}_2Pd\{V_{12}O_{32}(F)_2\}]_n$ and serendipitous formation of compound (2).

Mixture of $Pd(cod)Cl_2$ (75 mg, 0.26 mmol) and $AgBF_4$ (105 mg, 0.53 mmol) in 10 mL of acetonitrile was stirred for 2 hours and the resulting white precipitates of AgCl was removed by filtration. The filtered yellow solution was added to 10 mL of $\{n\text{-}Bu_4N\}_4[V_{12}O_{30}(F)_2]\cdot CH_3CN$ (250 mg, 0.12 mmol), and stirred to give deep green precipitate 200 mg.

This reaction was targeting a composition to potentially an a polymeric structure of hypothetic $\{n\text{-}Bu_4N\}_2Pd\{V_{12}O_{32}(F)_2\}]_n$.

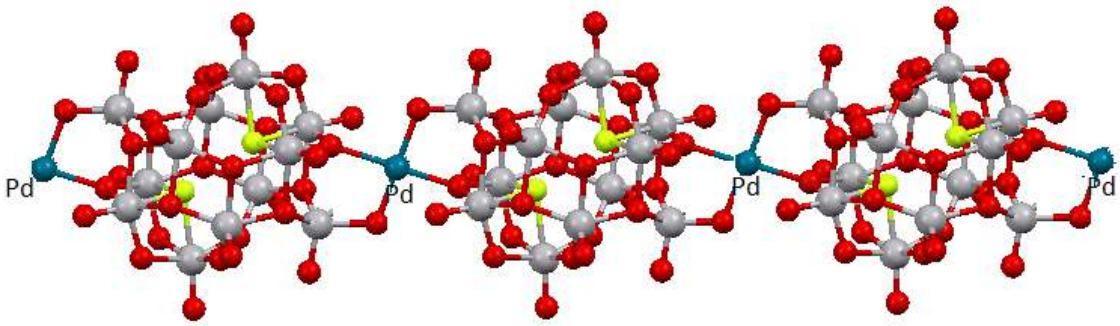

Figure 21 ***Imaginary view of 1-D V_{12} chain bridged by Pd^{2+}***

The reaction equation expected is as follows;

$Pd(cod)Cl_2 + 2AgBF_4 \rightarrow Pd(BF_4)_2 + 2AgCl + cod$

$Pd(BF_4)_2 + \{n\text{-}Bu_4N\}_4[V_{12}O_{30}(F)_2]\cdot CH_3CN \rightarrow [(n\text{-}Bu_4N)_2Pd\{V_{12}O_{32}(F)_2\}]_n + \{n\text{-}Bu_4N\}BF_4$

Unfortunately, the crystallizations did not succeed to prove the structure. Some crystallization method effort e.g. varying concentration, slow reactant diffusion, changing solvents was not successful so that structure determination by single crystal X-Ray could not be performed to prove to this 1-D polymeric structure. However this product can be used to form compound **(2)** in the following procedure.

4.2.2 Synthesis of [VO(DMSO)5]2[{Pd(DMSO)2}2V12O32(F)2] from hypothetic polymeric $[(n\text{-}Bu_4N)_2Pd\{V_{12}O_{32}(F)_2\}]_n$

Previous experiments by our group led to the formation of complex $[VO(DMSO)_5]_2[\{Pd(DMSO)_2\}_2V_{12}O_{32}(F)_2]$ with serendipity. Powder sample of hypothetic $[(n\text{-}Bu_4N)_2Pd\{V_{12}O_{32}(F)_2\}]_n$ (50 mg) was dissolved in 1.5 mL DMSO. Slow diffusion of 0.5 mL acetone into the solution gave crystal of $[VO(DMSO)_5]_2[\{Pd(DMSO)_2\}_2V_{12}O_{32}(F)_2]$. However, this method was not reproducible even using other methods, e.g. using air sensitive solvents and performing reaction in nitrogen-purged glovebox.

The synthesis of products $[VO(DMSO)_5]_2[\{Pd(DMSO)_2\}_2V_{12}O_{32}(F)_2]$ was expected from the breaking of hypothetic polymeric $[(n\text{-}Bu_4N)_2Pd\{V_{12}O_{32}(F)_2\}]_n$ so that we would have $\{Pd(DMSO)_2\}_2V_{12}O_{32}(F)_2]$ anion and $\{n\text{-}Bu_4N\}^+$ cations. In fact $[n\text{-}Bu_4N]^+$ cation was not obtained in the crystal structure, but $VO(DMSO)_5]^{2+}$ instead.

The complex [{Pd(DMSO)$_2$}$_2$V$_{12}$O$_{32}$(F)$_2$] which ever obtained serendipitously with this method, contained discrete anion [{Pd(DMSO)$_2$}$_2$V$_{12}$O$_{32}$(F)$_2$]$^{4-}$ accompanied with two counter cations [VO(DMSO)$_5$]$^{2+}$. The following will discuss the modified synthetic procedure to yield compound [VO(DMSO)$_5$]$_2$[{Pd(DMSO)$_2$}$_2$V$_{12}$O$_{32}$(F)$_2$].

4.2.3 Fair Yield Synthesis of [VO(DMSO)$_5$]$_2$[{Pd(DMSO)$_2$}$_2$V$_{12}$O$_{32}$(F)$_2$]

Mixture of Pd(cod)Cl$_2$ (20.5 mg, 0.07mmol) and AgBF$_4$ (28 mg, 0.14 mmol) in 2.5 mL Acetnitrile was stirred for 2 hours and the resulting white precipitates of AgCl was removed by filtration. The filtered yelllow filtrate was added to the solution of (*n*-Bu$_4$N)$_4$[V$_{12}$O$_{30}$F$_2$] (77 mg, 0.04 mmol) which was previously added and stirred in small amount of hot DMSO (75 ^{o}C). After standing overnight, dark green crystal 63 mg was obtained. Yield 72% based of V. (cod = 1,5-cyclooctadiene). Elemental Analysis calcd for C18H54F2O42Pd2S9V13 : C 12.93%, H 3.25%, N 0%, F: 1.46%, S 17.21% found : C 13.14%, H 3.48%, N 0%, F 1.38% S 17.68%

Upon the investigation of the reaction procedures by comparing with DMSO crystallization of hypothetic polymeric [(*n*-Bu$_4$N)$_2$Pd{V$_{12}$O$_{32}$(F)$_2$}]$_n$ before, it can be noticed that the succesfull synthesis and crystallization of [VO(DMSO)$_5$]$_2$[{Pd(DMSO)$_2$}$_2$V$_{12}$O$_{32}$(F)$_2$] is proceeded by dissolution of [V$_{12}$O$_{30}$F$_2$] in DMSO first before the reaction with Pd^{2+}. To improve the reaction rate by heating was maintained below the decomposition temperature of DMSO (boiling temperature of 189 °C at normal pressure).

Standing in closed vial with solvent evaporation is sufficient to grow single crystals. The fair yield of the synthesis of [VO(DMSO)$_5$]$_2$[{Pd(DMSO)$_2$}$_2$V$_{12}$O$_{32}$(F)$_2$] using {*n*-Bu$_4$N}$_4$[V$_{12}$O$_{30}$(F)$_2$]·CH$_3$CN precursor and Pd^{2+} cation from the product of Pd(cod)Cl$_2$ and AgBF$_4$. Instead of cation {*n*-Bu$_4$N}$^+$ from the salt of the precursor {*n*-Bu$_4$N}$_4$[V$_{12}$O$_{30}$(F)$_2$]·CH$_3$CN, the cation [VO(DMSO)$_5$]$^{2+}$ is present. This unexpected cation is the side product of V$_{12}$ decomposition. The reaction was performed in open air which can imply that the product is not air sensitive.

4.2.4 Improved Synthesis Method

As the cation VO(DMSO)$_5^{2+}$ is derived from decomposition product of mother product **[V$_{12}$O$_{30}$F$_2$]$^{4-}$**, this decomposition lowers the yield. Some efforts to increase the yield had been done, e.g. the use of other counter cations, TBABF$_4$, PPh$_4$BF$_4$, TEABF$_4$ with negative results.

4.3 Characterization

The sample was characterized with SCXRD, FTIR, UV Vis, TG, Elemental Analysis performed on the crystals.

Single Crystal X–ray Diffraction (SXRD)

The crystallographic data can be seen in Table 8. The atomic coordinates, anisotropic thermal parameters, selected bond distances and angles and bond valence sums calculations can be seen in the following tables 9-11:

Table 8 Crystallographic data for $[VO(DMSO)_5]_2[\{Pd(DMSO)_2\}_2V_{12}O_{32}(F)_2]$

Crystal System	monoclinic
Lattice Type	Primitive
Lattice Parameters	a = 15.3402(4) Å
	b = 16.9053(4) Å
	c = 21.3642(5) Å
	β = 105.0720(10) º
	V = 5349.8(2) $Å^3$
Space Group	P21/c (#14)
Z value	4
D_{calc}	3.016 g/cm^3
No. Observations (All reflections)	10507
Residuals: R (I>2.00σ(I))	0.0874
Residuals: R (All reflections)	0.0000
Residuals: wR (All reflections)	0.2575
Goodness of Fit Indicator	0.959

Table 9 Atomic coordinates and Biso/Beq

atom	x	y	z	Beq
C0Z	0.5396(7)	0.1378(5)	0.4947(4)	1.90(14)
C1	0.6440(9)	0.3385(9)	0.7665(6)	4.5(3)
C12	0.3672(8)	0.1687(6)	0.7348(5)	7.3(5)
C12	1.2046(10)	0.2265(15)	0.8132(8)	7.3(6)
C13	0.4254(8)	0.3650(6)	0.8166(5)	2.76(16)
C15	0.3690(7)	0.0823(5)	0.4937(4)	2.37(16)
C17	0.8571(8)	0.3973(9)	0.6568(7)	4.7(3)
C19	0.3405(10)	0.3990(8)	0.8094(6)	4.0(2)
C1B	0.5124(10)	0.0797(7)	0.7269(5)	4.0(3)
C1H	1.0223(12)	0.4559(12)	0.7265(11)	7.1(5)
C33	1.1195(9)	0.1538(9)	0.7930(6)	4.4(3)
C6	0.7669(19)	0.1125(14)	0.6502(17)	13.3(8)
F1	0.4956(2)	0.5866(2)	0.50619(17)	0.54(7)
N1E	0.2714(11)	0.4263(10)	0.8018(8)	7.1(4)
O1	0.4801(3)	0.2897(3)	0.5508(2)	0.81(8)
O10	0.5401(3)	0.5674(3)	0.6365(2)	0.83(8)
O11	0.4218(4)	0.6887(3)	0.6436(2)	1.34(9)
O111	0.5166(5)	0.0342(3)	0.5812(3)	2.33(14)
O12	0.3574(3)	0.5612(3)	0.5607(2)	1.00(8)
O13	0.2068(3)	0.4936(3)	0.4915(3)	1.41(11)
O14	0.3614(3)	0.4032(3)	0.5482(2)	0.88(8)
O15	0.4112(4)	0.4509(3)	0.6755(2)	1.16(9)
O16	0.4276(4)	0.2986(3)	0.6631(2)	1.11(9)
O17	0.9740(19)	0.4835(17)	0.5496(14)	16.0(9)
O18	1.1056(5)	0.3067(5)	0.6012(4)	3.77(18)
O19	0.9065(12)	0.1440(11)	0.8451(15)	22.6(11)
O1G	0.9753(11)	0.2921(17)	0.8966(10)	15.2(10)
O2	0.6176(3)	0.3035(3)	0.4906(2)	0.92(9)
O20	0.7961(7)	0.2821(7)	0.8293(10)	9.5(4)
O21	0.8588(8)	0.2207(8)	0.7227(11)	11.0(4)
O22	0.9305(8)	0.3606(7)	0.7790(6)	6.7(3)
O23	1.0349(7)	0.2262(10)	0.7999(9)	11.0(5)
O24	0.3510(7)	0.0571(5)	0.6451(4)	4.8(2)
O3	0.6602(4)	0.2798(3)	0.6158(2)	1.28(9)
O4	0.5538(3)	0.4099(3)	0.6269(2)	0.77(8)
O5	0.6701(3)	0.4336(3)	0.5685(2)	0.74(8)
O6	0.6986(4)	0.5065(3)	0.6941(2)	1.21(9)
O7	0.6667(3)	0.5764(3)	0.5701(2)	0.77(8)
O8	0.6916(4)	0.7298(3)	0.5294(3)	1.28(11)
O9	0.5582(3)	0.7028(3)	0.5813(2)	0.87(9)
Pd1	0.44987(4)	0.20726(3)	0.60952(2)	0.996(13)
S0B	0.9576(2)	0.3659(2)	0.7146(2)	5.62(9)
S1	0.7443(3)	0.3640(2)	0.8272(2)	3.22(9)
S10	1.1248(2)	0.2148(3)	0.8553(2)	5.62(10)
S11	0.8585(4)	0.0994(4)	0.8907(7)	10.5(3)
S12	0.7509(6)	0.3465(6)	0.7714(5)	4.3(2)
S2	0.8728(5)	0.1497(4)	0.6849(9)	20.3(5)
S8	0.47382(15)	0.10656(10)	0.54739(9)	1.57(3)
S9	0.41273(18)	0.12064(12)	0.67713(10)	2.30(4)

V0A	0.92406(15)	0.2593(2)	0.8251(2)	9.60(15)
V1	0.43859(8)	0.38913(7)	0.62716(5)	0.68(2)
V2	0.62341(8)	0.50555(6)	0.62579(5)	0.56(2)
V3	0.31413(7)	0.49702(7)	0.49864(6)	0.67(2)
V4	0.59962(8)	0.33803(6)	0.56214(5)	0.63(2)
V5	0.60956(8)	0.66850(6)	0.52376(5)	0.61(2)
V6	0.45134(8)	0.64020(7)	0.58753(5)	0.66(2)

Table 3.3: Anisotropic displacement parameters

atom	U11	U22	U33	U12	U23
O1	0.018(2)	0.004(2)	0.008(2)	-0.0003(18)	0.0013(17)
F1	0.0110(18)	0.0038(17)	0.0056(17)	0.0008(14)	-0.0003(13)
V1	0.0168(6)	0.0039(5)	0.0064(5)	0.0001(4)	0.0006(4)
C33	0.042(6)	0.064(8)	0.049(7)	0.018(6)	0.005(6)
O24	0.114(8)	0.039(4)	0.036(4)	-0.051(5)	-0.008(3)
O23	0.027(5)	0.170(14)	0.218(17)	0.017(7)	0.151(14)
O22	0.075(7)	0.090(8)	0.072(7)	-0.023(6)	0.049(6)
O21	0.041(6)	0.061(7)	0.29(2)	0.011(5)	-0.020(11)
O20	0.037(5)	0.064(7)	0.241(19)	0.006(5)	0.066(10)
C1	0.049(7)	0.083(10)	0.032(6)	-0.003(7)	0.023(6)
O11	0.028(3)	0.012(2)	0.014(2)	0.006(2)	-0.002(2)
O13	0.010(2)	0.019(3)	0.025(3)	0.002(2)	0.002(2)
S12	0.055(5)	0.060(6)	0.058(6)	0.027(4)	0.028(4)
O12	0.020(2)	0.008(2)	0.012(2)	0.0026(19)	0.0037(18)
S1	0.029(2)	0.036(2)	0.055(3)	-0.0022(15)	0.0164(18)
O111	0.068(5)	0.005(3)	0.014(3)	0.010(3)	0.002(2)
V2	0.0122(5)	0.0043(5)	0.0035(5)	0.0008(4)	-0.0001(4)
O2	0.019(3)	0.005(2)	0.011(2)	0.0037(18)	-0.0014(18)
S2	0.083(4)	0.080(4)	0.60(3)	0.002(3)	-0.090(9)
V6	0.0165(6)	0.0039(5)	0.0058(5)	0.0029(4)	-0.0010(4)
O6	0.020(3)	0.012(2)	0.009(2)	0.002(2)	-0.0015(19)
C6	0.123(19)	0.075(14)	0.23(3)	-0.027(13)	0.051(18)
O3	0.022(3)	0.011(2)	0.013(2)	0.006(2)	0.003(2)
V3	0.0086(5)	0.0070(5)	0.0107(6)	0.0017(4)	0.0010(4)
O4	0.017(2)	0.006(2)	0.007(2)	0.0002(18)	-0.0009(17)
V4	0.0135(6)	0.0033(5)	0.0065(5)	0.0034(4)	0.0009(4)
O5	0.011(2)	0.007(2)	0.010(2)	0.0021(17)	0.0010(18)
V5	0.0129(6)	0.0030(5)	0.0069(5)	-0.0012(4)	0.0001(4)
O8	0.021(3)	0.010(2)	0.017(3)	-0.006(2)	0.002(2)
O7	0.012(2)	0.006(2)	0.011(2)	0.0002(17)	0.0005(18)
O9	0.020(3)	0.005(2)	0.007(2)	-0.0012(18)	0.0006(17)
C12	0.037(7)	0.18(2)	0.061(9)	-0.013(10)	0.030(12)
S11	0.049(3)	0.066(4)	0.312(15)	0.035(3)	0.106(7)
S10	0.0392(17)	0.092(3)	0.081(3)	0.0096(17)	0.008(2)

O10	0.019(2)	0.006(2)	0.007(2)	0.0000(18)	-0.0011(17)
O15	0.026(3)	0.008(2)	0.013(2)	0.002(2)	-0.0005(19)
O14	0.017(2)	0.006(2)	0.012(2)	0.0002(18)	0.0000(18)
O16	0.025(3)	0.009(2)	0.010(2)	-0.001(2)	0.0023(18)
O19	0.175(17)	0.167(17)	0.61(5)	0.095(13)	0.24(2)
O18	0.024(3)	0.072(6)	0.057(5)	-0.012(3)	-0.013(4)
C1B	0.102(10)	0.034(6)	0.019(4)	0.036(6)	0.009(4)

Table 10 Bond lengths (Å)

atom	atom	distance		atom	atom	distance
Pd1	O1	2.008(5)		Pd1	S8	2.247(2)
Pd1	S9	2.232(2)		Pd1	O16	2.004(5)
O1	V4	1.964(5)		O1	V5[1]	1.947(4)
F1	V6	2.217(4)		F1	V4[1]	2.186(3)
F1	V5	2.185(3)		V1	O4	1.803(5)
V1	O15	1.600(5)		V1	O14	1.807(4)
V1	O16	1.740(5)		C33	O23	1.82(2)
C33	C12	1.76(2)		C33	S10	1.669(15)
O24	S9	1.477(9)		O23	V0A	1.993(15)
O23	S10	1.578(13)		O22	V0A	1.991(13)
O22	S0B	1.540(15)		O21	S2	1.49(2)
O21	V0A	2.25(2)		O20	S12	1.658(19)
O20	S1	1.591(12)		O20	V0A	2.025(13)
C1	S12	1.621(17)		C1	S1	1.788(12)
O11	V6	1.611(5)		O13	V3	1.615(5)
S12	S1	1.258(12)		O12	V6	1.939(5)
O12	V3	1.708(5)		O111	S8	1.484(6)
V2	O6	1.608(4)		V2	V3[1]	3.0515(18)
V2	O4	1.941(5)		V2	V4	3.1216(14)
V2	O5	1.987(5)		V2	O7	1.924(5)
V2	O10	1.712(5)		O2	V6[1]	1.973(4)
`O2	V4	1.724(5)		S2	C6	1.72(3)
V6	V4[1]	3.1098(15)		V6	V5	3.1138(18)
V6	O9	1.985(5)		V6	O10	1.929(5)
O3	V4	1.610(5)		V3	O5[1]	1.916(5)
V3	V5[1]	3.1178(16)		V3	O7[1]	2.002(5)
V3	O14	1.940(5)		O4	V4	2.095(5)
V4	O5	1.929(5)		V5	O8	1.610(6)
V5	O7	1.929(5)		V5	O9	1.724(5)
V5	O14[1]	2.095(5)		S8	C0Z	1.776(11)
S8	C15	1.764(9)		S9	C12	1.765(12)
S9	C1B	1.761(13)		V0A	O19	2.03(2)
V0A	O1G	1.62(2)		S0B	C17	1.787(12)
S0B	C1H	1.80(2)		C12	S10	1.709(19)
S11	O19	1.56(3)		C13	C19	1.395(19)
C19	N1E	1.13(2)				

4.4 Results and Discussion

4.4.1 Single Crystal X-ray Diffraction (SXRD) Analysis

A new Pd supported polyoxometalate compound has been synthesized in mixed CH_3CN/DMSO media. The title compound $[VO(DMSO)_5]_2[\{Pd(DMSO)_2\}_2V_{12}O_{32}(F)_2].2CH_3CN$, crystallizes in the monoclinic space group, P21/c (#14), $Z = 4$. The crystallographic data is presented in Table 8 which includes the unit cell parameters and other relevant information. Tables 9 and 10 provide the atomic and anisotropic displacement parameters for the title compound, respectively. Figure 18 illustrates the structure of the compound **(2)** anion.

Single crystal X-ray analysis revealed that the asymmetric unit of the title compound consists of one half of the $[\{Pd(DMSO)_2\}_2V_{12}O_{32}(F)_2]^{4-}$ anions. Two molecules $[VO(DMSO)_5]^{2+}$ cations are the symmetrically dependent parts generated through the crystallographic center of symmetry to compensate the anion. The acetonitrile molecules present in the crystal structure is confirmed by TG Analysis.

Compound **(2)** consists of Pd supported fluoride incorporated anion. As described in figure 18, $[\{Pd(DMSO)_2\}_2V_{12}O_{32}(F)_2]^{4-}$ anion is composed of two tetrahedral VO_4 units (red) and ten square pyramid VO_5 units (green and blue), and two F^- reside inside the cage (green sphere). Each tetrahedral VO_4 is connected to Pd. Two DMSO ligands are connected to Pd to from Pd square planar coordination geometry.

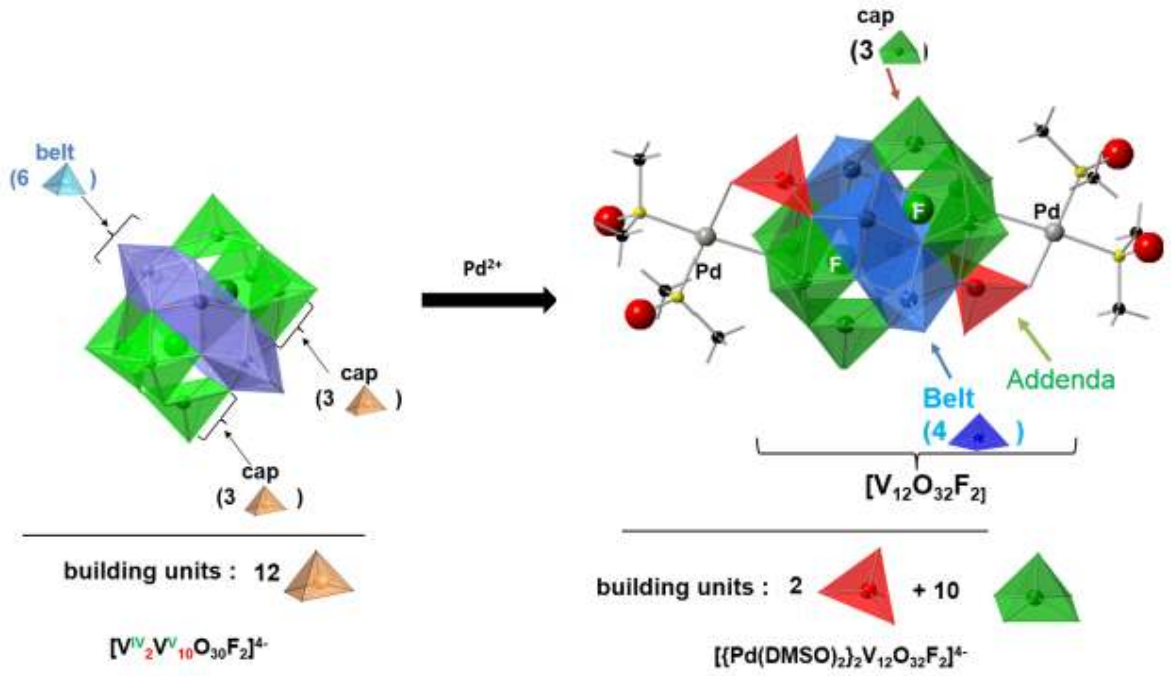

Figure 22 The comparison of precursor and anionic $[\{Pd(DMSO)_2\}_2V_{12}O_{32}F_2]^{4-}$, the VO_4 unit (red tetrahedral) and the VO_5 unit (green and blue square pyramids, Pd (brown, F (dark green), O (red, C (black), S (yellow)and H atoms are omitted for clarity.

Like the precedented difluoride-incorporated polyoxovanadates that possess the structure of $[V_{12}O_{32}(F_2)]^{n-}$ or its lacunary type structure,[7] anion **2** has three layers of one belt layer sandwiched by two cap layers. The belt layer has edge-sharing VO_5 units and three corner-sharing VO_5 units to form $[V_3O_{13}]$ fragment for each of the two cap layers.[7]

The structure is similar to the structures of reported $[H_6V^V_2V^{IV}_{10}O_{30}F_2]^{6-}$[60] $[V^{IV}_2V^V_{12}O_{36}F_4]^{8-}$[61] and $[HV^V_{11}O_{29}F_2]^{4-}$[51]. The V- μ_3-F distances of all these anions are in the range 2.217 and 2.185 Å. Like other F incorporated POV, F^- ion is too small to be a single guest in the cavity, so two F ions are needed. F- V bond, however creates a strong V-F interaction. [62] The repulsion of the F- ions in the center determine the structure (F…F = 2.946 Å).

Pd-DMSO bond

DMSO was chosen firstly in the experiment to deal with probable polymeric structure generated because DMSO has great dissolving ability and also DMSO is a common ligand in coordination chemistry. In the other hand, DMSO which have basic character is an excellent ligand.

From the structure of compound **(2)**, Pd atoms support the structure at both ends. The square planar Pd^{2+} ion are accomplished with two DMSO molecules with S coordination to form coordination number four of Palladium ion. The bond length of Pd-S is 2.232 Å. This value of long distance Pd-S indicates the weak bonding between Pd and DMSO ligand that make DMSO as a leaving group. The anion is discrete because the Pd-coordinated DMSO was not connected to the other moieties.

In the providing Pd^{2+} cation, it is important to have the anions with very small coordinating ability for the preparation of the Pd complexes where Pd(II) is bound directly to the neutral monodentate ligands. The anions tetrafluoroborate were found to satisfy this requirement.[28] So the use of non-coordinating BF_4^- in the synthesis of $[VO(DMSO)_5]_2[\{Pd(DMSO)_2\}_2V_{12}O_{32}(F)_2]$ is essential for the general preparation of complexes $[VO(DMSO)_5]_2[\{Pd(DMSO)_2\}_2V_{12}O_{32}(F)_2]$ because Pd(II) is bound directly to neutral monodentate ligands DMSO.

There are 12 terminal V=O units that fix at around 1.601 – 1.614 Å.Two types of oxido bridges are present in the structure, with V-μ-O bridges with bond lengths in the range 1.712–1.930(1) Å and V-μ_3-O bridges with bond lengths in the range 1.917–2.114 Å. Heavy disorder was found in cation $[VO(DMSO)_5]^{4+}$.

The dimethylsulfoxide oxovanadyl(IV) cation, $VO(DMSO)_5^{2+}$ have a short V=O bond, $d_{V=O}$ = 1.623 Å, four longer ones perpendicular to the V=O bond in the range of 1.991–2.028 Å, mean 2.009 Å, and the fifth DMSO molecule which is trans to the V=O bond is more weakly bound, d_{V-O} = 2.253 Å.

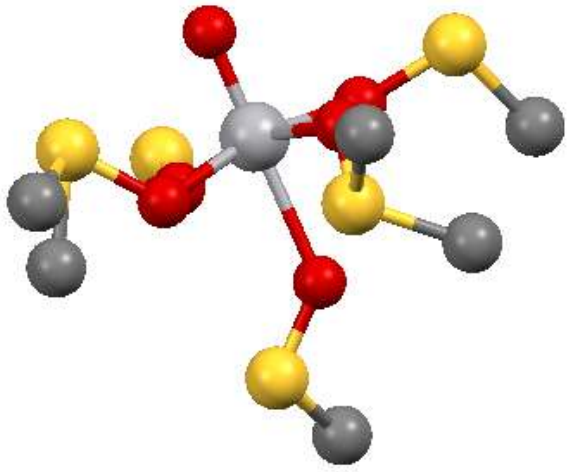

Figure 23 Ball stick structure of the $VO(DMSO)_5^{2+}$ cation in disordered form. O (red), C (black), S (yellow) and H atoms are omitted for clarity.

4.4.2 The IR spectrum

The IR spectra of compound **(2)** (figure 24) shows characteristic POV peaks below 1000 cm^{-1}. Strong bands at 985 cm^{-1} corresponding to the *v*(V=O) frequencies, and a bands with maxima at 600, 736 cm^{-1} corresponding to the Oxido bridges which are different form the precursor $[V_{12}O_{30}(F)_2]$ confirm the change in the spherical shapes from $V_{12}O_{30}(F)_2$ to $V_{12}O_{32}(F)_2$ main cluster.

Some small peaks in the region of far IR is indicative of presence of Pd-S bonding.[63] However, there is no evidence for exclusive oxygen bonding in the far-ir spectrum which should exhibit a single strong band (478 cm^{-1}) attributable to Pd-O stretching.[63] This means DMSO coordination Pd is only through S atom as described in X-ray structure analysis.

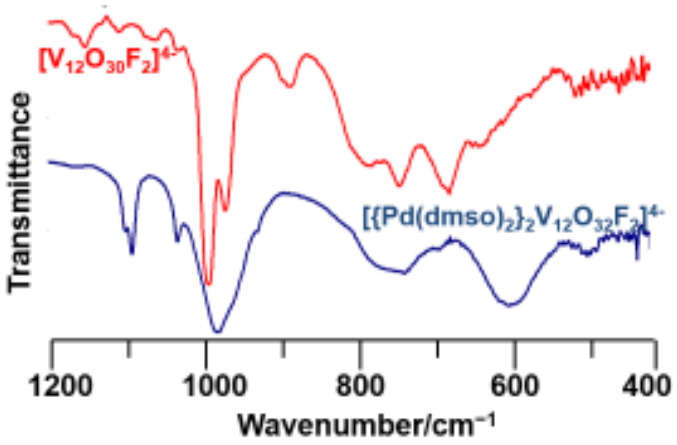

Figure 24 IR spectrum of compound (2) (blue) compared with compound (1) (red). Peak at 1045 cm^{-1} is the S=O stretching of DMSO

4.4.3 Bond Valence Sum (BVS) Calculation

The charges of V atoms as mixed valences of 4+ and 5+ as indicated by the bond valence sums calculations shown in Table 11. The bond valence sums of V6 is 4+ and the rest are 5+.

Table 11 BVS calculation of anion of compound (2)

			V1	V2	V3	V4	V5	V6	Pd1
2 V^{IV}	10 V^{V}	V^{IV}	4.66	4.74	4.72	4.77	4.8	4.36	
		V^{V}	4.91	4.99	4.97	5	5.04	4.58	
2 Pd^{II}	0 Pd^{IV}	Pd^{II}							2.46
		Pd^{IV}							2.36

Table 12 BVS calculation of cation of compound (2)

			V00A
2 V^{IV}	OV^{V}	V^{IV}	4.161
		V^{V}	4.380

So, the BVS suggests the mixed valence POV with formula $[V^{IV}O(DMSO)_5]_2[\{Pd^{II}(DMSO)_2\}_2V^{IV}_2V^{V}_{10}O_{32}F_2].2CH_3CN$. From the charge balance this is equal as there are two $[V^{IV}O(DMSO)_5]^{2+}$ cation and a $[\{Pd^{II}(DMSO)_2\}_2V^{IV}_2V^{V}_{10}O_{32}(F)_2]^{4-}$ anion.

4.4.4 Thermogravimetric (TG) Analysis

TGA measurements of compound **(2)** is illustrated in Figure 23.

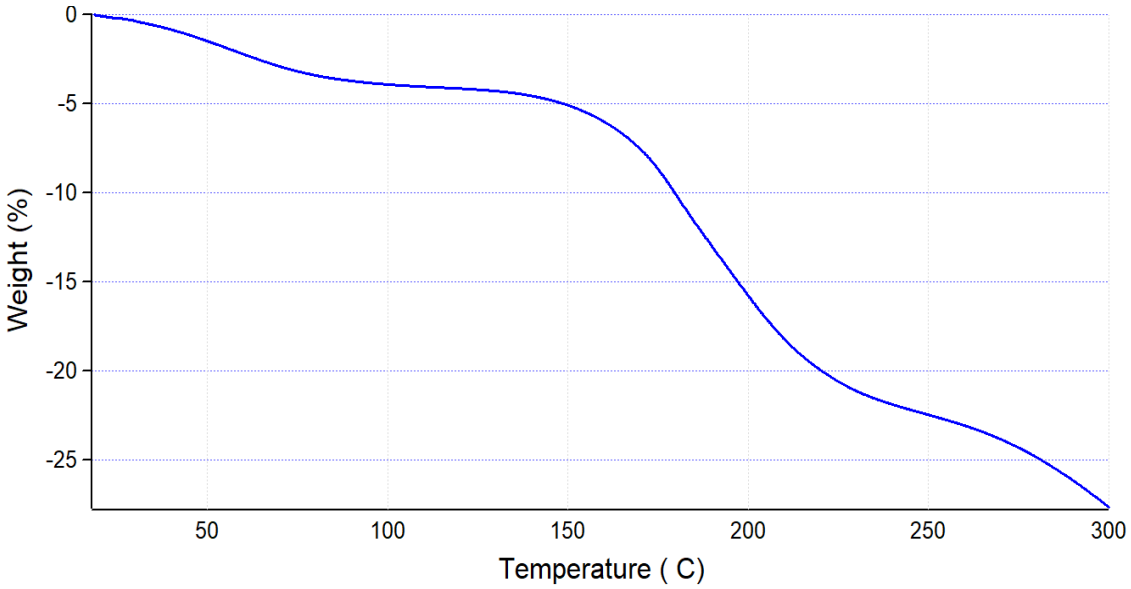

Figure 25 Thermogravimetric analysis (TGA) plots for $[VO(DMSO)_5]_2[\{Pd(DMSO)_2\}_2V_{12}O_{32}(F)_2].2CH_3CN$.

TGA measurement shows that the title compound $[VO(DMSO)_5]_2[\{Pd(DMSO)_2\}_2V_{12}O_{32}(F)_2].2CH_3CN$ starts to release solvent of crystallization acetonitrile at 50 °C up to 100 °C. The weight loss at the point is about 3 % equal to two molecules of acetonitrile. The loss of mass observed between 150 °C and 240 °C is likely the result of a loss of four molecules DMSO ligands of the anion and five molecules of DMSO ligands of the cation which should correspond totally to approximately 26% of the total formula weight. Acetonitrile has lower boiling point than DMSO that result in earlier than DMSO on evaporation as performed on TG data above.

4.4.5 UV-Vis Absorption Spectra

UV-Vis spectrum is a finger print characterization method to find whether the POM is reduced or oxidized. Most of the POMs in their highest oxidation state only give Metal to Oxygen charge transfer band at the short wavelength. Most of POMs do not have peak above 600 nm attributed intervalence charge transfer.

If POM get reduced, it shows intense blue color based on intervalence band, so that POM is often referred as polyoxo blue (Heteropoly blue). So we can check whether our POM is reduced compound or not by seeing the appearance of intervalence band peak of peak maximize around 800-900 nm.

UV/Vis spectrum of compound **(2)** in DMSO is illustrated in figure 22.

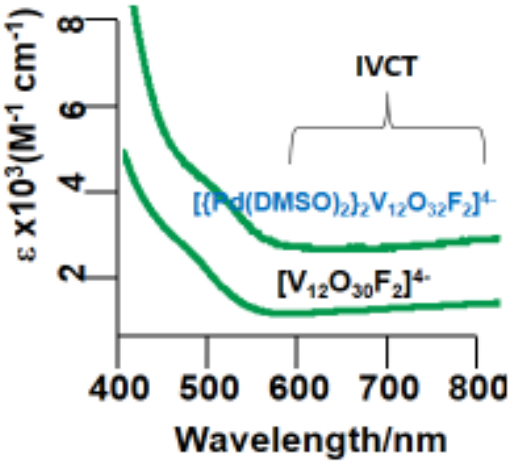

Figure 26 UV-vis spectrum data of compound (2)

UV/Vis spectrum of compound **(2)** in DMSO compared with compound **(1)** clearly shows a peak above 600 nm which is attributed to Intervalence Charge Transfer (IVCT) of these two POVs. This imply that there are mixed valence Vanadium atoms in compound **(2)** like previously discussed compound **(1)**. This confirms the BVS calculation before.

4.4.5 Stability of complex 2

Sometimes reduced POVs complex are highly air sensitive so that they are difficult to handle under the conventional environment. In our case, this is not significantly seen as the complex **2** is stable enough that did not need a moisture-free and oxygen-free environment in a nitrogen filled glove box for preparation. The preparation of complex **2** both in a glove box and outside a glove box produced the same result.

4.4.6 Low solubility of complex 2

Compound **(2)** is insoluble in most organic solvents, except in polar aprotic solvents DMSO and DMF. This insolubility of the complex make it restricted in exploring its reaction with others. The solution of this problem should be on choosing appropriate counter ions, so that compound **(2)** will be soluble in organic solvents with specific polarity. Research on the use of counter cation $\{n\text{-}Bu_4N\}^+$, PPh_4^+, TEA^+ and so is on progress.

4.5 Potential Application

4.5.1 POMOF

The anionic $[\{Pd(DMSO)_2\}_2V_{12}O_{32}(F)_2]^{4-}$ is a potential linker in Polyoxometalate based Metal Organic Framework Chemistry. Ligand DMSO can be considered a leaving ligand

which can be replaced by other bidentate ligands to grow a framework structure as illustrated in figure 23.

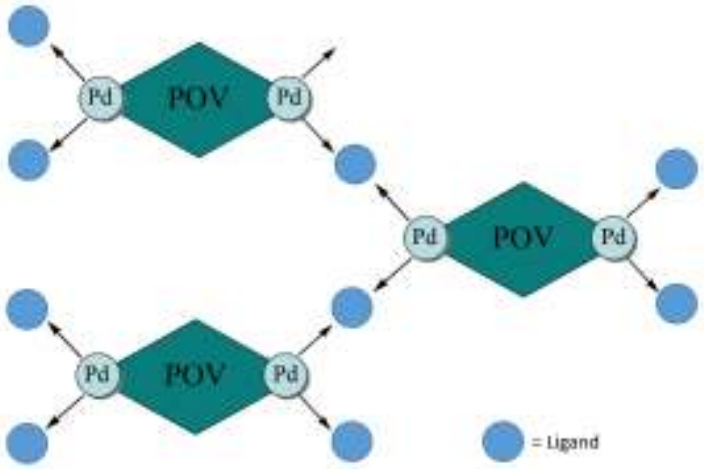

Figure 27 Illustration of how bi-dentate ligands (L) as linker and the binding of two Pd metal centers can help Pd-POV fragments to grow in any direction for forming POMOFs.

So, $[\{Pd(DMSO)_2\}_2V_{12}O_{32}(F)_2]^{4-}$ is considered as a building block for making 3-D framework structures. Besides that, making use of the catalytic active Pd site in addition to catalytic active V is also interesting to explore in catalysis field.

4.5.2 Catalysis

The direct supporting of metal ions onto the surface oxygens of polyoxometalates at molecular levels is the improvement in polyoxometalate-based catalysts.[64] The design of molecules based on a combination of noble metals like Pd and V atoms is very interesting for developing new oxidation catalysts because each of them is effective for catalysis.

For this reason, complex $[VO(DMSO)_5]_2[\{Pd(DMSO)_2\}_2V_{12}O_{32}(F)_2]$ is potential for the catalysis. Due to the its insolubility in most organic solvent, the complex still can be used in heterogeneous system.

4.6 Conclusions

Here, a new Pd supported F^- inclusion dodecavanadate clusters is presented. We have achieved an inorganic linker by supporting Pd^{2+} on both end of dodecavanadate cluster. This complex is the inorganic linker unit that has the composition of dodecavanadate moiety and Pd atoms support the structure at both ends. The square planar Pd ion are accomplished with two DMSO molecules with S coordination mode to form coordination

number four for Palladium ion. The BVS calculation and thermal analysis suggests the mixed valence $[VO(DMSO)_5]_2[\{Pd(DMSO)_2\}_2V_2^{IV}V_{10}^{V}O_{32}F_2].2CH_3CN$ formula.

In conclusion, we have reported direct preparation of a new Pd supported fluorinated dodecavanadate inorganic linker in reduced form. The next chapter 5 will discuss the synthesis of the fully oxidized one.

4.6.1 Future Work

Even though the complex compound **(2)** is ionic, the compound is not soluble in most organic solvents, except DMF and DMSO. It would be interesting to see if the yield and solubility of the title compound could essentially be increased and tuned by replacing the cation $VO(DMSO)_5^{2+}$ with other cations which would result in more soluble complex and higher yield.

In addition, it is needed to explore the properties with respect to catalytic activity of the title compound and the utility of the compound in formation of novel frameworks. The POMOF construction from compound **(2)** is also interesting by making use of e.g. symmetric linking ligands bidentate 4,4'-bipyridine, 4,4'-Trimethylenedipyridine, 4-Dimethylaminopyridine etc. Apart from coordination polymer, $[\{Pd(DMSO)_2\}_2V_{12}O_{32}(F)_2]^{4-}$ is also possible to form a discrete Pd(II) complex with 2,2'-bipyridine.

CHAPTER 5 SYNTHESIS OF A FULLY OXIDIZED PALLADIUM SUPPORTED FLUORIDE INCORPORATED DODECAVANADATE {*n*-Bu_4N}$_4$[{$Pd(NO_3)(DMSO)$}$_2V_{12}O_{32}(F)_2$]·2DMSO

Abstract

In the objective of obtaining stable Pd-Polyoxovanadate linker unit against oxidation, complex {*n*-Bu_4N}$_4$[{$Pd(NO_3)(DMSO)$}$_2V_{12}O_{32}(F)_2$]·2DMSO **(3)** was synthesized. The air stable complex **3** can be obtained by oxidation of both complex **2** as precursor and some other POVs.

This chapter will describe the synthesis and characterization of a fully oxidized form of Pd-supported fluoro dodecavanadate. In addition to fully oxidized form, the compound **(3)** have Nitrate ligand beside DMSO ligand that make it different form the previously synthesized compound **(2)**. Full characterization of the complex will be described.

The complex **(3)** is an air stable complex which can be synthesized from precursor {*n*-Bu_4N}$_4$[$V_{10}O_{26}$]. This chapter will also mention some synthetic procedures by which the title compound can be obtained by different ways. The synthesis of complex **3** was done on the use of the solution-based synthetic methods and the crystallization by slow evaporation technique.

Graphical Abstract

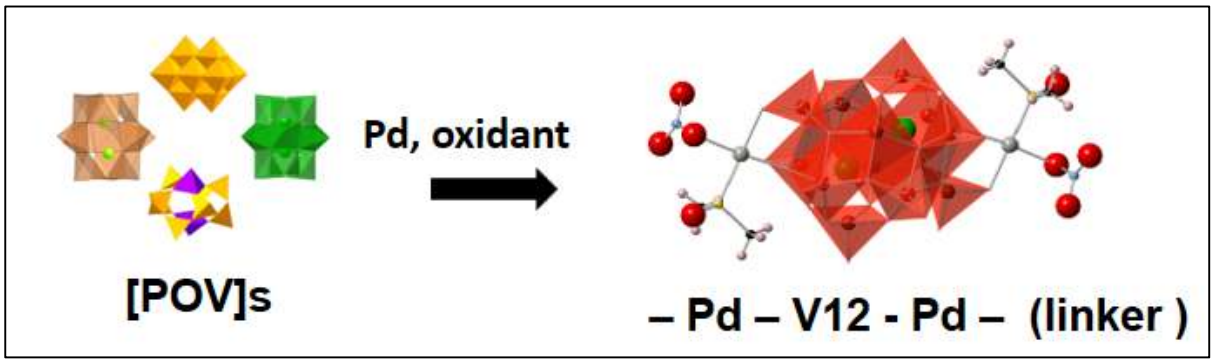

Figure 28 Synthetic Scheme to the anionic (3)

5.1 Introduction

As mentioned in chapter 4, the negatively charged polyoxometalate can serve as an inorganic ligand that is able to form a metal complex through the coordination of the oxido groups to a metal. The tetrahedral-VO_4-unit in particular has coordination ability and it binds cations to act as a ligand[5665] This happens again in the formation of fully oxidized Pd-fluoro dodecavanadate cluster **(3)**.

As described at complex **(2)** in the previous chapter, not like other single anion in the sphere,[21] two anion F^- sit in the sphere to stabilize the structure of the sphere of the fluoride-incorporated polyoxovanadates. [51,66] .

Furthermore, some fluoride-incorporated polyoxovanadates such as $[V_7O_{19}(F)]^{n-}$, is constructed from VO_5 and VO_4 units, while most of anion-incorporated–polyoxovanadates consist of only VO_5 units. The VO_5 and VO_4 units present together in Polyoxovanadates have potential to stabilize both anions and metal cations.

In studying other possible ligand for Pd beside DMSO, nitrate ligand is also interesting to explore. Playing role as a ligand in coordination chemistry, Nitrate ($O{-}NO_2^-$) is a monoanionic and a monodentate ligand. As palladium prefers tetra-coordinate square planar arrangement, so the nitrates are bonded in monodentate binding motif.

In this work, we demonstrated the formation of a fully oxidized Pd supported fluoro decavanadate by deliberately choosing F^- as the incorporated anions and Nitrate as the other ligand beside DMSO for the Pd-V12 complex. This give rise to a spherical fluoride-incorporated polyoxovanadate which are also have Pd^{2+} units on the polyoxovanadate framework ready to use as linker sites (figure 29).

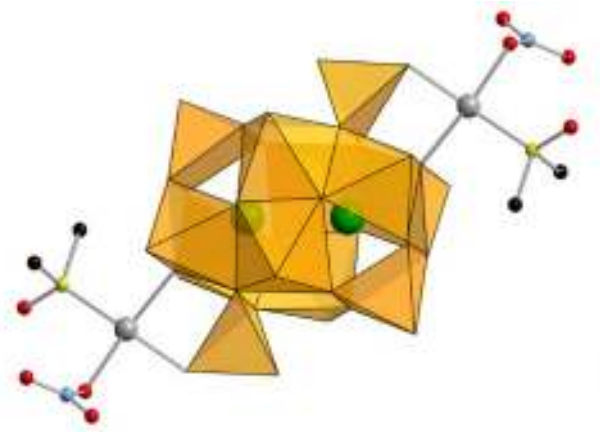

Figure 29 Polyhedral and ball-and-stick representation of the anion part of compound (3). Orange polyhedra and green, gray, red, light blue, yellow and black spheres represent vanadium-oxygen units, fluorine, palladium, oxygen, nitrogen, sulfur, and carbon atoms, respectively. Hydrogen atoms are omitted for clarity.

5.2 Experimental

Compound **(3)** can be approached from many choices of POV which imply the stability of this compound. For some consideration of best approach, the main precursor for the synthesis of complex **(3)** is $\{n\text{-}Bu_4N\}_4[V_{10}O_{26}]$. The yield obtained was the best among other POV precursors. At the same time, $\{n\text{-}Bu_4N\}_4[V_{10}O_{26}]$ is an easily prepared metastable species which can convert to VO_5-based polyoxovanadates.

In-situ prepared $Pd(NO_3)_2$ was used. $Pd(cod)Cl_2$ (11 mg, 0.038 mmol, cod = 1,5-cyclooctadiene) was dissolved in the mixed solvent of nitromethane and DMSO (4:1, v/v, 1.25 mL). $AgNO_3$ (13 mg, 0.077 mmol) was added to the solution, and the white precipitates of AgCl were removed by filtration. The filtrate was mixed with the nitromethane solution of $\{n\text{-}Bu_4N\}_4[V_{10}O_{26}]$ (23 mM, 1 mL). Addition of 30% H_2O_2 (0.05 mL, 4.4 mmol) and HNO_3 (0.33 M, 0.015 mL diluted by DMSO) give reddish yellow solution. The slow evaporation of the solvent yielded red crystals of **1**. Red crystals were collected by filtration, washed by acetone and dried (60% yield based on Pd). Anal. Calcd. for $\{n\text{-}Bu_4N\}_4[\{Pd(NO_3)(DMSO)\}_2V_{12}O_{32}(F)_2]\cdot 2DMSO$: C, 31.10; H, 6.09; N, 3.02; F, 1.37; S, 4.61, found: C, 31.84; H, 6.34; N, 2.99; F, 1.32; S, 4.78. IR (KBr pellet; 4000−400 cm^{-1}): 2961, 2931, 2876, 2839, 1509, 1483, 1463, 1382, 1353, 1296, 1143, 1112, 1047, 1023, 984, 852, 808, 707, 624, 580, and 488 cm^{-1}. ^{51}V NMR (105.15 MHz, CD_3CN, 25°C): δ −444, −458, −525, and −542 ppm. ^{19}F NMR (376.17 MHz, CD3CN, 25°C, CF_3COOH (δ = 0 ppm)): δ −71 ppm. ^{1}H NMR (399.78 MHz, CD_3CN, 25°C): δ 0.97 (24H), 1.38(16H), 1.62(16H), 2.50 (6H), 3.17 (16H), 3.37 (4.5H), and 4.41 ppm (1.5H).

5.2.1 Alternative Synthetic Routes for Synthesis of Compound (3)

Basically complex **3** can be obtained by oxidation of complex **2** synthesized before. However, the cation $VO(DMSO)_5^{2+}$ lower the yield of resulting complex **3** because the cation $VO(DMSO)_5^{2+}$ also contain Vanadium.

To obtain better POV precursors, some other POVs are also tested. This results in the other synthetic procedures toward the synthesis of complex **3** beside the beside the best one $\{n\text{-}Bu_4N\}_4[V_{10}O_{26}]$:

*a. Synthesis of of **(3)** with precursor complex $\{n\text{-}Bu_4N\}_4[V_{12}O_{30}(F)_2]\cdot CH_3CN$*

Mixture of $Pd(cod)Cl_2$ (12 mg, 0.04mmol) and $AgBF_4$ (16 mg, 0.08 mmol) in 0.5 mL Acetonitrile was stirred for 2 hours and the resulting white precipitates of AgCl was removed by filtration. The filtered yellow filtrate was added to the solution of $(n\text{-}Bu_4N)_4[V_{12}O_{30}F_2]$ [**1**] (44 mg, 0.02 mmol) which was previously added and stirred in small amount of hot DMSO (75 ^oC). After standing overnight, dark green crystal of [3] obtained is filtered, and the green filtrate was added with H_2O_2 50 µL. The red filtrate gave red crystal of compound **(3)** after standing overnight.

*b. Synthesis of of **(3)** with precursor complex $\{n\text{-}Bu_4N\}_3[V_{10}O_{28}H_3]$*

Mixture of $Pd(cod)Cl_2$ (0.04 mmol) and $AgBF_4$ (0.08 mmol) in 0.5 mL Nitromethane was stirred for 2 hours and the resulting white precipitates of AgCl was removed by filtration. The filtered yelllow filtrate was added to the small amount of hot DMSO (75 ^oC) solution of $\{n\text{-}Bu_4N\}_3[V_{10}O_{28}H_3]$ (0.02 mmol). After standing 1 week, the mixture turned brown. Red crystal was obtained was obtained by Ether diffusion.

*c. Synthesis of of **(3)** with precursor complex $\{n\text{-}Bu_4N\}_4[HV_{11}O_{29}F_2]$*

$AgNO_3$ (77 µmol, 13 mg) was dissolved in 0.25 mL DMSO, and 1 mL Nitromethane was added. $Pd(cod)Cl_2$ (38 µmol, 11 mg)) was then added, and stirred for 2 min. The resulting white precipitates of AgCl was removed by filtration. The filtered filtrate was added to the 1 mL nitromethane solution of $\{n\text{-}Bu_4N\}_4[HV_{11}O_{29}F_2]$ (23 µmol). The mixture was stirred, and then oxidant H_2O_2 50 µL was added so that the solution turns red. $HNO_3$15 µmol (46.7 µL, 0.328 M in DMSO) was added finally to conclude the reaction. After standing overnight, few amount red crystal complex **(3)** was obtained.

5.3 Characterization

5.3.1 Materials and Measurements.

{*n*-Bu_4N}F, $AgNO_3$, and solvents were purchased from commercial sources and used as received. $Pd(cod)Cl_2$ and {*n*-Bu_4N}$_4[V_{10}O_{26}]$ were prepared according to the reported procedures[67 68 45] .

^1H, ^{51}V and ^{19}F NMR spectra were measured at 399.78, 105.15, and 376.17 MHz, respectively recorded with JEOL JNM-LA400. All spectra were obtained in the indicated solvent, at 25ºC unless otherwise noted. ^{19}F NMR spectra were referenced to neat CF_3COOH ($\delta = 0.00$). ^{51}V NMR spectra were referenced using a sample of 10 mM $NaVO_3$ in 2.0 M NaOH (−541.2 ppm).

Voltammetric experiments was performed with ALS/CH Instruments electrochemical analyzer (Model 600A). The working electrode was glassy carbon, the counter electrode was Pt wire, and the reference electrode was Ag/Ag^+. The voltage scan rate was set at 100 mV s^{-1}. The potentials in all voltammetric experiments were converted using data derived from the oxidation of ferrocene (ferrocene / ferrocenium) as an external reference.

5.3.2 X-ray crystallographic analysis.

Single crystal structure analysis was performed at 90 K by using a Bruker D8 VENTURE diffractometer with graphite monochromated Cu Kα radiation (λ = 1.54178 Å). The data reduction and absorption correction were done using *APEX3* program. the structural analyses were performed using *APEX3*, and *WinGX*[4] for Windows software. The structures were solved by SHELXS-2014 (direct methods) and refined by SHELXL-2014. Non-hydrogen atoms were refined anisotropically. Hydrogen atoms are positioned geometrically and refined using a riding model.

The crystallographic data can be seen in Table 12. The atomic coordinates, anisotropic thermal parameters, selected bond distances and angles and bond valence sums calculations can be seen in tables 13-15.

Table 13 Crystallographic data

Empirical Formula	C72H168F2N6O42Pd2S4V12
Formula Weight	2780.47
Crystal Color, Habit	orange, block
Crystal Dimensions	0.200 x 0.200 x 0.200 mm
Crystal System	Orthorhombic
Lattice Type	Primitive
Cell Determination (2q range)	9600 (5.8 - 144.8o)
Lattice Parameters	a = 20.0743(4) Å
	b = 19.1110(4) Å
	c = 30.3484(6) Å
	V = 11642.9(4) Å3
Space Group	Pbca (#61)
Z value	4
Dcalc	1.586 g/cm3
Reflection/Parameter Ratio	16.12
Residuals: R (I>2.00s(I))	0.0499
Residuals: R (All reflections)	0.0000
Residuals: wR (All reflections)	0.1396
Goodness of Fit Indicator	1.027
Max Shift/Error in Final Cycle	0.001

Table 14 Atomic coordinates and Biso/Beq

atom	x	y	z	Beq
S201	0.47532(6)	0.24876(6)	0.34286(4)	2.96(3)
C201	0.5313(3)	0.2324(3)	0.38683(19)	3.95(13)
C202	0.4050(3)	0.2001(3)	0.36000(19)	3.87(12)
C301	0.5964(3)	0.4905(3)	0.28775(18)	3.68(12)
C302	0.6262(3)	0.4393(3)	0.25439(19)	4.45(14)
C303	0.6120(3)	0.3641(3)	0.26755(19)	4.47(14)
C304	0.6424(4)	0.3099(4)	0.2375(2)	5.50(18)
C305	0.5465(3)	0.5681(3)	0.23001(16)	3.24(11)
C306	0.4819(3)	0.5285(4)	0.2315(2)	4.87(16)
C307	0.4412(3)	0.5389(4)	0.1890(2)	4.58(16)
C308	0.4708(5)	0.5063(6)	0.1493(3)	8.1(3)
C309	0.6562(3)	0.5957(4)	0.25914(19)	4.08(13)
C310	0.7059(4)	0.5999(5)	0.2964(3)	6.8(2)
C311	0.7715(8)	0.6284(10)	0.2770(6)	4.8(4)
C312	0.8041(5)	0.5908(8)	0.2368(4)	6.5(4)
C361	0.7621(14)	0.6587(19)	0.2887(9)	6.5(8)
C362	0.8091(9)	0.6753(13)	0.3268(6)	6.3(5)
C313	0.5562(3)	0.6066(3)	0.30853(16)	3.34(11)
C314	0.5537(3)	0.6849(3)	0.30385(18)	3.87(13)
C315	0.5173(4)	0.7173(3)	0.3420(2)	5.11(16)
C316	0.5173(4)	0.7956(4)	0.3416(2)	5.18(17)
C401	0.2675(3)	0.6913(3)	0.4880(2)	4.84(14)
C402	0.2624(4)	0.7287(5)	0.4446(3)	7.0(2)
C403	0.2920(4)	0.6884(4)	0.4071(3)	6.0(2)
C404	0.2936(5)	0.7252(6)	0.3644(3)	8.8(3)
C405	0.2383(4)	0.7993(4)	0.5298(2)	6.6(2)
C406	0.3088(4)	0.8197(4)	0.5407(3)	6.7(2)
C407	0.3322(8)	0.9049(9)	0.5402(6)	5.3(4)
C408	0.2998(6)	0.9468(7)	0.5769(5)	6.1(4)
C457	0.2995(10)	0.8934(9)	0.5438(6)	3.7(4)
C458	0.3659(10)	0.9206(9)	0.5549(6)	4.5(4)
C409	0.2468(4)	0.6830(5)	0.5676(3)	8.4(3)
C410	0.2096(6)	0.7089(9)	0.6093(4)	15.2(5)
C411	0.2351(6)	0.6698(11)	0.6501(5)	16.0(5)
C412	0.2220(6)	0.5993(10)	0.6527(6)	17.2(6)
C413	0.1559(6)	0.7237(8)	0.5249(5)	3.9(3)
C414	0.1297(6)	0.6503(7)	0.5296(6)	5.3(4)
C415	0.0573(7)	0.6428(11)	0.5143(10)	7.7(5)
C416	0.0195(10)	0.6100(17)	0.5311(7)	10.2(8)
C463	0.1486(6)	0.7006(9)	0.5068(6)	3.0(3)
C464	0.1288(7)	0.6256(8)	0.4949(7)	4.6(4)

C465	0.0518(9)	0.6218(12)	0.4848(8)	5.8(5)
C466	0.0350(18)	0.5608(18)	0.499(3)	32(3)
S501	0.1903(3)	0.5096(2)	0.38711(13)	10.19(13)
S551	0.1728(5)	0.4596(7)	0.3632(4)	9.1(3)
O501	0.1507(4)	0.5331(4)	0.3509(2)	7.97(18)
C502	0.1530(11)	0.4346(12)	0.4101(7)	21.1(11)
C501	0.2570(6)	0.4713(11)	0.3681(5)	14.8(6)
N101	0.3484(4)	0.3331(5)	0.2758(2)	7.0(2)
N301	0.5896(2)	0.5655(2)	0.27144(13)	3.21(9)
N401	0.2265(3)	0.7221(4)	0.5259(2)	6.13(16)
O1	0.51924(14)	0.63045(15)	0.44595(9)	1.89(6)
O2	0.63575(14)	0.60894(16)	0.40658(9)	2.17(6)
O3	0.39131(14)	0.59502(15)	0.47212(9)	1.85(5)
O4	0.28158(14)	0.51669(17)	0.47942(10)	2.42(6)
O5	0.53244(13)	0.51034(14)	0.40182(9)	1.67(5)
O6	0.39284(13)	0.47304(14)	0.43044(9)	1.77(5)
O7	0.42087(15)	0.58661(16)	0.37617(10)	2.18(6)
O8	0.43146(15)	0.46535(17)	0.33689(9)	2.35(6)
O9	0.62311(13)	0.47886(15)	0.45321(9)	1.76(5)
O10	0.38081(13)	0.41495(14)	0.50268(9)	1.79(5)
O11	0.61283(15)	0.39713(16)	0.37774(9)	2.26(6)
O12	0.36152(15)	0.33302(16)	0.42738(10)	2.26(6)
O13	0.48346(14)	0.38126(15)	0.40333(9)	1.88(5)
O14	0.58667(14)	0.34198(15)	0.45483(9)	1.95(6)
O15	0.46531(15)	0.30931(15)	0.47890(9)	2.02(6)
O16	0.56873(16)	0.26868(16)	0.53018(10)	2.46(6)
O102	0.4108(3)	0.3498(3)	0.27687(15)	6.21(13)
O103	0.3076(5)	0.3866(5)	0.2762(4)	12.7(3)
O104	0.3388(4)	0.2748(3)	0.2758(2)	8.1(2)
O201	0.5039(2)	0.21723(19)	0.30281(12)	3.68(8)
Pd1	0.45032(2)	0.36165(2)	0.34025(2)	2.306(7)
V1	0.44459(3)	0.50811(4)	0.38604(2)	1.729(13)
V2	0.58411(3)	0.57186(3)	0.43930(2)	1.548(12)
V3	0.36081(3)	0.51275(4)	0.48506(2)	1.658(13)
V4	0.56944(3)	0.41402(4)	0.42050(2)	1.653(12)
V5	0.42090(3)	0.37555(4)	0.45065(2)	1.663(12)
V6	0.54156(3)	0.34041(4)	0.51000(2)	1.777(12)
F1	0.50334(11)	0.43659(12)	0.47669(7)	1.73(4)

Table 15 Anisotropic displacement parameters

atom	U11	U22	U33	U12	U13	U23
S201	0.0466(7)	0.0327(6)	0.0330(6)	-0.0011(5)	-0.0022(5)	-0.0133(5)
C201	0.066(4)	0.036(3)	0.048(3)	0.010(3)	-0.016(3)	-0.016(2)
C202	0.058(3)	0.042(3)	0.047(3)	-0.009(3)	0.008(3)	-0.013(2)
C301	0.052(3)	0.051(3)	0.037(3)	0.014(3)	0.007(2)	0.023(2)
C302	0.057(4)	0.071(4)	0.041(3)	0.028(3)	0.014(3)	0.021(3)
C303	0.066(4)	0.067(4)	0.037(3)	0.027(3)	0.007(3)	0.008(3)
C304	0.077(5)	0.082(5)	0.050(4)	0.031(4)	0.004(3)	-0.001(3)
C305	0.044(3)	0.047(3)	0.032(2)	0.007(2)	0.001(2)	0.015(2)
C306	0.056(4)	0.078(5)	0.051(3)	-0.009(3)	-0.004(3)	0.023(3)
C307	0.055(4)	0.057(4)	0.062(4)	-0.003(3)	-0.013(3)	0.009(3)
C308	0.091(7)	0.119(8)	0.097(7)	0.006(6)	-0.017(5)	-0.034(6)
C309	0.040(3)	0.073(4)	0.042(3)	0.003(3)	0.005(2)	0.026(3)
C310	0.052(4)	0.137(8)	0.068(5)	-0.020(4)	-0.018(3)	0.047(5)
C311	0.031(6)	0.076(11)	0.076(11)	-0.003(6)	-0.009(7)	0.015(7)
C312	0.037(6)	0.114(12)	0.095(10)	-0.002(6)	-0.002(6)	0.031(9)
C361	0.046(12)	0.13(3)	0.071(16)	-0.003(16)	0.008(11)	0.027(17)
C362	0.042(9)	0.127(19)	0.072(13)	0.006(10)	-0.011(8)	0.014(12)
C313	0.048(3)	0.052(3)	0.027(2)	0.003(2)	0.005(2)	0.014(2)
C314	0.066(4)	0.048(3)	0.033(3)	-0.011(3)	0.000(2)	0.012(2)
C315	0.092(5)	0.047(3)	0.055(4)	0.005(3)	0.019(3)	0.015(3)
C316	0.088(5)	0.052(4)	0.057(4)	-0.004(4)	-0.003(3)	0.006(3)
C401	0.037(3)	0.051(3)	0.096(5)	0.024(3)	0.006(3)	0.019(3)
C402	0.074(5)	0.092(6)	0.101(6)	0.056(5)	0.039(5)	0.041(5)
C403	0.080(5)	0.071(5)	0.076(5)	0.032(4)	-0.034(4)	-0.005(4)
C404	0.098(7)	0.145(9)	0.090(6)	0.062(7)	0.018(5)	0.030(6)
C405	0.081(5)	0.100(6)	0.068(4)	0.071(5)	0.031(4)	0.035(4)
C406	0.105(6)	0.080(5)	0.070(5)	0.060(5)	0.022(4)	0.011(4)
C407	0.038(9)	0.089(11)	0.073(9)	0.013(9)	0.009(8)	0.007(8)
C408	0.043(6)	0.078(9)	0.110(12)	-0.006(6)	-0.002(7)	-0.013(8)
C457	0.042(10)	0.043(8)	0.057(9)	0.022(8)	0.000(8)	0.007(7)
C458	0.046(10)	0.050(9)	0.075(12)	0.000(7)	-0.010(8)	0.011(8)
C409	0.052(4)	0.144(8)	0.125(7)	0.055(5)	0.035(4)	0.097(7)
C410	0.115(8)	0.34(2)	0.123(9)	0.152(11)	0.080(7)	0.157(12)
C411	0.090(8)	0.35(2)	0.167(12)	0.107(12)	0.054(8)	0.191(15)
C412	0.084(8)	0.29(2)	0.28(2)	-0.023(11)	-0.045(10)	0.220(19)
C413	0.037(6)	0.067(9)	0.044(8)	0.021(6)	-0.005(6)	0.004(6)
C414	0.050(7)	0.061(8)	0.091(12)	0.014(6)	-0.004(7)	0.008(8)
C415	0.040(7)	0.083(12)	0.17(2)	0.003(7)	-0.017(11)	0.072(15)
C416	0.079(12)	0.20(3)	0.108(15)	0.007(16)	-0.012(11)	0.077(17)
C463	0.018(5)	0.060(10)	0.036(8)	0.019(6)	-0.006(5)	0.007(7)
C464	0.036(7)	0.043(8)	0.094(14)	0.006(6)	-0.001(7)	0.017(8)
C465	0.045(9)	0.093(15)	0.082(13)	-0.002(8)	-0.012(9)	-0.030(12)

C466	0.08(2)	0.08(2)	1.06(19)	-0.032(17)	-0.16(5)	0.17(5)
S501	0.173(4)	0.116(3)	0.098(3)	0.050(3)	-0.091(3)	-0.036(2)
S551	0.097(7)	0.148(10)	0.102(7)	0.012(6)	-0.031(5)	-0.007(7)
O501	0.124(5)	0.100(5)	0.079(4)	0.024(4)	-0.046(4)	-0.003(3)
C502	0.30(3)	0.27(3)	0.23(2)	0.01(2)	-0.011(19)	0.18(2)
C501	0.071(7)	0.35(3)	0.142(11)	0.017(11)	-0.039(7)	-0.093(14)
N101	0.100(6)	0.102(6)	0.063(4)	-0.003(5)	-0.024(4)	-0.029(4)
N301	0.037(2)	0.055(3)	0.030(2)	0.0075(19)	0.0050(17)	0.0197(19)
N401	0.041(3)	0.098(5)	0.094(4)	0.046(3)	0.026(3)	0.057(4)
O1	0.0279(15)	0.0243(14)	0.0196(13)	0.0003(11)	-0.0007(11)	0.0026(11)
O2	0.0259(14)	0.0332(16)	0.0232(14)	-0.0099(12)	0.0036(11)	0.0018(12)
O3	0.0219(13)	0.0258(14)	0.0225(13)	0.0036(11)	-0.0010(11)	0.0006(11)
O4	0.0187(14)	0.0432(18)	0.0301(15)	0.0012(13)	-0.0027(12)	-0.0009(13)
O5	0.0194(13)	0.0263(14)	0.0178(12)	-0.0024(11)	-0.0001(10)	0.0014(11)
O6	0.0206(13)	0.0254(14)	0.0213(13)	-0.0007(11)	-0.0012(11)	-0.0005(11)
O7	0.0280(15)	0.0304(15)	0.0244(14)	0.0000(12)	-0.0001(12)	0.0030(12)
O8	0.0326(16)	0.0373(17)	0.0193(14)	0.0029(13)	-0.0011(12)	0.0007(12)
O9	0.0199(13)	0.0274(14)	0.0194(13)	-0.0007(11)	0.0010(10)	-0.0003(11)
O10	0.0188(13)	0.0276(14)	0.0215(13)	-0.0041(11)	0.0005(10)	-0.0010(11)
O11	0.0286(15)	0.0337(16)	0.0236(14)	0.0029(13)	0.0050(12)	-0.0022(12)
O12	0.0289(15)	0.0329(16)	0.0242(14)	-0.0100(13)	-0.0014(12)	-0.0020(12)
O13	0.0262(14)	0.0266(14)	0.0188(13)	-0.0001(12)	-0.0015(11)	-0.0028(11)
O14	0.0252(14)	0.0261(14)	0.0226(14)	0.0017(12)	0.0010(11)	-0.0020(11)
O15	0.0314(15)	0.0221(14)	0.0231(14)	-0.0030(12)	0.0026(11)	-0.0014(11)
O16	0.0365(17)	0.0258(15)	0.0312(16)	0.0037(13)	-0.0001(13)	0.0046(12)
O102	0.109(4)	0.078(3)	0.049(3)	0.029(3)	-0.031(3)	-0.033(2)
O103	0.142(7)	0.140(7)	0.201(10)	0.071(6)	-0.073(7)	-0.045(7)
O104	0.170(7)	0.067(4)	0.072(4)	0.012(4)	0.006(4)	-0.014(3)
O201	0.058(2)	0.042(2)	0.0397(19)	-0.0017(17)	0.0067(17)	-0.0191(16)
Pd1	0.03446(18)	0.03231(18)	0.02086(16)	-0.00228(13)	-0.00300(12)	-0.00737(12)
V1	0.0217(3)	0.0263(4)	0.0177(3)	-0.0017(3)	-0.0013(2)	0.0004(3)
V2	0.0178(3)	0.0233(3)	0.0177(3)	-0.0043(3)	0.0013(2)	0.0021(2)
V3	0.0169(3)	0.0263(4)	0.0198(3)	0.0006(3)	-0.0019(2)	0.0003(3)
V4	0.0211(3)	0.0227(3)	0.0190(3)	0.0003(3)	0.0023(2)	-0.0023(2)
V5	0.0216(3)	0.0226(3)	0.0190(3)	-0.0058(3)	0.0005(2)	-0.0028(2)
V6	0.0233(3)	0.0215(3)	0.0227(3)	0.0013(3)	0.0011(3)	0.0001(3)
F1	0.0216(11)	0.0245(11)	0.0198(10)	-0.0008(9)	0.0011(9)	-0.0004(9)

Table 16 Bond lengths (Å)

atom	atom	distance		atom	atom	distance
S201	C201	1.772(6)		S201	C202	1.769(6)
S201	O201	1.473(4)		S201	Pd1	2.2165(12)
C301	C302	1.530(8)		C301	N301	1.523(7)
C302	C303	1.519(8)		C303	C304	1.509(9)
C305	C306	1.502(9)		C305	N301	1.527(7)
C306	C307	1.540(9)		C307	C308	1.481(12)
C309	C310	1.510(10)		C309	N301	1.503(7)
C310	C311	1.542(19)		C310	C361	1.61(3)
C311	C312	1.56(2)		C311	C361	0.70(4)
C311	C362	1.91(3)		C361	C362	1.53(3)
C313	C314	1.504(8)		C313	N301	1.528(7)
C314	C315	1.503(9)		C315	C316	1.496(10)
C401	C402	1.502(11)		C401	N401	1.532(9)
C402	C403	1.497(12)		C403	C404	1.475(13)
C405	C406	1.505(11)		C405	N401	1.499(11)
C406	C407	1.695(19)		C406	C457	1.424(19)
C407	C408	1.52(2)		C407	C457	0.70(3)
C407	C458	0.86(3)		C408	C457	1.43(2)
C408	C458	1.57(2)		C457	C458	1.47(3)
C409	C410	1.551(16)		C409	N401	1.525(11)
C410	C411	1.53(2)		C411	C412	1.38(3)
C413	C414	1.50(2)		C413	C463	0.72(2)
C413	N401	1.418(13)		C414	C415	1.53(2)
C414	C463	1.24(2)		C414	C464	1.15(3)
C415	C416	1.11(3)		C415	C464	1.59(2)
C415	C465	0.99(4)		C415	C466	1.69(5)
C416	C465	1.56(3)		C416	C466	1.39(7)
C463	C464	1.53(2)		C463	N401	1.718(15)
C464	C465	1.58(2)		C465	C466	1.29(5)
S501	S551	1.250(13)		S501	O501	1.429(8)
S501	C502	1.76(2)		S501	C501	1.631(16)
S551	O501	1.520(15)		S551	C502	1.55(2)
S551	C501	1.711(16)		N101	O102	1.293(10)
N101	O103	1.310(13)		N101	O104	1.131(11)
O1	V2	1.729(3)		O1	V6[1]	1.894(3)
O2	V2	1.601(3)		O3	V3	1.732(3)
O3	V6[1]	1.906(3)		O4	V3	1.601(3)

O5	V1	1.828(3)		O5	V2	1.937(3)
O5	V4	2.064(3)		O6	V1	1.829(3)
O6	V3	1.933(3)		O6	V5	2.041(3)
O7	V1	1.602(3)		O8	Pd1	2.020(3)
O8	V1	1.721(3)		O9	V2	1.987(3)
O9	$V3^1$	1.908(3)		O9	V4	1.919(3)
O10	$V2^1$	1.913(3)		O10	V3	1.985(3)
O10	V5	1.926(3)		O11	V4	1.596(3)
O12	V5	1.606(3)		O13	Pd1	2.061(3)
O13	V4	1.909(3)		O13	V5	1.911(3)
O14	V4	1.761(3)		O14	V6	1.904(3)
O15	V5	1.770(3)		O15	V6	1.894(3)
O16	V6	1.597(3)		O102	Pd1	2.093(5)
V2	$V3^1$	3.0177(9)		V2	V4	3.0841(10)
V3	V5	3.0693(10)		V4	V6	3.1096(9)
V4	F1	2.203(2)		V5	V6	3.0923(9)
V5	F1	2.174(2)		V6	F1	2.234(2)

5.4 Results and Discussion

5.4.1 Single Crystal X-ray Diffraction (SXRD) Analysis

Into the solution of $Pd(NO_3)_2$, $\{n\text{-}Bu_4N\}_4[V_{10}O_{26}]$ and $\{n\text{-}Bu_4N\}F$ was added. The addition of excess amount of hydrogen peroxide was to assure the full oxidation of all vanadium atoms. To control the speciation of polyoxovanadate nitric acid was added[51]. Red crystal suitable for single X-ray crystallographic analysis compound **(3)** were obtained from the solution in ca 50% yield based on Pd^{2+} (Figure 25).

Four tetra-*n*-butyl ammonium cations per one polyoxovanadate were determined. The anion structure of compound **(3)** exhibited the basal fluoride-incorporated polyoxovanadates with three layers of one belt layer of four VO_5 units and two cap layers of $[V_3O_{13}]$ fragments.

If compound **(2)** was grown in acetonitrile-DMSO media, then compound **(3)** is a new fully oxidized Pd supported polyoxometalate compound synthesized in mixed CH_3NO_2/DMSO media. It crystallizes in Orthorhombic space group Pbca, Z = 4. The crystallographic data in Table 12 includes the unit cell parameters and other relevant information. Tables 13, 14 and 15 provide the atomic coordinate and anisotropic displacement parameters and bond length for the title compound, respectively. Figures 26 illustrate the structure of the anion of compound **(3)** with all building units.

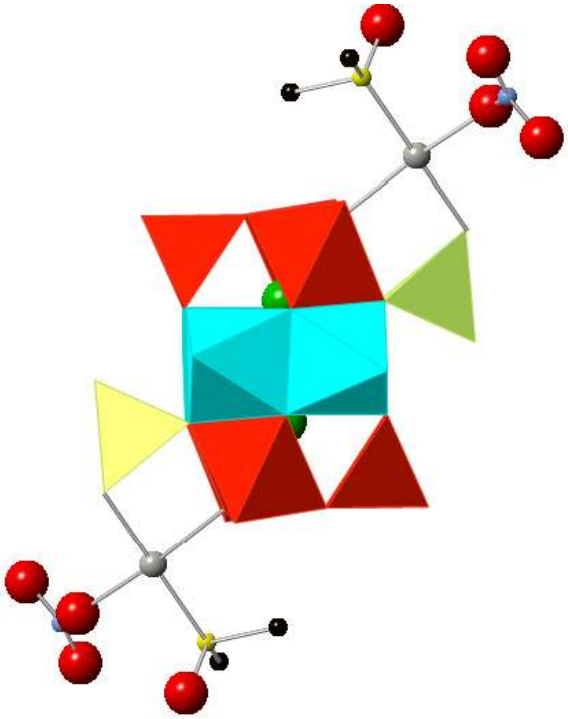

Figure 30 belt (blue) and cap layers (red) and addenda VO_4 unit (yellow) in the anion structure of (3)

Like previous compound **(2)**, compound **(3)** possessed two F^- surrounded by ten VO_5 units. The shortest V· ·F distance (2.17 Å) is longer than that of the usual V−F bonds (ca. 1.8 Å). This suggests that the vanadium atoms and a fluoride anion are not directly bonded like other fluoride-incorporated polyoxovanadates. In addition to the parent structure, two VO_4 units existed between the belt and cap layers.

The two Pd^{2+} atoms have square planar geometry bridged by an oxygen atom from a VO_4 unit and a bridging oxygen atom between edge-shared VO_5 units on the cap layer. The square planar Pd^{2+} ion are accomplished with DMSO and NO_3^- molecules. The bond length of Pd-S is 2.2165 Å and Pd-O is 2.093 Å against both ligands respectively. These values of long distances indicate the weak bonding between Pd and DMSO ligand and Pd and NO_3^- ligand that make DMSO and NO_3^- as a good leaving group.

The peripheral sites of the anion are occupied by an oxygen atom from NO_3^- and a sulfur atom of DMSO. The N−O distances of NO_3^- are 1.22, 1.24, and 1.43 Å. The N−O distance with O coordinated to Pd is longer than the others.

While free DMSO has S-O distance 1.531 Å, the S−O and S−C distances of Pd-coordinated DMSO are 1.47, 1.77, and 1.78 Å, respectively. These values are comparable to those of free DMSO, indicating the weak interaction between Pd and DMSO. The anion is discrete because the Pd-coordinated NO_3^- and DMSO were not connected to the other moieties. In the other report, $Pd(DMSO)_2(NO_3)_2$ exhibit dimer configuration bridged by nitrate.[69]

From X-ray crystallographic, elemental, and thermogravimetric analyses show that the formula of **(3)** is $\{n\text{-}Bu_4N\}_4[\{Pd(NO_3)(DMSO)\}_2V_{12}O_{32}(F)_2]\cdot 2DMSO$.

The reaction equation for the formation of **(3)** can be expressed by the following equation (2):

$$10Pd^{2+} + 6\,[V_{10}O_{26}]^{4-} + 10F^- + 6H_2O_2 + 4H^+ + 10NO_3^-$$

$$\rightarrow 5[\{Pd(NO_3)\}_2V_{12}O_{32}(F)_2]^{4-} \quad (2)$$

Compound (**3)** is the first example of fully oxidized polyoxovanadates with available metal coordination sites as a linker unit, to best of our knowledge.

5.4.2 Bond Valence Sum (BVS) Calculation

The charges of V atoms are all pentavalent by the bond valence sums calculations shown in Table 16.

Table 17 BVS calculation of compound (3)

V^{IV}	V^{V}		Bond Valence Sum											
			V1	V2	V3	V4	V5	V6	V7	V8	V9	V10	V11	V12
0	12	V^{IV}	4.594	4.744	4.752	4.861	4.825	4.821						
		V^{V}	4.836	4.994	5.003	5.104	5.064	5.062						

The BVS calculation confirm the formula of compound **(3)** in term of charge balance and the missing of IVCT peak in UV Vis spectra.

5.4.3 The IR spectrum

The IR spectra of compound **(3)** shows characteristic POV peaks in the region of 1000−400 cm^{-1}. Interestingly these peaks are similar in shape to that of $[HV_{11}O_{29}F_2]^{4-}$, [54] which possess the similar fully oxidized structure (figure 30).

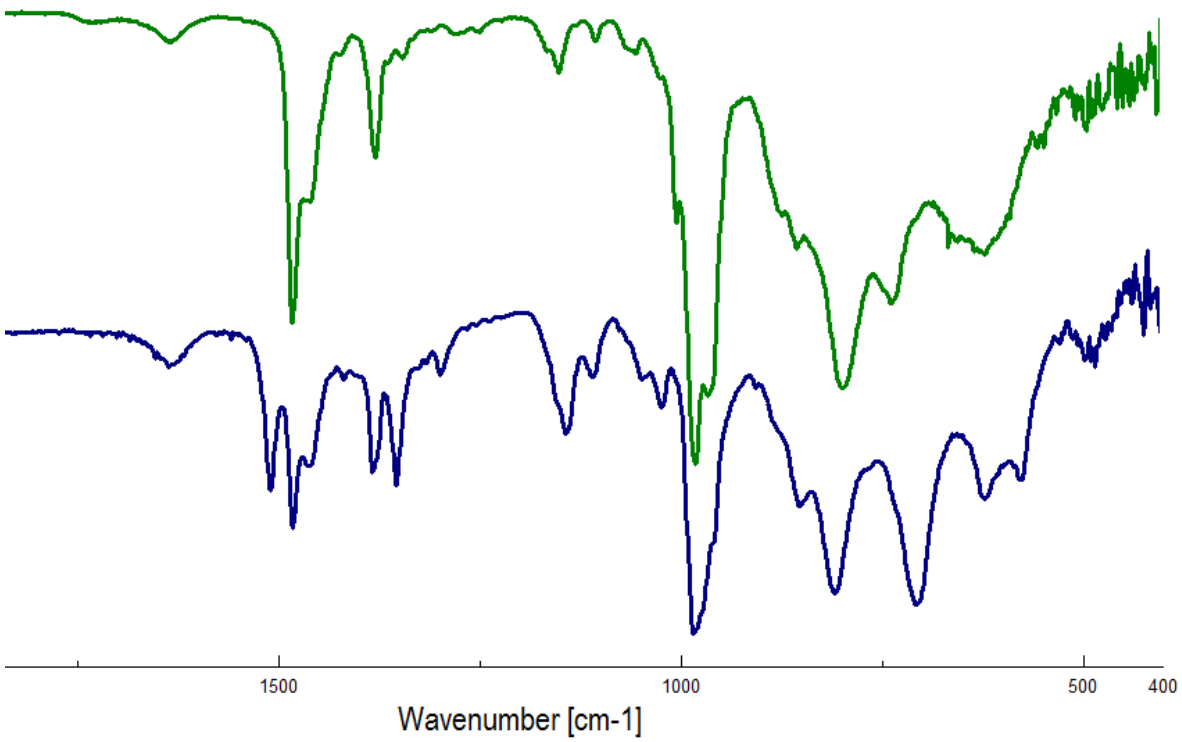

Figure 31 The IR spectrum of 3 in the region of (3) (blue) comparable with that of $[HV_{11}O_{29}F_2]^{4-}$(green)

Two peaks of S−O stretching vibration at 1050 and 1110 cm^{-1}, are due to free and coordinated DMSO, respectively. The higher wavenumber of coordinated DMSO suggested the coordination to palladium center via sulfur atom, as shown in crystallographic analysis[70]. Peaks due to symmetric and asymmetric vibration of NO_3^- were observed at 1356 and 1511 cm^{-1}, respectively[70].

5.4.4 NMR Spectroscopy Analysis

The solution state of compound **(3)** was studied by NMR spectra measurement in CD_3CN. The ^{51}V NMR spectrum show the four resonance peaks at −444, −458, −525, and −542 ppm with the intensity ratio of 2:1:2:1 (figure 32).

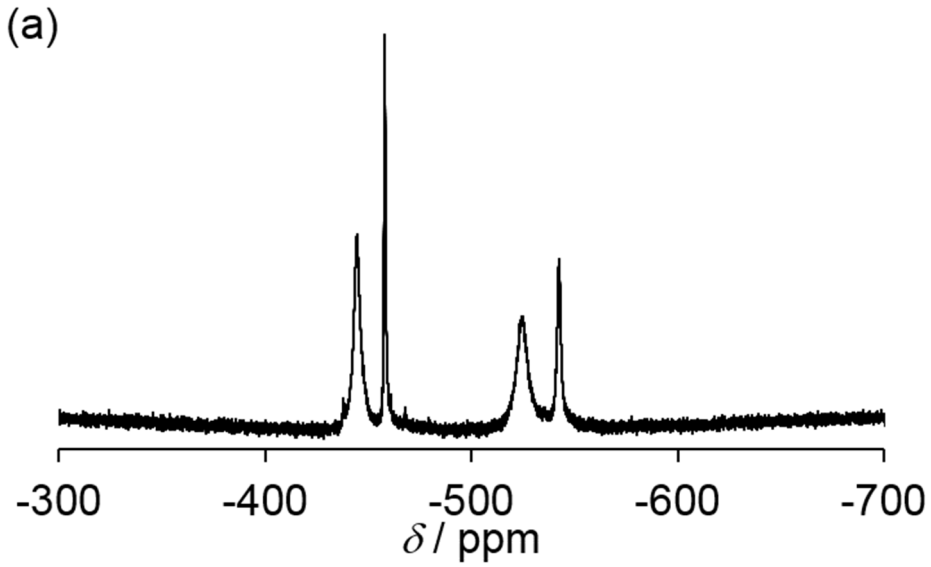

Figure 32 ^{51}V NMR spectra of complex 3 in CD_3CN.

The ^{51}V NMR spectra of the anion **(3)** is in perfect agreement with data of the crystal data by SCXRD as illustrated in figure 29.

As we can see from the crystal structure of anion **3,** there two possible ways of assigning based on the symmetry of V atoms. However, based on the previous report, we can take to account the V atom coordinated to Pd atoms, where vanadium-supported noble metal complex tends to resonate downfield[56].

So, the downfield peak with intensity ratio 2 can be assigned to the equivalent vanadiums (the blue color V4, V5) and the downfield with intensity ratio 1 can be assigned at the green color V6, which are all connected with Pd^{2+} through an oxygen bridge. The upfield peaks at intensity ratio 2 were assigned to the residual vanadiums (V2 and V3 red color) at belt position and the last peak with intensity ratio1 is assigned to the brown color V7 at cap position not connected to O-Pd.

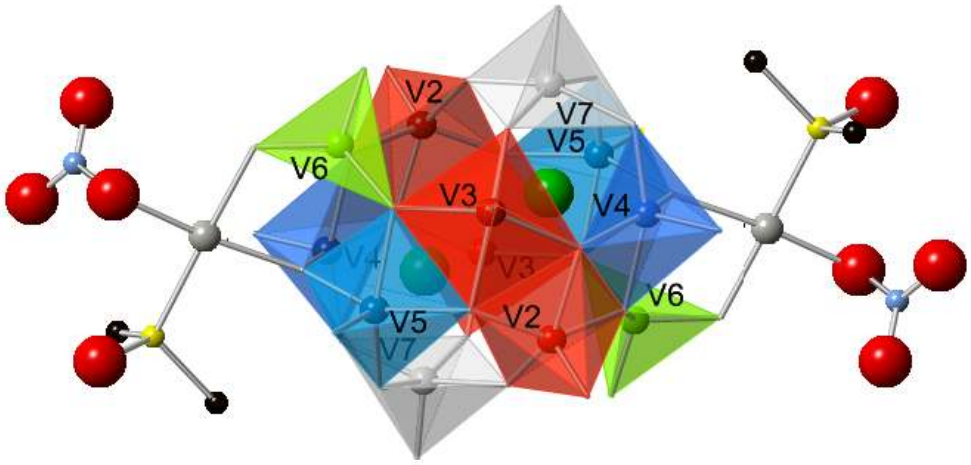

Figure 33 Assignment of ^{51}V NMR of V atoms differentiated by different colors.

This is the assignment based the factor that the ^{51}V NMR signal of a vanadium-supported noble metal complex tends to resonate downfield [56]. So all the intensity ratio was in accordance with the symmetry of the crystal structure of **3**. However, it is also possible for the other alternative assignment, where the green V atoms come to grey, and the red one comes to blue.

The result of ^{19}F NMR spectrum (figure 34) that shows single signal at −71 ppm ascertains both the presence of F in the sphere and the structural integrity of the dodecavanadate framework of **3** in the solution state.

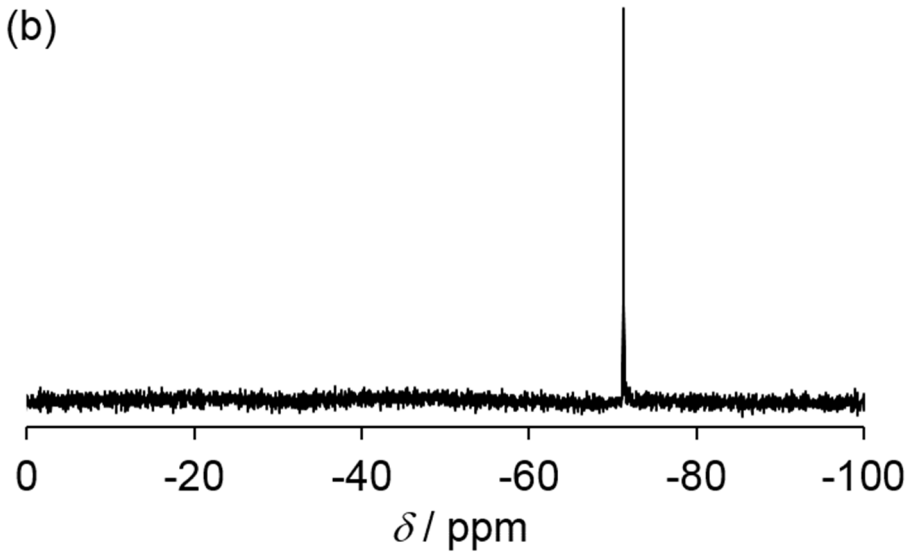

Figure 34 ^{19}F, NMR spectra of 3 in CD_3CN.

For the ^{1}H NMR spectrum, the four peaks observed at 0.97, 1.38, 1.62, and 3.17 ppm are due to tetra-*n*-butylammonium as counter cations. A peak observed at 2.50 ppm is to free DMSO.

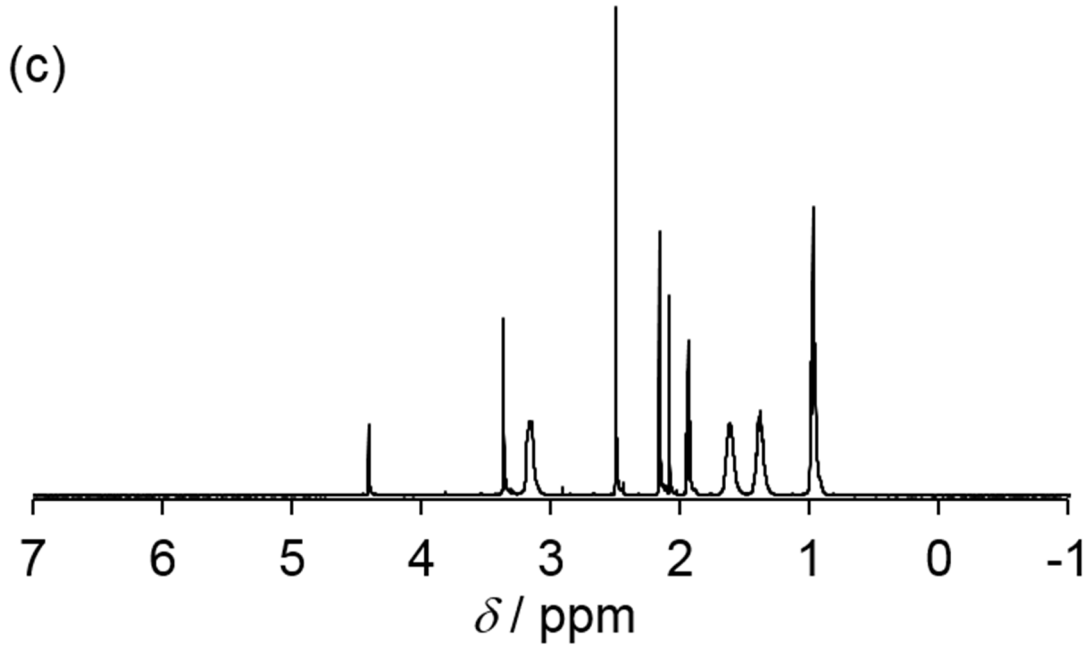

Figure 35 ^{1}H NMR spectra of 3 in CD_3CN.[13]

Furthermore, two singlet peaks with intensity ratio 3:1 at 3.37 and 4.41 ppm were observed. The total peak area was same as that of free DMSO. If mixed solvent DMSO-d_6 and CD_3CN were used instead, these two peaks disappeared. These suggests that peaks at 3.37 and 4.41 ppm are because of the exchangeable Pd-coordinated DMSO. It is also known that ^{1}H NMR peak due to Pd-coordinated DMSO via sulfur is observed at lower field than that via oxygen [59].

Compared with the previous works, the peak at 3.37 ppm is due to Pd-coordinated DMSO via oxygen, and the other is due to that via sulfur, indicating that in the solution state DMSO coordination via oxygen atom to the Pd center is preferable.[59] The peak at 2.16 ppm and 2.08 ppm are due to the presence of small amount of water and aceton respectively in the measured solution.

5.4.5 UV-Vis Absorption Spectra

From the measurement of UV/Vis spectrum of **3** in CH_3CN, there are peaks at 244 and 470 nm and shoulders at 300 and 370 nm, with $\varepsilon = 5.6\times10^4$, 7.4×10^3, 2.4×10^4, and 1.1×10^4 $M^{-1}cm^{-1}$, respectively (Figure 36).

This results is similar adsorption band in the similar region with the fully oxidized fluoride-incorporated polyoxovanadate, $[HV_{11}O_{29}F_2]^{4-}$, which also has similar structural units with compound **(3)**, (shoulders at 330 and 465 nm with $\varepsilon = 1.1\times10^4$ and $\varepsilon = 2.3\times10^3$ $M^{-1}cm^{-1}$, respectively).[51]

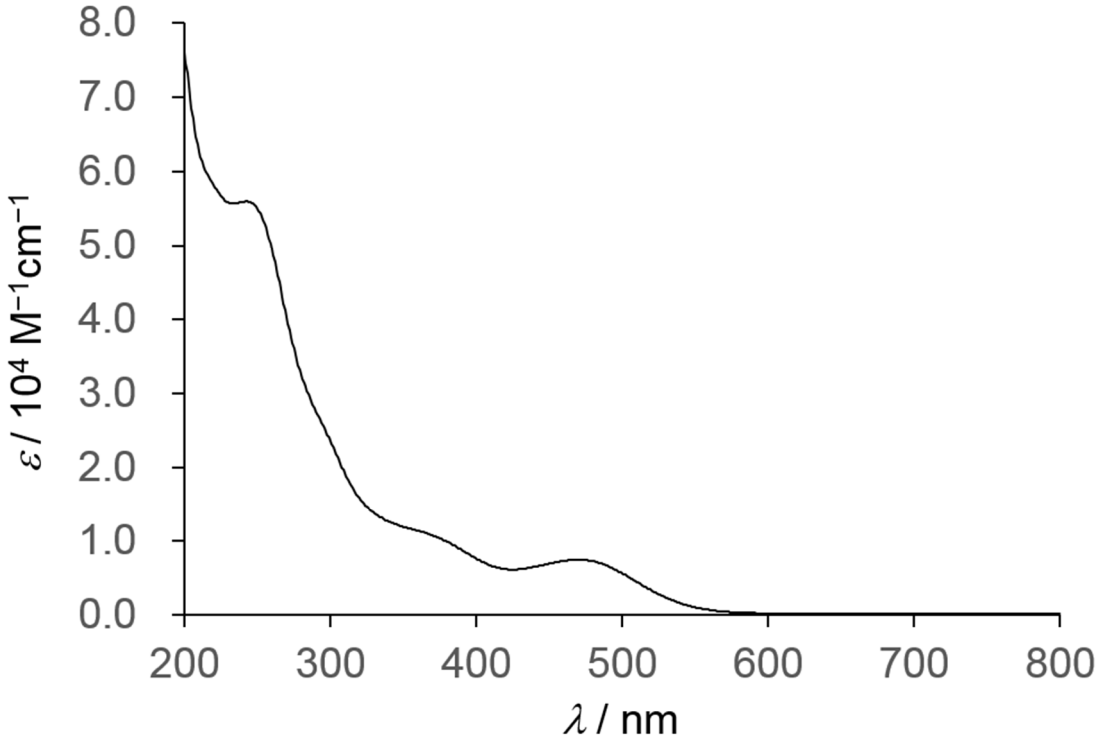

Figure 36 UV/vis spectrum of compound (3).

The UV−vis spectrum of the compound **(3)** showed no absorption band above 600 nm, proving that the vanadium species are not mixed valence of V^{IV} / V^{V}. Compound **(3)** that only has Vanadium(V) does not contain *d* electrons, obviously is restricted to intra-ligand LMCT absorptions only. The observed red color of compound **(3)** is because LMCT bands lie in the visible region (absorbed blue-green color in 490 nm).

5.4.6 Cyclic voltammetry Analysis

Cyclic voltammogram result of compound **(3)** in CH_3CN showed a reductive peak at −0.50 V and an oxidative peak at −0.37 V versus ferrocene/ferrocenium (Figure 37).

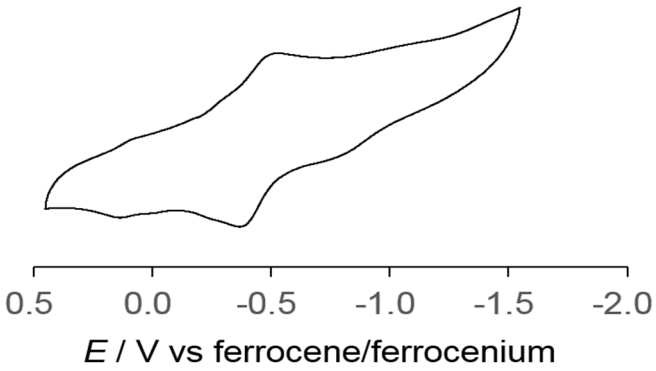

Figure 37 Cyclic voltammogram of compound (3)

This redox pair was observed in the higher potential in comparison with the that of $[HV_{11}O_{29}F_2]^{4-}$.[51]

5.4.7 Thermogravimetric (TG) Analysis

TGA measurements were done on ground powders (~10 mg). The heating profile for the measurement included a heating rate of 10 °C/min from room temperature to 300 °C, followed by a return cooling rate of 10 °C/min.

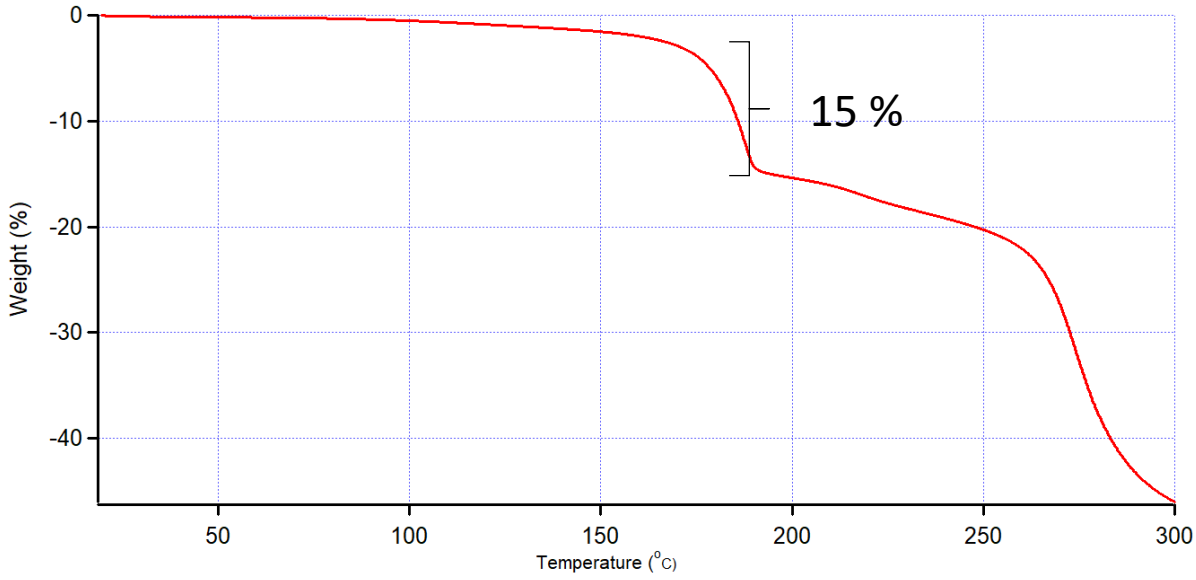

Figure 38 TG of compound 3

TGA measurements illustrated in Figure 10 show that compound **(3)** starts to release both ligands (DMSO and NO_3^-) 160 °C up to 180 °C at a point about 15% weight loss occurs.

5.5 Conclusion

In this chapter, we have successfully overcome the weakness of complex **2** before for becoming best linker for MOF or supramolecular frameworks. We can get rid of annoying counter cation $VO(DMSO)_5^{2+}$ away as found in complex **2**. We can also get a soluble in organic solvent linker because the counter cation is a very popular $\{n\text{-}Bu_4N\}^+$ cation. The complex is stable in the air with it fully oxidized state. Its diamagnetic properties allow for ^{51}V NMR study. By NMR evidence the structure integrity is kept in solution too. So, this is very good for supramolecular MOF linker.

Anionic **(3)** is a new building block of polyoxometalates designed by utilizing the unique structural features of fluoride-incorporated polyoxometalates. By the combination of both tetrahedrally and square-pyramidally coordinated vanadium atoms, both cations and anions are stabilized by one polyoxovanadate framework. Measurement of ^1H NMR shows the ligand exchange property of Pd-coordinated DMSO with at the same time maintaining the polyoxovanadate framework.

5.5.1 Potential Application

Different form complex **(2)** which is insoluble in most solvents, complex **(3)** is soluble in most organic solvents. This enable the exploration of the chemistry of the complex better than previously prepared complex **(2)**. Like anionic $[\{Pd(DMSO)_2\}_2V_{12}O_{32}(F)_2]^{4-}$ in complex **(2)**, anion $\{Pd(NO_3)(DMSO)\}_2V_{12}O_{32}(F)_2]^{4-}$ is also potential linker in Polyoxometalate based Metal Organic Framework Chemistry. Ligand DMSO and Nitrate are weakly bonded and considered as the leaving group which can be replaced by other organic multidentate ligands to grow a framework structure as described chapter 4. Apart from coordination polymer / POMOF linker, catalytic activity of complex **(3)** is also very interesting subject to study.

CONCLUDING REMARKS

Even if POMs can afford high negative charge, in general they still have weak coordination ability because their high negative charges are delocalized along the cluster. This problem hinders the use of POMs as the building units (linkers) for the construction of framework structures. This projects were successful in dealing with the mentioned problem by successful synthesis of transition metal supported polyoxovanadate.

During this experiment we have successfully performed a systematic stepwise synthesis of Pd-POV linker units. We started from the synthesis of precursor fluoride-incorporated dodecavanadate $[V_{12}O_{30}F_2]^{4-}$ through the modification of other polyoxovanadate $[HV_{11}O_{29}F_2]^{4-}$. The two types of linkers successfully obtained afterwards are a reduced Palladium Supported Fluoride Incorporated Dodecavanadate $[\{Pd(DMSO)_2\}_2V_{12}O_{32}(F)_2]^{4-}$ and a fully oxidized $[\{Pd(DMSO)_2\}_2V_{12}O_{32}(F)_2]^{4-}$.

The synthesized anions $[\{Pd(DMSO)_2\}_2V_{12}O_{32}(F)_2]^{4-}$ and $[\{Pd(DMSO)(NO_3)\}_2V_{12}O_{32}F_2]^{4-}$ provides two available metal coordination sites at both ends of POMs which in turn would play role as a linker unit. The attached ligands DMSO and nitrate are leaving groups which are easily removed by additional ligands. Furthermore, the definite square planar 90°-degree coordination of Pd^{2+} is very good for rational synthesis of framework structures. The diamagnetic properties of $[\{Pd(DMSO)(NO_3)\}_2V_{12}O_{32}F_2]^{4-}$ anion allows their study later by NMR spectroscopy.

These complexes are also useful for researchers who need inorganic linkers. Therefore, this research opens up the future works in the new field of POM chemistry, a so called POM based frameworks (POMOFs) or Metal Inorganic Frameworks fields.

Lastly, the complexes are very potential for catalysis due to the availability of catalyst active sites V and Pd at the same time. The redox active $[V_{12}O_{30}F_2]^{4-}$ anion synthesized is interesting because it can store and release electrons that make it potential for high capacity energy storage electrode materials.

REFERENCE

(1) Car, P.-E.; Patzke, G. *Inorganics* **2015**, *3* (4), 511–515.

(2) Long, D.; Tsunashima, R.; Cronin, L. *Angew. Chemie Int. Ed.* **2010**, *49* (10), 1736–1758.

(3) Müller, A.; Beckmann, E.; Bögge, H.; Schmidtmann, M.; Dress, A. *Angew. Chemie Int. Ed.* **2002**, *41* (7), 1162–1167.

(4) Long, D.-L.; Cronin, L. *Chem. Eur. J* **2006**, *12*, 3698–3706.

(5) Abbas, H. Controllable Growth of Polyoxometalate Based Building Blocks : Towards the Construction of Clusters , Arrays and, University of Glasgow, 2006.

(6) Kurata, T.; Hayashi, Y.; Uehara, A.; Isobe, K. *Chem. Lett.* **2003**, *32* (11), 1040–1041.

(7) Rhule, J. T.; Hill, C. L.; Judd, D. A.; Schinazi, R. F. *Chem. Rev.* **1998**, *98* (1), 327–358.

(8) Yamase, T. *J. Mater. Chem.* **2005**, *15* (45), 4773–4782.

(9) Sharpless, N. E.; Munday, J. S. *Anal. Chem.* **1957**, *29* (11), 1619–1622.

(10) Tsigdinos, G. a.; Hallada, C. J. *Inorg. Chem.* **1968**, *7* (3), 437–441.

(11) Brown, D. H. *Spectrochim. Acta* **1963**, *19* (1962), 1683–1685.

(12) Jackson, M. N.; Kamunde-Devonish, M. K.; Hammann, B. A.; Wills, L. A.; Fullmer, L. B.; Hayes, S. E.; Cheong, P. H.-Y.; Casey, W. H.; Nyman, M.; Johnson, D. W. *Dalt. Trans.* **2015**, *44* (39), 16982–17006.

(13) Ohlin, C. A. *Chem. - An Asian J.* **2012**, *7* (2), 262–270.

(14) Wilson, E. F.; Miras, H. N.; Rosnes, M. H.; Cronin, L. *Angew. Chemie - Int. Ed.* **2011**, *50* (16), 3720–3724.

(15) Pope, M. T.; Müller, A. *Angew. Chem. Int. Ed. Engl.* **1991**, *30*, 34–48.

(16) Miras, H. N.; Yan, J.; Long, D.-L.; Cronin, L. *Chem. Soc. Rev.* **2012**, *41* (22), 7403.

(17) Rehder, D. *Bioinorganic vanadium chemistry*; John Wiley & Sons, 2008; Vol. 30.

(18) Monakhov, K. Y.; Bensch, W.; Kögerler, P. *Chem. Soc. Rev.* **2015**, *44* (23), 8443–8483.

(19) Tidmarsh, I. S.; Laye, R. H.; Brearley, P. R.; Shanmugam, M.; Sañudo, E. C.; Sorace, L.; Caneschi, A.; McInnes, E. J. L. *Chem. Commun.* **2006**, *22* (24), 2560–2562.

(20) Manos, M. J.; Tasiopoulos, A. J.; Tolis, E. J.; Lalioti, N.; Woollins, J. D.; Slawin, A. M. Z.; Sigalas, M. P.; Kabanos, T. A. *Chem. - A Eur. J.* **2003**, *9* (3), 695–703.

(21) Hayashi, Y. *Coord. Chem. Rev.* **2011**, *255* (19–20), 2270–2280.

(22) Day, P. Brown, D. B., Ed.; Springer Netherlands: Dordrecht, 1980; pp 3–24.

(23) Xie, X.; Nie, Y.; Chen, S.; Ding, W.; Qi, X.; Li, L.; Wei, Z. *J. Mater. Chem. A* **2015**, *3* (26), 13962–13969.

(24) Hayashi, Y.; Fukuyama, K.; Takatera, T.; Uehara, A. *Chem. Lett.* **2000**, *29* (7), 770–771.

(25) Randall, W. J.; Weakley, T. J. R.; Finke, R. G. **1993**, *20*, 1068–1071.

(26) Neumann, R.; Abu-Gnim, C. *J. Am. Chem. Soc.* **1990**, *112* (16), 6025–6031.

(27) Albéniz, A. C.; Espinet, P. In *Encyclopedia of Inorganic Chemistry*; John Wiley & Sons, Ltd, 2006.

(28) Wayland, B. B.; Schramm, R. F. *Inorg. Chem.* **1969**, *8* (4), 971–976.

(29) Espinet, A. C. A. & P. *Encycl. Inorg. Chem.* **2006**.

(30) Du, D.-Y.; Qin, J.-S.; Li, S.-L.; Su, Z.-M.; Lan, Y.-Q. *Chem. Soc. Rev.* **2014**, *43* (13), 4615–4632.

(31) Wang, J.; Zhao, J.; Niu, J. *J. Mol. Struct.* **2004**, *697* (1–3), 191–198.

(32) Qin, C.; Wang, X.; Qi, Y.; Wang, E.; Hu, C.; Xu, L. *J. Solid State Chem.* **2004**, *177* (10), 3263–3269.

(33) Streb, C.; Ritchie, C.; Long, D.; Kögerler, P.; Cronin, L.; Streb, C.; Ritchie, C.; Long, D.; Cronin, P. L. **2007**.

(34) Lisnard, L.; Dolbecq, A.; Mialane, P.; Francis, S. **2005**, 3913–3920.

(35) Dolbecq, A.; Dumas, E.; Mayer, R.; Mialane, P. **2010**, 6009–6048.

(36) Rao, C. N. R. *Mater. Sci. Eng. B* **1993**, *18* (1), 1–21.

(37) Bruker AXS, Inc.: Madison, Wisconsin, USA, 2015.

(38) Farrugia, L. J. *J. Appl. Crystallogr.* **1999**, *32* (4), 837–838.

(39) G. M. Sheldrick. 2014.

(40) Ito, N.; Saji, T.; Aoyagui, S. *J. Organomet. Chem.* **1983**, *247* (3), 301–305.

(41) Sharp, M.; Petersson, M.; M, K. E. *J. Electroanal. Chem.* **1980**, *109* (c), 271–288.

(42) Montenegro, M. I.; Pletcher, D. *J. Electroanal. Chem.* **1986**, *200* (1–2), 371–374.

(43) Okaya, K.; Kobayashi, T.; Koyama, Y.; Hayashi, Y.; Isobe, K. *Eur. J. Inorg. Chem.* **2009**, No. 34, 5156–5163.

(44) *Organometallics in Synthesis, Third Manual*; Schlosser, M., Ed.; John Wiley & Sons, 2013.

(45) Baxter, S. M.; Wolczanski, P. T. **1989**, *0* (7), 3263–3264.

(46) Gale, P. A. *Chem. Commun.* **2011**, *47* (1), 82–86.

(47) Reichenbächer, K.; Süss, H. I.; Hulliger, J. *Chem. Soc. Rev.* **2005**, *34* (1), 22–30.

(48) Krivosudský, L.; Schwendt, P.; Gyepes, R.; Filo, J. *Inorg. Chem. Commun.* **2014**, *49*, 48–51.

(49) Müller, A.; Rohlfing, R.; Krickemeyer, E.; Bögge, H. *Angew. Chemie Int. Ed. English* **1993**, *32* (6), 909–912.

(50) Müller, A.; Rohlfing, R.; Barra, A.-L.; Gatteschi, D. *Adv. Mater.* **1993**, *5* (12), 915–917.

(51) Kikukawa, Y.; Yokoyama, T.; Kashio, S.; Hayashi, Y. *J. Inorg. Biochem.* **2015**, *147*, 221–226.

(52) Gouzerh, P.; Proust, A. *Chem. Rev.* **1998**, *98* (1), 77–112.

(53) Chen, Q.; Chen, Q.; Goshorn, D. P.; Goshorn, D. P.; Scholes, C. P.; Scholes, C. P.; Tan, X. L.; Tan, X. L.; Zubieta, J.; Zubieta, J. *J. Am. Chem. Soc.* **1992**, *114* (12), 4667–4681.

(54) Okaya, K.; Kobayashi, T.; Koyama, Y.; Hayashi, Y.; Isobe, K. **2009**, 5156–5163.

(55) Brown, I. D.; Altermatt, D. *Acta Crystallogr. Sect. B Struct. Sci.* **1985**, *41* (4), 244–247.

(56) Kurata, T.; Uehara, A.; Hayashi, Y.; Isobe, K. *Inorg. Chem.* **2005**, *44* (7), 2524–2530.

(57) Hayashi, Y.; Miyakoshi, N.; Shinguchi, T.; Uehara, A. *Chem. Lett.* **2001**, *36* (2), 170–171.

(58) Calligaris, M. *Coord. Chem. Rev.* **2004**, *248* (3–4), 351–375.

(59) Diao, T.; White, P.; Guzei, I.; Stahl, S. S. *Inorg. Chem.* **2012**, *51* (21), 11898–11909.

(60) Muller, A.; Rohlfing, R.; Krickemeyer, E.; Bagge, H. *Angew. Chemie Int. Ed. English* **1993**, *32* (6), 909–912.

(61) Ninclaus, C.; Riou, D. **2000**, *3*, 851–852.

(62) Miller, B. A.; Rohlfing, R.; Krickemeyer, E. **1993**, *0*, 3–6.

(63) Price, J. H.; Williamson, A. N.; Schramm, R. F.; Wayland, B. B. *Inorg. Chem.* **1972**, *11* (6), 1280–1284.

(64) Ii, M. M.; Ii, F.; Ii, C.; Ii, N.; Cu, I.; Ii, C.; Ii, Z.; Weiner, H.; Hayashi, Y.; Finke, R. G. **1999**, No. c, 2579–2591.

(65) Nishio, M.; Inami, S.; Hayashi, Y. **2013**, 1876–1881.

(66) Ninclaus, C.; Riou, D.; Ferey, G. *Chem. Commun.* **1997**, *3* (9), 851–852.

(67) Drew, D.; Doyle, J. R.; Shaver, A. G. In *Inorganic Syntheses*; John Wiley & Sons, Inc., 1972; pp 47–55.

(68) Long, D.-L.; Burkholder, E.; Cronin, L. *Chem. Soc. Rev.* **2007**, *36* (1), 105–121.

(69) Johansson, M. H.; Oskarsson, Å. *Acta Crystallogr. Sect. C Cryst. Struct. Commun.* **2001**, *57* (11), 1265–1267.

(70) Nakamoto, K. *Infrared and Raman spectra of inorganic and coordination compounds, Part B: Applications in Coordination, Organometallic, and Bioinorganic Chemistry*, 5th ed.; Wiley: New York, 1997.